

**TREATMENT OF WATER USING HYBRID OZONATION-  
MEMBRANE SYSTEM**

**FORMATION OF BROMATE AND OTHER  
BROMINATED DISINFECTION BYPRODUCTS DURING  
THE TREATMENT OF WATERS USING A HYBRID  
OZONATION-MEMBRANE FILTRATION SYSTEM**

By

**MOHAMMADREZA MOSLEMI**

B.Sc., M.Sc.

A Thesis Submitted to the School of Graduate Studies  
in Partial Fulfillment of the Requirements for the  
Degree Doctor of Philosophy

McMaster University

© Copyright by Mohammadreza Moslemi

August 2011

Doctor of Philosophy (2011)  
Civil Engineering

McMaster University  
Hamilton, Ontario

Title: Formation of Bromate and Other Brominated Disinfection  
Byproducts during the Treatment of Waters Using a Hybrid  
Ozonation-Membrane Filtration System

Author: Mohamandreza Moslemi  
M.Sc. (Sharif University of Technology)  
B.Sc. (Sharif University of Technology)

Supervisor: Dr. Susan J. Masten

Number of Pages: xxiii, 181

## Abstract

In this research, ozone hydrodynamics and disinfection by-products formation in a novel hybrid ozonation-ceramic membrane filtration system was studied to minimize membrane fouling while also ensuring that the system meets regulatory criteria for disinfection by-products. The influence of important operating parameters including inlet ozone mass injection rate, initial bromide concentration, membrane molecular weight cut off (MWCO), membrane coating, hydroxyl radical scavenger (*t*-butanol), pH, and temperature on bromate concentration in the absence and presence of natural organic matter (NOM) was examined. Experiments were also conducted under various operating conditions to investigate the formation of total trihalomethanes (TTHMs) and halo-acetic acids (HAAs) in the water distribution system due to post chlorination. Moreover, variations in the TOC, UV<sub>254</sub>, color and turbidity with respect to operating parameters were monitored.

Bromate and TTHMs formation increased with increasing ozone mass injection rate, and initial bromide concentration. An increase in the bromate concentration was observed with decreasing membrane MWCO. Less bromate and TTHM was formed with the coated membrane and *t*-butanol significantly reduced bromate and TTHM formation. Bromate formation decreased significantly with decreasing pH. Increasing the temperature resulted in enhanced bromate formation. NOM exerted a favorable effect on bromate formation as the

bromate concentration was observed to decrease as the NOM content was increased.

Experimental results indicated that ozonation can greatly reduce color and turbidity of water and can be used to overcome membrane fouling. Ensuring a minimum ozone residual in the system enables the continuous treatment of water at a relatively high permeate flux (up to 85% of the clean water flux) and eliminates the need for membrane cleaning procedures.

An empirical model was developed to predict bromate formation in the hybrid ozone- membrane system ( $R^2=0.903$ ). Theoretical models were developed to estimate the rate of bromate formation and to describe the ozone mass transfer in a hybrid system. In all cases, good correlation between the model predictions and the experimental data was achieved.

## **Acknowledgements**

I would like to express my sincerest gratitude to those individuals who without their help this work would not have been possible.

First and foremost, I would like to express my utmost gratitude to my research supervisor, Dr. Susan J. Masten and also Dr. Simon H. Davies for their excellent guidance, support, and patience through out my research. I am also extremely thankful to the members of the supervisory committee, Dr. Sarah Dickson and Dr. Carlos Filipe for their valuable guidance and kind supports throughout this research work.

I wish to express my deep appreciation to Mrs. Anna Robertson, the supervisor of the environmental lab, for her technical advice and assistance during the experimental phases of this research.

I also acknowledge the financial support from the National Science Foundation, the Natural Sciences and Engineering Research Council of Canada and the Department of Civil Engineering at McMaster University.

Finally and most importantly, I am indebted to my family for their constant support and encouragement. This thesis is dedicated to my parents, Simin and Ali, for their unconditional love and support.

## **Table of Contents**

<b>Abstract</b>	iii
<b>Acknowledgements</b>	v
<b>Table of Contents</b>	vi
<b>List of Tables</b>	x
<b>List of Figures</b>	xii
<b>List of Abbreviations</b>	xvi
<b>Summary of Publications</b>	xix
<b>Declaration of Academic Achievement</b>	xxi
<b>1. Introduction</b>	1
1.1. Drinking Water Treatment Methods	1
1.1.1. Conventional Methods	1
1.1.2. Advent of Membrane Technology	3
1.1.3. Fouling: Major Drawback	6
1.2. Hybrid Ozonation-Membrane System	9
1.2.1. Ozonation as a Solution to Fouling	9
1.2.2. Additional Benefits of Ozonation	11
1.3. Research Summary	13
1.3.1. Research Significance	13
1.3.2. Theory & Background	16
1.3.3. Historical Perspective	27
1.3.4. Strategies to Cope with $\text{BrO}_3^-$ Formation	30
1.3.5. Objectives & Scope of Research	34

<b>2. Ozone Mass Transfer in a Recirculating Loop Semibatch Reactor Operated at High Pressure</b>	38
2.1. Abstract	38
2.2. Introduction	39
2.3. Materials and Methods	42
2.3.1. Experimental Apparatus	42
2.3.2. Experimental Conditions	43
2.3.3. Analytical Methods	44
2.4. Determination of the Ozone Mass Transfer	45
2.5. Results and Discussion	48
2.5.1. Water Flow Rate	48
2.5.2. Inline Mixer	50
2.5.3. Inlet Ozone Gas Concentration	54
2.5.4. Inlet Gas Flow Rate	56
2.5.5. Temperature	58
2.5.9. pH	59
2.5.10. Mass Balance on Ozone	60
2.6. Conclusion	62
2.7. Acknowledgements	62
2.8. References	63
<b>3. Bromate Formation in a Hybrid Ceramic Membrane Filtration – Ozonation</b>	66
3.1. Abstract	66
3.2. Introduction	66
3.3. Materials and Methods	69
3.3.1. Experimental Setup	69

3.3.2. Analytical Methods	72
3.3.4. Reagents	73
3.4. Results and Discussion	73
3.4.1. Effect of pH	74
3.4.2. Effect of Inlet Ozone Mass	75
3.4.3. Initial Bromide Concentration	78
3.4.5. Effect of MWCO	78
3.5. Bromate Formation Model	81
3.6. Acknowledgements	82
3.7. Supplemental Data	83
3.8. Supporting Documentation	84
3.9. References	86
<b>4. Empirical Modeling of Bromate Formation during Drinking Water Treatment Using a Hybrid Membrane Filtration–Ozonation</b>	<b>90</b>
4.1. Abstract	90
4.2. Introduction	91
4.3. Materials and Methods	94
4.4. Results and Discussion	95
4.4.1. The Role of the Hydroxyl Radical	95
4.4.2. Membrane Coating	97
4.4.3. Temperature	99
4.5. Empirical Model for Bromate Formation	100
4.6. Model Validation	102
4.7. Conclusion	104
4.8. Supporting Documentation	107
4.9. References	110

<b>5. Disinfection By-products Formation in the Presence of NOM in a Hybrid Ceramic Membrane Filtration – Ozonation</b>	117
5.1. Abstract	117
5.2. Introduction	118
5.3. Materials and Methods	121
5.3.1. Experimental Setup	121
5.3.2. Analytical Methods	124
5.3.3. Reagents	127
5.4. Results and Discussion	128
5.4.1. Effect of Inlet Ozone Mass	129
5.4.2. Effect of Initial Bromide Concentration	132
5.4.3. Effect of NOM Concentration	134
5.4.4. Effect of Ph	136
5.4.5. Effect of OH Radical Scavengers	138
5.4.6. Effect of Membrane Coating	141
5.4.7. Effect of MWCO	145
5.4.8. Fouling	149
5.5. Empirical Bromate Model	151
5.6. References	154
<b>6. Conclusions and Recommendations</b>	158
6.1. Conclusions	158
6.2. Recommendations for Future Research	162
6.3. Implications of Research for Full-scale Operation	163
<b>References</b>	165
<b>Appendix</b>	178

## List of Tables

### Chapter 1:

Table 1- Drinking water regulations and guidelines for DBPs.	15
Table 2- Reactions occurring during ozone self-decomposition.	21
Table 3- Reactions and rate constants involved in bromate formation via molecular ozone pathway.	24
Table 4- Reactions and rate constants involved in bromate formation via hydroxyl radical pathway.	26

### Chapter 2:

Table 1- Dimensionless Henry's law constants.	48
Table 2- Water flow rates versus flow regime.	49
Table 3- $K_L a$ values calculated by modelling experimental results at various water flow rates.	50
Table 4- $K_L a$ values calculated by modelling experimental results under various mixing conditions.	54
Table 5- $K_L a$ values calculated by modelling experimental results at various gaseous ozone concentrations.	56
Table 6- $K_L a$ values calculated by modelling experimental results at various inlet gas flow rates.	57
Table 7- Ozone uptake at various inlet gas flow rates.	58
Table 8- $K_L a$ values calculated by modelling experimental results at various temperatures.	59

### Chapter 3:

Table 1- Steady state bromate concentration in the permeate under various operating conditions	74
Table 2- Steady state $[\text{BrO}_3^-]$ at various MWCOs	79

Table 3- Retention time in the membrane for various MWCOs	80
Table 4- Rate constants for the formation of bromate in the hybrid ozonation-membrane system	82
<b>Chapter 4:</b>	
Table 1- Steady state aqueous $[O_3]$ at various pH values.	98
Table S1- Steady state bromate concentration in the permeate under various operating conditions	110
<b>Chapter 5:</b>	
Table 1- TTHMs concentrations in the permeate under various operating conditions.	128
Table 2- Effects of MWCO, [NOM] and $O_3$ dosage on permeate flux.	150

## List of Figures

### Chapter 1:

- Fig. 1- Typical pore size of various membrane filtration processes. 5
- Fig. 2- Permeate flux decline due to fouling. 8
- Fig. 3- Bromate formation diagram during ozonation of Br<sup>-</sup> containing waters. 25

### Chapter 2:

- Fig. 1- Schematic of the experimental apparatus. 44
- Fig. 2- Simplified control volume for modeling ozone mass transfer. 45
- Fig. 3- Dissolved ozone concentration vs. time at various water flow rates. 50
- Fig. 4- Dissolved ozone concentration versus time - The effect of inline mixer. 53
- Fig. 5- Dissolved ozone concentration versus time at various gaseous ozone concentrations. 55
- Fig. 6- Dissolved ozone concentration versus time at various inlet gas flow rates. 57
- Fig. 7- Dissolved ozone concentration versus time at various temperatures. 59
- Fig. 8- Dissolved ozone concentration versus time at various pH vales. 60

### Chapter 3:

- Fig. 1- Bromate formation - Molecular ozone and hydroxyl radical pathways. 69
- Fig. 2- Schematic of the experimental setup. 70
- Fig. 3- Bromate concentration in the permeate vs. time at various pH values. 75

Fig. 4- Dissolved ozone concentration in the permeate vs. time at various inlet O <sub>3</sub> mass rates.	76
Fig. 5- Bromate concentration in the permeate vs. time at various inlet O <sub>3</sub> mass rates.	77
Fig. 6- Steady state bromate concentration in the permeate vs. steady state aqueous O <sub>3</sub> concentration.	77
Fig. 7- Steady state bromate concentration in the permeate vs. initial bromide concentration.	78
Fig. 8- Steady state bromate concentration in the permeate vs. retention time in the membrane.	80
Fig. S1- Bromate concentration in the permeate vs. time at various initial bromide concentrations.	83
Fig. S2- Bromate concentration in the permeate vs. time at various MWCOs.	84

#### **Chapter 4:**

Fig. 1- Formation of bromate in aquatic systems.	92
Fig. 2- The effect of <sup>•</sup> OH scavenger on the steady state bromate and ozone concentrations in the permeate at various pHs.	96
Fig. 3- Steady state bromate concentration in the permeate vs. pH.	99
Fig. 4- Bromate concentration in the permeate vs. time at various temperatures.	100
Fig. 5- Predicted bromate concentration vs. observed values.	103
Fig. 6- Measured and simulated bromate concentrations vs. contact time.	104
Fig. 7- Measured and simulated bromate concentrations vs. contact time.	104
Fig. 8- Measured and simulated bromate concentrations vs. contact time.	105
Fig. 9- Measured and simulated bromate concentrations vs. contact time.	105
Fig. S1- The effect of <sup>•</sup> OH scavenger on the dissolved ozone concentration in the permeate vs. time at various pHs.	108

Fig. S2- The effect of $\cdot\text{OH}$ scavenger on the bromate concentration in the permeate vs. time at various pHs.	108
Fig. S3- Bromate concentration in permeate vs. time at various pH values.	109
Fig. S4 - Bromate concentration in the permeate vs. time in the presence of t-BuOH.	109
<b>Chapter 5:</b>	
Fig. 1- Schematic of the experimental setup.	124
Fig. 2- Bromate concentration in the permeate vs. time at various inlet ozone mass injection rates.	130
Fig. 3- Percent reduction in the steady state DBPs concentration at various inlet ozone mass rates.	131
Fig. 4- Percent reduction at various inlet ozone mass rates.	131
Fig. 5- Bromate concentration in the permeate vs. time at various initial bromide concentrations.	133
Fig. 6- Percent reduction in DBPs concentration at various initial bromide concentrations.	133
Fig. 7- Bromate concentration in the permeate vs. time at various NOM concentrations.	135
Fig. 8- Percent reduction at various NOM concentrations.	135
Fig. 9- Bromate concentration in the permeate vs. time at various pHs.	137
Fig. 10- Percent reduction in DBPs concentration at various pHs.	137
Fig. 11- Percent reduction at various NOM concentrations.	138
Fig. 12- Bromate concentration in the permeate vs. time in the presence of scavenger.	140
Fig. 13- Percent reduction in DBPs concentration in the presence of scavenger.	140
Fig. 14- Percent reduction in the presence of scavenger.	141

Fig. 15- Bromate concentration in the permeate vs. time. The effect of membrane coating.	143
Fig. 16- Percent reduction in DBPs concentration. The effect of membrane coating.	144
Fig. 17- Percent reduction. The effect of membrane coating.	144
Fig. 18- Bromate concentration in the permeate vs. time using various MWCOs.	146
Fig. 19- Percent reduction in DBPs concentration using various MWCOs.	147
Fig. 20- Percent reduction using various MWCOs.	147
Fig. 21- Percent reduction in color using various MWCOs.	148
Fig. 22- Percent reduction in turbidity using various MWCOs.	148
Fig. 23- Percent reduction in UV <sub>254</sub> using various MWCOs.	149
Fig. 24- Effect of ozone dosage on permeate flux.	151
Fig. 25- Predicted bromate concentration vs. observed values.	153
Fig. A1- Experimental apparatus: Hybrid ozoantion – membrane filtration.	178
Fig. A2- High-pressure stainless steel tank.	179
Fig. A3- Water coil inside the tank.	180
Fig. A4- Ceramic membranes (from left to right: one, three and seven channel).	181

## List of Abbreviations

$\text{Al}_2\text{O}_3$	Aluminum oxide
AOP	Advanced oxidation process
$b_i$	Regression coefficients
$\text{Br}^-$	Bromide ion
$\text{BrO}_3^-$	Bromate ion
C	$\text{O}_3$ concentration in the bulk water
$C_G$	Inlet $\text{O}_3$ gas concentration
$\text{CHBr}_2\text{Cl}$	Dibromochloromethane (DBCM)
$\text{CHBr}_3$	Bromoform (TBM)
$\text{CHBrCl}_2$	Bromodichloromethane (BDCM)
$\text{CHCl}_3$	Chloroform (TCM)
$C_{\text{in}}$	Concentration of bromate in the inflow into the
$\text{CO}_3^{2-}$	Carbonate
$C_P$	Concentration of bromate in the permeate
$C_R$	Concentration of bromate in the retentate
$C_s$	Aqueous $\text{O}_3$ concentration at equilibrium with the inlet $\text{O}_3$ gas concentration ( $C_G$ )
$C_{\text{ss}}$	Steady state ozone concentration in the reactor
DBPs	Disinfection by-products
DDI	Distilled deionized water
DOC	Dissolved organic carbon
F	Bleed flow rate
Fe	Iron
$\text{Fe}_2\text{O}_3$	Iron oxide
H'	Dimensionless Henry's law constant
$\text{H}_3\text{PO}_4$	Phosphoric acid
HAAs	Halo acetic acids

$\text{HCO}_3^-$	Bicarbonate
HO	Hydroxyl
$\text{HO}^\bullet$	Hydroxyl radicals
HOB <sub>r</sub>	Hypobromous acid
J	Steady state permeate flux
k	First order rate constant
kD	kilo Dalton
$K_{La}$	Overall mass transfer coefficient
MCL	Maximum contaminant level
MF	Microfiltration
Mn	Manganese
MWCO	Molecular weight cut off
NaOH	Sodium hydroxide
NF	Nanofiltration
NOM	Natural organic matter
O <sub>3</sub>	Ozone
$\text{OBr}^-$	Hypobromite ion
$\text{OH}^-$	Hydroxyl ion
PES	Polyethersulfone
pK <sub>a</sub>	Dissociation constant
PP	Polypropylene
PS	Polysulfone
PVDF	Polyvinylidene fluoride
Q	Flow rate
Q <sub>B</sub>	Bleed flow rate
Q <sub>in</sub>	Inlet flow rate
Q <sub>P</sub>	Permeate flow rate
R	Universal gas constant

Re	Reynolds number
RO	Reverse osmosis
SUVA	Specific UV absorbance
t	Time
T	Water temperature
t-BuOH	Tertiary butyl-alcohol
THMs	Trihalomethanes
TiO <sub>2</sub>	Titanium dioxide
TMP	Trans-membrane pressure
TOC	Total organic carbon
UF	Ultrafiltration
USEPA	United States Environmental Protection Agency
UV	Ultraviolet
UV <sub>254</sub>	UV absorbance at a wavelength of 254nm
V	Total volume of water in the system
v	Cross flow velocity
V <sub>0</sub>	Initial volume of water in the reactor
V <sub>mp</sub>	Total volume of the membrane
V <sub>mp</sub>	Porous volume
V <sub>p</sub>	Total volume of the membrane pores
WHO	The World Health Organization
W <sub>m</sub>	Weight of the membrane
ZrO <sub>2</sub>	Zirconium dioxide
θ	Retention time in the membrane
ρ	Density of the ceramic membrane material
τ	Retention time in the entire system

## **Summary of Publications**

This thesis consists of the following papers:

### **Paper I**

Moslemi, M., Davies, H.S., Masten, S.J. (2010) Ozone Mass Transfer in a Recirculating Loop Semibatch Reactor Operated at High Pressure. *Journal of Advanced Oxidation Technologies*, 13 (1) 79-88.

*Preface:* In this article the effects of water flow rate, mixing, gaseous ozone concentration, inlet gas flow rate, temperature, and pH on ozone hydrodynamics in a recirculating loop semibatch reactor under high pressure is studied. A mathematical model was also developed to describe the ozone mass transfer in the corresponding reactor.

### **Paper II**

Moslemi, M., Davies, H.S., Masten, S.J. (2011) Bromate Formation in a Hybrid Ozonation – Ceramic Membrane Filtration System. *Water Research*, 45, 5529-5534.

*Preface:* In this paper the effect of pH, inlet ozone mass rate, initial bromide concentration, and membrane molecular weight cut off (MWCO) on bromate formation in a hybrid membrane filtration–ozonation reactor is discussed. A model to estimate the rate of bromate formation was also developed.

### **Paper III**

Moslemi, M., Davies, H.S., Masten, S.J. Empirical Modeling of Bromate Formation during Drinking Water Treatment Using a Hybrid Membrane Filtration – Ozonation. *Journal of Membrane Science*, Submitted for publication, 2011.

*Preface:* The existing work studies the influence of the nature of the membrane surface, hydroxyl radical scavengers, and temperature, on bromate formation in a hybrid membrane filtration–ozonation reactor. An empirical model was also developed using multiple linear regression method to predict bromate formation in a hybrid ozone-ceramic membrane filtration system. The model, takes into account the effects of important experimental variables including initial bromide concentration, inlet ozone mass rate, pH, temperature, and reaction time.

### **Paper IV**

Moslemi, M., Alpatova, A.A., Byun, S., Davies, H.S., Masten, S.J. Disinfection By-products Formation in the Presence of NOM in a Hybrid Ceramic Membrane Filtration – Ozonation. To be submitted for publication.

*Preface:* This research investigates the effect of pH, inlet ozone mass injection rate, natural organic matter concentration, initial bromide concentration, membrane coating, hydroxyl radical scavenger, and membrane molecular weight cut off on the formation of disinfection by-products (including bromate, trihalomethanes, and halo acetic acids) in a hybrid membrane filtration–ozonation reactor.

## **Declaration of Academic Achievement**

This thesis has been prepared in accordance with the regulations for a “Sandwich” thesis format or as a compilation of papers stipulated by the Faculty of Graduate Studies at McMaster University and has been co-authored.

### **Chapter 2: Ozone Mass Transfer in a Recirculating Loop Semibatch Reactor Operated at High Pressure**

*M. Moslemi:* Designed and constructed a bench-scale experimental apparatus; conducted laboratory experiments and analysis the effects of water flow rate, mixing, gaseous ozone concentration, inlet gas flow rate, temperature, and pH on ozone hydrodynamics at high pressure; collected and analyzed data; developed a mathematical model to describe the ozone mass transfer; prepared the journal paper.

*Dr. S.J. Masten and Dr. S.H. Davies:* Supervised the research work; reviewed and revised the journal paper.

This work has been printed with written permission from the Journal of Advanced Oxidation Technologies.

### **Chapter 3: Bromate Formation in a Hybrid Ozonation – Ceramic Membrane Filtration System**

*M. Moslemi:* Designed and constructed a bench-scale experimental apparatus; conducted laboratory experiments and analysis to study the effect of pH, inlet ozone mass rate, initial bromide concentration, and membrane molecular weight cut off on

bromate formation; collected and analyzed data; developed a model to estimate the rate of bromate formation in the reactor tested; prepared the above named journal paper.

*Dr. S.J. Masten and Dr. S.H. Davies:* Supervised the research work; reviewed and revised the journal paper.

#### **Chapter 4: Empirical Modeling of Bromate Formation during Drinking Water Treatment Using a Hybrid Membrane Filtration – Ozonation**

*M. Moslemi:* Designed and constructed a bench-scale experimental apparatus; conducted laboratory experiments and analysis to investigate the effect of the nature of the membrane surface, hydroxyl radical scavengers, and temperature, on bromate formation; collected and analyzed data; developed an empirical model to predict bromate formation in a hybrid ozone-ceramic membrane filtration system; prepared the journal paper.

*Dr. S.J. Masten and Dr. S.H. Davies:* Supervised the research work; reviewed and revised the journal paper.

#### **Chapter 5: Disinfection By-products Formation in the Presence of NOM in a Hybrid Ceramic Membrane Filtration – Ozonation**

*M. Moslemi:* Designed and constructed a bench-scale experimental apparatus; conducted laboratory experiments and analysis to study the influence of pH, inlet ozone mass injection rate, natural organic matter concentration, initial bromide concentration, membrane coating, hydroxyl radical scavenger, and membrane molecular weight cut off on the formation of disinfection by-products including

bromate, trihalomethanes and halo acetic acids in a hybrid ozonation-membrane system; collected and analyzed data; prepared the journal paper.

*A.A. Alpatova and S. Byun:* Measured TTHMs and HAAs in the samples which they were provided.

*Dr. S.J. Masten and Dr. S.H. Davies:* Supervised the research work; reviewed and revised the journal paper.

## **Chapter 1: Introduction**

### **1.1. Drinking Water Treatment Methods**

#### **1.1.1. Conventional Methods**

Various conventional treatment methods are available for water purification, each being suitable for waters with a particular origin and type of contamination. Therefore, a combination or series of methods is usually used to effectively treat the water and meet the applicable water regulations. Common conventional water treatment steps can be classified as follows [1]:

- 1- Screening
- 2- Coagulation/flocculation/sedimentation
- 3- Granular media filtration
- 4- Disinfection

Although conventional water treatment has high productivity, such methods are associated with a number of drawbacks, which may in part limit their application. Conventional methods, involving coagulation/flocculation, usually include considerable amounts of chemical addition, which results in large volumes of sludge, which must be further treated and disposed of. Chemical addition often requires extensive safety precautions. In addition, these processes may be insufficient to ensure compliance with the current and future rigorous standards, especially when low quality water supplies are employed [2,3]. Moreover, finished

water quality obtained from these methods is largely subject to knowledge, experience and judgment of the operators who are monitoring the treatment process, which could bring about disasters as happened in Milwaukee in 1993.

The year of 1993 is considered to be a turning point in the recent history of water treatment owing to the incident occurred in that year. *Cryptosporidium* oocysts passed through the conventional treatment system (granular media filters) in Milwaukee, Wisconsin. This incident in turn, caused over 400,000 illnesses and almost 100 deaths. It was not long after that engineers and designers tried to develop and employ more sophisticated water treatment methods, which can prevent the repeat of such tragic incidents. Membrane filtration is one of the processes that, due to its numerous advantages has attracted great attention since 1993 [1,4,5]. Membranes exclude and thus remove microorganisms and pollutants according to their size and irrespective of raw water quality, and operator judgment. Hence, a revolution in treatment strategies has been brought about by the advent of membranes.

As the world's population continues to increase and anthropogenic chemicals are released into our water supplies, the quality of water continues to deteriorate, leading to a reduction in the number of suitable drinking water supplies. Population growth has also given rise to higher demands for safe drinking water. At the same time, water quality regulations have been tightened and the public has become both more knowledgeable and more discriminating regarding water quality [6]. These facts have in turn emphasized the necessity for development of

safe and effective water treatment strategies, which has in turn made water utilities use robust treatment methods such as membrane filtration.

### **1.1.2. Advent of Membrane Technology**

Throughout the last century, membrane technology has been one of the most important developments in the history of drinking water treatment since chlorination and filtration. Microporous membranes were first patented in 1922 and their application was, until the 1950s, limited to laboratory investigations. The first interest in the application of membranes for potable water treatment was in the 1980s as drinking water facilities and regulators became increasingly concerned about microbial contamination [6,7]. In the past 15 years, membrane filtration has proved to be a safe and reliable technology offering high quality drinking water that complies with the stringent regulatory requirements. Over the same period, operational costs of membrane filtration utilities have dropped significantly due to advances in technology and mass production of membranes, which made membrane technology cost competitive with conventional treatment methods [2].

The initial motivation to use membranes for water treatment was to remove turbidity and microorganisms from raw water. Membranes are semi-permeable and usually porous barriers, which are permeable to some constituents of the feed stream (water) and almost impermeable to others (impurities), and hence they can selectively exclude and remove impurities from raw water. The predominant

membrane filtration mechanism and driving force that are employed in water industry are size exclusion and pressure, respectively.

Membranes have gained widespread applications in drinking water industry including, disinfection and microorganisms removal, particle/turbidity removal, desalination of sea/brackish water, water softening, color removal, and etc, which can be accomplished through various types of pressure driven membrane processes [8]:

- Microfiltration (MF)
- Nanofiltration (NF)
- Ultrafiltration (UF)
- Reverse osmosis (RO)

Due to different pore sizes and molecular weight cut off values (MWCO), various membrane processes strain solutes of different sizes. Figure 1 indicates the typical pore dimensions and operating conditions for the processes mentioned above.

Membranes used in water treatment applications can be fabricated from various materials including polymers (such as polypropylene (PP), polysulfone (PS), polyethersulfone (PES) and polyvinylidene fluoride (PVDF)), and inorganic materials such as ceramics [9]. Owing to the various advantages offered by pressure-driven membrane modules, their application in surface water treatment has dramatically increased within the past few decades and a large number of membrane filtration plants have been constructed during the last two decades. Although at present, granular media filtration is the most widely used filtration technology throughout the world, the intense development of membrane filtration units is expected to continue [6].

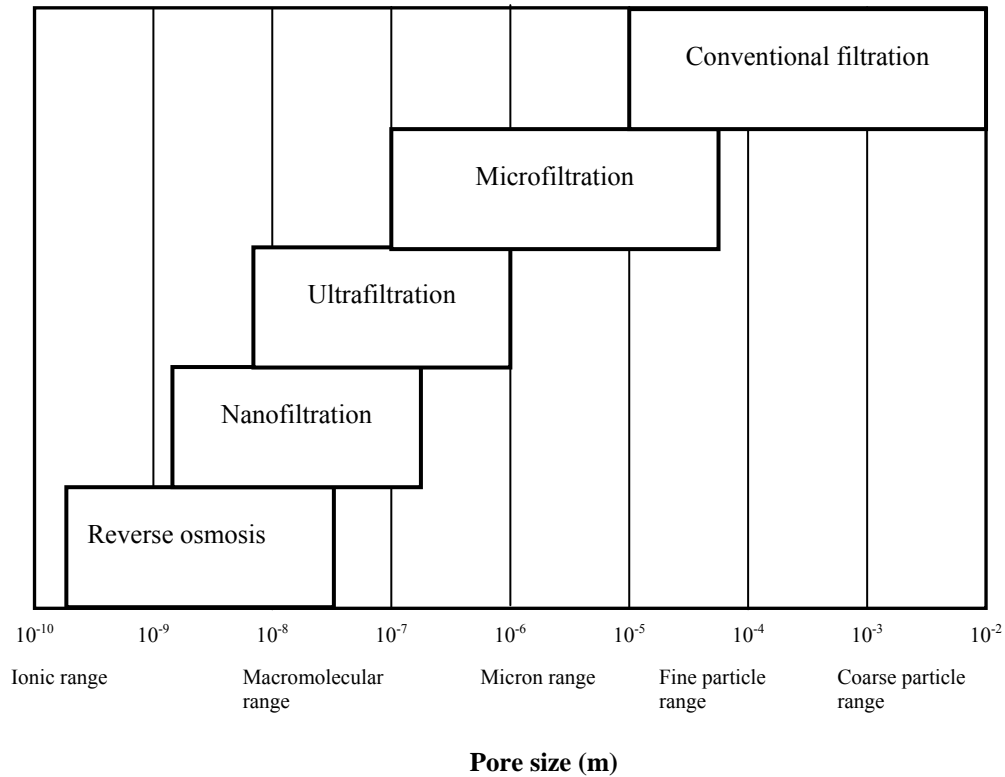


Fig. 1- Typical pore size of various membrane filtration processes. Adapted from [14].

Membrane filtration has several advantages that make it very suitable and promising in terms of drinking water production [10-12]:

- Effective rejection/removal of impurities (suspended solids, turbidity, microorganisms)
- High quality water production (complying with the strict drinking water regulations)
- Less chemical reagent and disinfectant consumption (by avoiding coagulation/flocculation step)
- Less waste production

- More compact construction (requiring smaller footprints)
- Easier operational control (having the capability to be automated)

In spite of all these advantages, membrane processes suffer from a major drawback, which is dealt with in the following section.

### **1.1.3. Fouling: Major Drawback**

One of the major challenges associated with the operation of membrane filtration plants is dealing with the fouling problem, which is brought about by natural organic matter (NOM) and some inorganic species present in the water body [8,10,13].

Fouling is the adsorption or deposition of solute molecules (NOM) or particulate material on the membrane surface or within the pores due to electrostatic adsorption, hydrophobic interactions or van der Waals forces [14,15]. Larger particles, which are removed by sieving, will deposit on the membrane surface and block the pores (surface cake formation), while smaller particles will diffuse into the pores and attach to the walls, thus restricting or blocking the pathways [16,17]. The typical fouling mechanisms are internal fouling (deposition of NOM within the membrane pores) and or external fouling (deposition of NOM on the membrane surface) [14]. Fouling can adversely affect the performance of membrane systems in following ways:

- Decline in the permeate flux and concomitant drop in productivity
- Need for membrane cleaning and recovery followed by a pause in the operation
- Reduction in membrane lifetime due to successive cleaning and irreversible fouling

- Increase in energy consumption and operational costs
- Change in rejection of various ions

As it is depicted in Figure 2, as a result of fouling, the permeate flux drops appreciably. Therefore, to maintain a constant flux and compensate for the fouling effect, the operating pressure has to be continually increased.

The two strategies that are often employed in drinking water utilities to treat fouled membranes include back-flushing and chemical cleaning [18]. The former involves pushing clean water through the membrane in the reverse direction, from the permeate-side to the feed-side, in order to dislodge foulants. The latter, includes soaking the clogged membrane in chemical cleaning agents such as acids and bases to detach and remove foulants from the membrane surface and pores. Because of the cost, time loss and difficulty incurred by cleaning and or back-flushing of fouled membranes in large filtration plants, it is preferable to find a way to prevent and suppress membrane fouling. As an alternative method, ozonation has shown to be very effective in terms of membrane fouling prevention and removal [19-22]. Considering the oxidative nature of ozone, it is necessary that membrane is made of ozone resistant materials such as Teflon or ceramic. Hence, a hybrid membrane/ozonation system, which will be subsequently discussed in more detail, was proposed by Masten and colleagues [13].

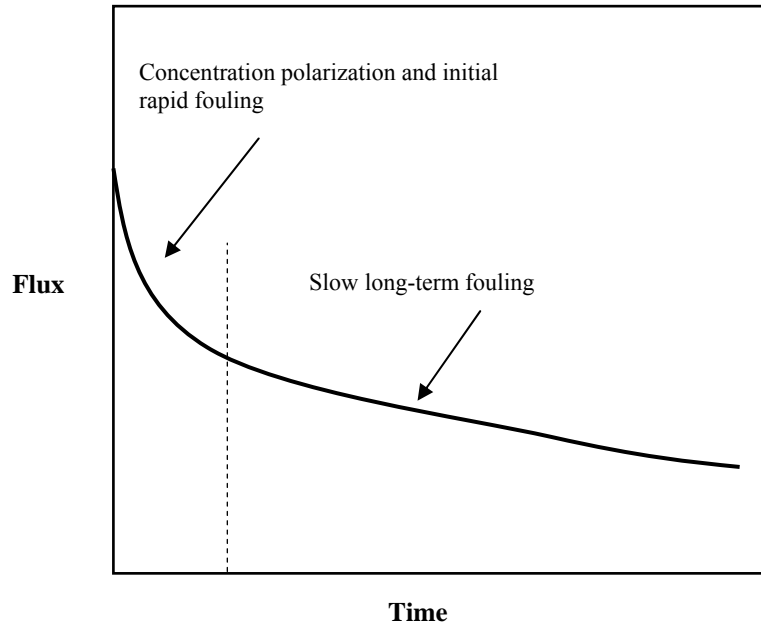


Fig. 2- Permeate flux decline due to fouling. Adapted from [14].

In the following sections, incorporation of ozonation within the membrane filtration system and the advantages and disadvantages that ozonation could bring about will be addressed. Afterwards, the major defect of hybrid ozonation/membrane systems, which is the formation of disinfection by-products (DBPs) and measures to minimize it, will be discussed. Lastly, the proposed research project, along with the supporting theories/hypotheses and also a summary of the research progress made thus far will be presented.

## **1.2. Hybrid Ozonation-Membrane System**

### **1.2.1. Ozonation as a Solution to Fouling**

With most surface waters, NOM is the main cause of membrane fouling [17]. Coagulation/flocculation, which involves the addition of chemicals to enhance the coagulation process, is typically used prior to membrane filtration to partially remove NOM from raw water and thus suppress fouling. However, especially in case of potable water production, due to health concerns it is desirable to avoid chemical addition as far as possible. An alternative solution to eliminating or reducing membrane clogging during filtration is the incorporation of ozonation into the process.

Several research groups have demonstrated that the hybrid ozonation/membrane system can considerably overcome fouling problems and achieve substantially higher permeate fluxes, compared to conventional membrane filtration systems. This method allows continuous operation and eliminates the need for cleaning or back-flushing of fouled membranes [13,18-22].

Ozone is a strong oxidant that can oxidize and decompose much of the natural organic matter present in surface waters [19,23]. In such a hybrid system, aqueous ozone will react with NOM deposited on the membrane surface or attached to the pores walls, resulting in a lessening of its bond with membrane surface. Concomitantly, water stream inside the membrane module would flush away partly dissociated foulants and thus recovering the permeable membrane surfaces and the clean water permeate flux [19]. Considering the oxidizing nature of

ozone, employed membranes have to be reasonably ozone resistant. Polymeric membranes that are commonly used in water treatment would rapidly erode out as a result of ozonation.

Karnik et al., 2005 [13] proposed the use of ceramic tubular membranes, which are made of metal oxides, such as alumina, titania and zirconia, and are believed to be ozone resistant. Despite their higher price, ceramic membranes have several advantages over polymeric membranes such as higher thermal, chemical and mechanical durability, capability to withstand higher pressures and longer lifetime. Besides that, the presence of various metal oxides in their structure could catalytically promote ozone decomposition on the membrane surface to form hydroxyl radicals ( $\text{HO}^\bullet$ ). Hydroxyl radicals contain an unpaired electron, which gives them unusually fast reactivity.  $^\bullet\text{OH}$  is a stronger oxidant than ozone and hence can more effectively decompose natural organic matter and remove foulants [24].

During their investigations, Karnik and associates [13] achieved up to about 100% permeate flux recovery in a hybrid ozonation/ceramic ultrafiltration membrane system, which was operated as a cross-flow configuration under a constant trans-membrane pressure (TMP). According to their experimental results, after about 12 hr the permeate flux dropped to about 60% of the initial value, on account of membrane fouling. Thereafter, gaseous ozone was injected into the circulating water stream for a period of 2 hr. Soon after, permeate flux started to recover, and eventually as a result of different ozone dosages various

enhancements in permeate flux were achieved. The greater the ozone concentration, the greater the permeate flux recovery. It has been exhibited that, by applying about 12.5 (g O<sub>3</sub> /m<sup>3</sup> gas) over a short course, up to approximately 100% flux recovery can be obtained.

In another set of experiments, Karnik et al. [13] compared the effect of continuous ozonation (1.5 g/m<sup>3</sup>) with that of pure oxygenation at the same gas injection flow rates. The results imply that flux enhancement is mainly due to the oxidative effect of ozone and hydroxyl radicals (which are formed on the membrane surface due to ozone decomposition), and not the scouring effect of gas sparging. Moreover, they demonstrated that ozonation at reasonably low dosages (1.5 g/m<sup>3</sup>) allows for continuous filtration without need for frequent chemical cleaning and back-flushing, which is a great benefit of such hybrid processes. Some other researchers including Schlichter et al. 2004, [22] and Mozia et al. 2005 [21] also tried hybrid ozonation/membrane filtration systems. Their findings confirm that by maintaining a minimum ozone concentration in the water continuous operation at relatively high permeate fluxes (almost more than 90% of the initial flux) can be maintained and the need for other cleaning procedures can be eliminated. Ozonation offers several side advantages that make this method highly promising and effective in terms of potable water treatment.

### **1.2.2. Additional Benefits of Ozonation**

The application of ozone in the water industry has increased dramatically both in quantity and diversity since the first full scale installation of ozone for the

treatment of potable water in Nice, France (1906) [25-28]. Other than fouling prevention, ozonation has a number of benefits [23,29-32]:

- Disinfection and thus a reduction in final disinfectant demand
- Oxidation of organic compounds, and removal of taste, odour, and color compounds
- Removal of the precursors of some chlorination by-products, including trihalomethanes (THMs)
- The reduction of total organic carbon (TOC) levels by mineralization
- Aid to coagulation through transformation of NOM to smaller and more polar compounds
- Oxidation and removal of Fe (II) and Mn (II)

Nevertheless, the hybrid ozonation/membrane filtration process, like all ozonation processes suffers from a major drawback, which is the formation of ozonation disinfection by-products (DBPs). Oxidation of organic and inorganic compounds (present in water) through ozonation results in the formation of a number of by-products some of which are believed to be carcinogenic, and could exert adverse health effects [33]. Furthermore, albeit destruction of bacteria is much more rapid and effective by ozonation than by chlorination, ozone is very short-lived [34]. Therefore, it is not practical to maintain adequate ozone residuals in the distribution system to prevent bacterial regrowth. Hence, a secondary and long-lasting disinfectant such as chlorine still needs to be added to finished water as the last disinfection step, which could, in part, react with ozonation products to

form new disinfection by-products [31]. This issue and the pertinent treatment measures are elaborated in the following sections.

### **1.3. Research Summary**

#### **1.3.1. Research Significance**

Chlorine and its derivatives have long been used to inactivate microorganisms present in water and thus disinfect water. Due to the ease of its application, low price and relatively high persistence and long lifetime, chlorine disinfectants have gained widespread use for disinfection. However, chlorination can produce a number of by-products including trihalomethanes (THMs) and halo-acetic acids (HAAs) which can pose adverse health effects to humans [35]. The trihalomethane which are major chlorination by-products were first discovered in 1973 [26].

As our general knowledge about water chemistry and properties of various water constituents increased, the focus on drinking water safety and related standards deepened. In the last century, noticeable developments in the drinking water quality criteria and standards can be observed and water regulations have become more and more stringent. In the 21<sup>st</sup> century, the main focus of various drinking water regulations is on reducing microbial contamination and exposure to chemicals with adverse health effects and considerable attention is paid to monitoring and suppression of disinfection by-products that are identified as health concerns. The major chlorination and ozonation DBPs that are regulated by most drinking water guidelines are THMs, HAAs, bromate and chlorite.

During the last decade, several regulatory organizations have lowered or established new maximum contaminant levels (MCLs) for DBPs. The MCLs for some of the DBPs of concern, which are set by the World Health Organization (WHO), Ontario Ministry of the Environment, Guidelines for Canadian Drinking Water Quality, USEPA and European Union Regulations are presented in Table 1 [36-41]. In 1998, the U.S. EPA tightened the U.S. drinking water regulations by enacting a set of new guidelines, Stage 1 Disinfectant/Disinfection By-products Rule (D/DBP), concerning disinfection by-products, which was followed by another rule, Stage 2 D/DBP, which was promulgated in 2000 [39,40].

Under the Stage 1 D/DBP Rule, the MCL for the combination of four trihalomethanes [TTHMs: chloroform (TCM), bromodichloromethane (BDCM), dibromochloromethane (DBCM), and bromoform (TBM)] was lowered and new standards for five halo-acetic acids [HAA5: monochloroacetic acid (MCA), dichloroacetic acid (DCA), trichloroacetic acid (TCA), monobromoacetic acid (MBA), and dibromoacetic acid (DBA)], bromate, and chlorite were established. According to this rule, conventional treatment plants are required to employ enhanced coagulation process to achieve desired reduction in DBPs concentration [39]. Stage 2 of these rules does not alter MCLs mentioned in the Stage 1 DBP Rule. However, it obligates water treatment plants to assign new sampling locations along the distribution system in order to monitor THMs and HAA5 concentrations at the regions that are anticipated to contain the highest levels of DBPs [40].

While the formation of various bromine containing by-products in conventional ozonation systems has been studied [66-68], the formation of such disinfection by-products in a hybrid ozonation-membrane filtration has not been previously investigated. Hence, it is crucial to study bromate formation under various operating conditions in such hybrid systems. In this study, the effect of pH, inlet ozone mass injection rate, initial bromide concentration, and membrane molecular weight cut off on bromate formation in a membrane filtration–ozonation system was investigated.

Table 1- Drinking water regulations and guidelines for DBPs.

Regulations/ Guidelines	Year	MCL (mg/L)										
		TTHMs				HAA5					Bromate	Chlorite
		TCM	BDCM	DBCM	TBM	MCA	DCA	TCA	MBA	DBA		
WHO Guidelines	2006	0.30	0.06	0.10	0.10	0.02	0.05	0.20	---	---	0.01	0.70
Ontario Safe Drinking Water Act	2002	0.10				---					0.01	---
Canadian Drinking Water Quality	2010	0.10				0.08					0.01	1.00
USEPA, Stage 1 D/DBP Rule	1998	0.08				0.06					0.01	1.00
European Union Regulations	1998	0.10				---					0.01	---

### 1.3.2. Theory & Background

DBPs are formed as a result of the reaction of disinfectants with DBP precursors. The quality (type) and quantity of produced by-products depend on water characteristics such as TOC, pH, temperature, alkalinity, NOM and bromide content. Moreover, parameters such as disinfectant type and dosage and contact time are determining factors. NOM commonly serves as the organic precursor and bromide ( $\text{Br}^-$ ), and iodide ( $\text{I}^-$ ) act as important inorganic precursors [41,42].

The most frequently reported type of chlorination DBPs are THMs, with TCM and BDCM as the first and second most dominant species, respectively. HAAs are the second predominant group, with DCA and TCA being the first and second most frequently occurring species [42]. Several strategies have been proposed to minimize chlorination by-products formation, a summary of which is presented below:

I- Removal of precursors to chlorination DBPs, which are known to be dissolved NOM present in the water body. Strategies including activated carbon adsorption, ion exchange or enhanced coagulation process can be employed prior to chlorination to eliminate a portion of NOM and precursors [43-46]. However, such methods are costly due to the large amount of adsorbent consumed or coagulant required and also the large volumes of sludge produced during coagulation.

II- Reduction in the chlorine dosage or detention time, which is usually impractical, since a minimum chlorine residuals needs to be maintained in the

distribution system to prevent microbial regrowth along the pipeline. Therefore, dosage and exposure time is, to a large extent, dictated by regulatory requirements and water quality.

III- Removal of DBPs after formation. Air stripping can be used to eliminate semi-volatile constituents such as THM from water. Activated carbon filters can also remove these harmful compounds via adsorption. Reverse osmosis and or nanofiltration are other methods by which by-products could be filtered out from water. Nevertheless, these strategies are inefficient, since any remaining NOM will react with residual chlorine along the distribution system to regenerate DBPs [46,47].

IV- The last and the most promising method is to use an alternative and less troublesome disinfectant which can in part reduce the concentration of chlorination DBP precursors and also the demand for primary disinfectant. Ozone, which is known to be far stronger than common water disinfectants and can bring about several side advantages (see Section 2.2) was introduced to be an excellent alternative for water disinfection. Generally speaking, the ranking of various water disinfectants with respect to their oxidizing strength can be expressed as follows [6,33]:



However as mentioned earlier, ozone lacks an essential property which restricts its application as a primary disinfectant. According to the rate constants reported in the literature for the reaction of ozone with a variety of compounds, and depending

on the water quality, the half-life of ozone in aqueous solutions is short (mostly less than one hour) [48-50]. Hence, due to lack of persistent ozone residuals, the need for chlorination as a final disinfection step still persists [31]. Therefore, in the context of studying DBP formation, the impact of ozonation/membrane filtration on the precursors of chlorination DBPs needs to be evaluated.

The chemistry of ozone in aqueous solutions and its health effects are complicated. Reactions with ozone are largely dose and pH dependent, and hence the magnitude of by-products formed under various conditions will vary greatly. Nevertheless, investigations indicate that ozonation by-products overall appear to be less harmful compared to those produced during chlorination [25,26].

Ozone is an electrophile and has a high selectivity. Due to its dipolar structure, ozone preferentially reacts with unsaturated bonds including double bonds and activated aromatic systems and leads to a splitting of the bond. Therefore, the presence of electron-donating groups favours oxidation by ozone, whereas electron-withdrawing groups may exert an opposite effect. Ozone will react faster with certain types of aromatic compounds, e.g. those carrying electron supplying substituents such as the hydroxyl group. If there are no such substituents or if electron withdrawing groups such as chlorine are present, the rate of ozonation is much slower. In general, the ionized or dissociated forms of organic compounds react much faster with ozone than the neutral (non-dissociated) forms [13,25,51].

The reaction of ozone with organic and inorganic compounds present in water is a complicated process and happens via a series of chain reactions. In general,

these reactions proceed through two pathways, which are referred to as direct and indirect reactions. In general, ozone reacts with NOM to form simpler compounds with lower molecular weights and higher polarities. The importance of distinguishing between the different ozonation pathways lies in the different types of products that they may lead to [27]. As opposed to indirect reactions, the direct reactions of ozone with organic compounds are usually selective reactions happening at relatively slower rates. Generally speaking, the direct pathway is important if the indirect pathway is inhibited [25,52]. Direct ozonation of compound M can be stated by the following general equation:



Indirect reactions involve the contribution of secondary oxidants, which are generated as a result of ozone decomposition [25,27,53]. The most important secondary oxidants that are produced by ozone decomposition are hydroxyl radicals ( $HO^\bullet$ ), which are much stronger oxidants than ozone and react rapidly and non-selectively with nearly all electron-rich organic compounds [52,54,55].



Ozone decomposition and hydroxyl radical formation proceed through a series of reactions, which can be divided into two principal mechanisms:

I- Self-decomposition (Auto-decomposition):

Ozone self-decomposition occurs through a chain of complicated reactions and initiators such as hydroxide ion ( $\text{OH}^-$ ) can significantly contribute to this process [56]. Ozone decomposition in pure water has been studied by several researchers and so far numerous pathways have been presented, a collection of which is presented in Table 2 [54,57-61]. The overall stoichiometry of the process, which yields hydroxyl radicals, can be written as follows:



## II- Solute-induced decomposition:

A variety of organic solutes including humic acids, alcohols and also inorganic solutes such as ferrous ion ( $\text{Fe}^{2+}$ ) can react with  $\text{O}_3$  to initiate the ozone decomposition process. Therefore, such compounds that can start the ozone decomposition chain are referred to as initiators, and in general, the type and concentration of NOM in natural waters can considerably influence the ozone decomposition and its transformation into hydroxyl radicals. After the decomposition process is initiated,  $\cdot\text{OH}$  will be generated and the continuity and speed of the process relies on the presence of promoters such as ozone molecule itself that can convert  $\cdot\text{OH}$  into highly selective  $\text{O}_2\cdot^-$ . On the other hand, many inorganic and organic substances including bicarbonate and carbonate can react with hydroxyl radicals and thus remove them from the cyclic process. By such mechanism these compounds will scavenge  $\cdot\text{OH}$  and terminate the chain reaction.

Such compounds that act as obstacles to ozone decomposition are referred to as chain inhibitors [58,60,62,63].

Table 2- Reactions occurring during ozone self-decomposition [64].

Reaction	Reaction rate constant	
	constant	unit
$O_3 + OH^- \rightarrow HO_2^\bullet + O_2^- \bullet$	70	$M^{-1} s^{-1}$
$HO_2^\bullet \rightleftharpoons O_2^- \bullet + H^+$	$pK_a = 4.8$	–
$HO_2^\bullet \rightarrow O_2^- \bullet + H^+$	$3.2 \times 10^5$	$s^{-1}$
$O_2^- \bullet + H^+ \rightarrow HO_2^\bullet$	$2.0 \times 10^{10}$	$M^{-1} s^{-1}$
$O_2^- \bullet + O_3 \rightarrow O_3^- \bullet + O_2$	$1.6 \times 10^9$	$M^{-1} s^{-1}$
$HO_3^\bullet \rightleftharpoons O_3^- \bullet + H^+$	$pK_a = 8.2$	–
$HO_3^\bullet \rightarrow O_3^- \bullet + H^+$	$3.3 \times 10^2$	$s^{-1}$
$O_3^- \bullet + H^+ \rightarrow HO_3^\bullet$	$5.2 \times 10^{10}$	$M^{-1} s^{-1}$
$HO_3^\bullet \rightarrow HO^\bullet + O_2$	$1.1 \times 10^5$	$s^{-1}$
$O_3 + HO^\bullet \rightarrow HO_2^\bullet + O_2$	$9.0 \times 10^5$	$M^{-1} s^{-1}$
$HO^\bullet + HO^\bullet \rightarrow H_2O_2$	$5.0 \times 10^9$	$M^{-1} s^{-1}$
$O_3^- \bullet + H^+ \rightarrow HO_3^\bullet$	$1.0 \times 10^{10}$	$M^{-1} s^{-1}$
$HO^\bullet + HO_3^\bullet \rightarrow H_2O_2 + O_2$	$5.0 \times 10^9$	$M^{-1} s^{-1}$
$HO_3^\bullet + HO_3^\bullet \rightarrow H_2O_2 + 2O_2$	$5.0 \times 10^9$	$M^{-1} s^{-1}$
$HO_3^\bullet + O_2^- \bullet \rightarrow OH^- + 2O_2$	$1.0 \times 10^{10}$	$M^{-1} s^{-1}$
$H_2O_2 \rightleftharpoons HO_2^- + H^+$	$pK_a = 11.6$	–
$H_2O_2 \rightarrow HO_2^- + H^+$	$4.5 \times 10^{-2}$	$s^{-1}$
$HO_2^- + H^+ \rightarrow H_2O_2$	$1.0 \times 10^{10}$	$M^{-1} s^{-1}$
$O_3 + HO_2^- \rightarrow HO^\bullet + O_2^- \bullet + O_2$	$2.8 \times 10^6$	$M^{-1} s^{-1}$
$O_3 + H_2O_2 \rightarrow H_2O + \dot{O}_2$	$6.5 \times 10^{-3}$	$M^{-1} s^{-1}$
$HO^\bullet + H_2O_2 \rightarrow HO_2^\bullet + H_2O$	$2.7 \times 10^7$	$M^{-1} s^{-1}$
$HO^\bullet + HO_2^- \rightarrow O_2^- \bullet + H_2O$	$7.5 \times 10^9$	$M^{-1} s^{-1}$

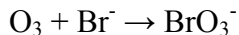
Humic substances are one of the main constituents of dissolved organic matter in natural waters and are produced by decay and leaching of organic debris. Ozone can break down humic substances, and transform them to non-humic substances [26,27]. Humic substances are the most important precursors of chlorination by-products. Therefore, by such mechanism ozone contributes to destruction of the chlorination precursors and reduces the risk of THM and HAA formation [32]. Hence, it is suggested that, ozonation can be employed to control and suppress the formation of chlorination by-products. Nevertheless, the ozonation mechanism is pH dependent and it is reported that ozone is more effective for the removal of precursors at low pHs [26]. As pH decreases, the concentration of  $\text{OH}^-$  in water decreases. Considering that  $\text{OH}^-$  is a very important initiator of ozone decay process, pH reduction will hinder ozone decomposition and hence ozone becomes more stable at low pHs. As a result, less hydroxyl radicals will be generated and in turn, the indirect pathway will be suppressed.

Usually under acidic conditions (pH less than about 4) the direct pathway is dominant, while at pH greater than about 10 the indirect pathway is the governing mechanism. At pH about 7 both direct and indirect pathways could be important [25,61]. Moreover, because of the high reactivity of OH radicals, the oxidation of a particular compound M by OH radicals will occur in competition with the oxidation of all scavengers, such as carbonate ( $\text{CO}_3^{2-}$ ) and bicarbonate ( $\text{HCO}_3^-$ ). Therefore, the presence of  $\cdot\text{OH}$  scavengers can also favour the direct pathway [52,53,55].

Aside from the impact of ozone on DBPs formation during post chlorination, ozone itself can produce a number of DBPs, some of which can be of health concern. Ozonation DBPs can be divided into two principal categories:

I- Organic by-products: As a result of the reaction of ozone with natural organic compounds, a number of organic by-products including aldehydes, ketones, carboxylic acids, and alcohols are generated, some of which are recognized to be mutagenic [108,109]. Humic substances, which consist of humic acids and fulvic acids, are again the main precursors of ozonation organic DBPs. Fulvic substances have generally lower aromatic contents and molecular weights than humic substances. Hence, humic acids are believed to be more reactive with ozone than are fulvic acids. In addition, the production of some chlorination DBPs has reported to be relatively higher upon chlorination of humic fraction as compared to that of fulvic fraction [10,42].

II- Inorganic by-products: Among the inorganic by-products of ozonation, bromate ( $\text{BrO}_3^-$ ), which is formed during the ozonation of bromide containing waters, is the main constituent of concern [65], which, as stated before, has been determined to be a human carcinogen and is regulated by drinking water guidelines [37,66,67]. As it is shown in Table 3, molecular ozone can directly react with bromide ion ( $\text{Br}^-$ ) present in natural waters via a number of steps to form bromate ion [6,68,69], and the overall reaction of the process can be written as follows:



However, the actual mechanism is much more complicated and involves a combination of series and parallel reactions, which include both direct and indirect ozonation pathways [42,59,62,70-72]. The reactions and the pertinent rate constants for the hydroxyl radical pathway are presented in Table 4. von Gunten et al., [66] also presented a diagram for bromate formation during the ozonation of bromide containing waters. This diagram, which is shown in Figure 3, involves both molecular ozone and hydroxyl radical reactions

Table 3- Reactions and rate constants involved in bromate formation via molecular ozone pathway [73].

Reaction	k or pKa (20° C)
$O_3 + Br^- \rightarrow O_2 + BrO^-$	$160 M^{-1}s^{-1}$
$O_3 + BrO^- \rightarrow 2O_2 + Br^-$	$330 M^{-1}s^{-1}$
$O_3 + BrO^- \rightarrow BrO_2^- + O_2$	$100 M^{-1}s^{-1}$
$O_3 + HOBr \rightarrow BrO_2^- + O_2 + H^+$	$\leq 0.013 M^{-1}s^{-1}$
$BrO_2^- + O_3 \rightarrow BrO_3^- + O_2$	$>10^5 M^{-1}s^{-1}$

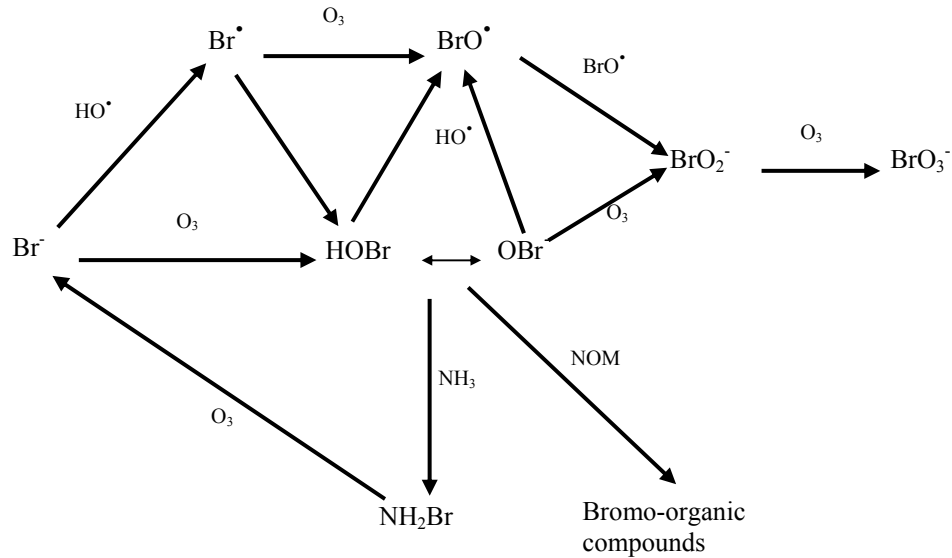


Fig. 3- Bromate formation diagram during ozonation of  $\text{Br}^-$  containing waters. Adapted from [66].

It is reported that low levels of bromide ( $<20 \mu\text{g/L}$ ) are not troublesome in terms of bromine-derived by-products formation, however for bromide levels above about  $50 \mu\text{g/L}$ , the concentration of bromate formed during ozonation may exceed the allowable concentration ( $10 \mu\text{g/L}$ ). If both NOM and bromide are present, several bromo-organic by-products such as bromoform, bromopicrin, dibromoacetonitrile, bromoacetone, bromoacetic acid, bromoalkanes, bromohydrins could also be formed. These are mostly formed by the reaction of hypobromous acid (HOBr, which is a product of the reaction between bromide and ozone) with NOM [33,68,76].

Table 4- Reactions and rate constants involved in bromate formation via hydroxyl radical pathway.  $k_+$ , forward reaction;  $k_-$ , backward reaction;  $K$ , equilibrium constant [74,75].

reaction	$k_+$ , $k_-$ , or $K$
$\text{Br}^- + \cdot\text{OH} \rightleftharpoons \text{BrOH}^-$	$10^{10} \text{ M}^{-1} \text{ s}^{-1}, 3.3 \times 10^7 \text{ s}^{-1}$
$\text{BrOH}^- \rightarrow \text{Br}\cdot + \text{OH}^-$	$4 \times 10^6 \text{ s}^{-1}$
$\text{Br}\cdot + \text{OH}^- \rightarrow \text{BrOH}^-$	$1.3 \times 10^{10} \text{ M}^{-1} \text{ s}^{-1}$
$\text{BrOH}^- + \text{H}^+ \rightarrow \text{Br}\cdot + \text{H}_2\text{O}$	$4.4 \times 10^{10} \text{ M}^{-1} \text{ s}^{-1}$
$\text{BrOH}^- + \text{Br}^- \rightarrow \text{Br}_2^- + \text{OH}^-$	$2 \times 10^8 \text{ M}^{-1} \text{ s}^{-1}$
$\text{Br}\cdot + \text{Br}^- \rightleftharpoons \text{Br}_2^-$	$10^{10} \text{ M}^{-1} \text{ s}^{-1}, 10^5 \text{ s}^{-1}$
$\text{Br}_2^- + \text{Br}_2^- \rightarrow \text{Br}_3^- + \text{Br}^-$	$2 \times 10^9 \text{ M}^{-1} \text{ s}^{-1}$
$\text{Br}_3^- \rightleftharpoons \text{Br}_2 + \text{Br}^-$	$8.3 \times 10^8 \text{ s}^{-1}, 10^{10} \text{ M}^{-1} \text{ s}^{-1}$
$\text{Br}_2 + \text{H}_2\text{O} \rightleftharpoons \text{HOBr} + \text{H}^+ + \text{Br}^-$	$5.8 \times 10^{-9} \text{ M}^2$
$\text{HOBr} \rightleftharpoons \text{OBr}\cdot + \text{H}^+$	$1.58 \times 10^{-9} \text{ M}$
$\text{Br}_2^- + \text{OBr}^- \rightarrow \text{BrO}\cdot + 2\text{Br}^-$	$8 \times 10^7 \text{ M}^{-1} \text{ s}^{-1} ?$
$\text{Br}\cdot + \text{OBr}^- \rightarrow \text{BrO}\cdot + \text{Br}^-$	$4 \times 10^9 \text{ M}^{-1} \text{ s}^{-1}$
$\cdot\text{OH} + \text{OBr}^- \rightarrow \text{BrO}\cdot + \text{OH}^-$	$4.5 \times 10^9 \text{ M}^{-1} \text{ s}^{-1}$
$\cdot\text{OH} + \text{HOBr} \rightarrow \text{BrO}\cdot + \text{H}_2\text{O}$	$2 \times 10^9 \text{ M}^{-1} \text{ s}^{-1}$
$2\text{BrO}\cdot + \text{H}_2\text{O} \rightarrow \text{OBr}^- + \text{BrO}_2^- + 2\text{H}^+$	$5 \times 10^9 \text{ M}^{-1} \text{ s}^{-1}$
$\text{BrO}\cdot + \text{BrO}_2^- \rightarrow \text{OBr}^- + \text{BrO}_2$	$3.4 \times 10^8 \text{ M}^{-1} \text{ s}^{-1}$
$\text{Br}_2^- + \text{BrO}_2^- \rightarrow \text{OBr}^- + \text{BrO}\cdot + \text{Br}^-$	$8 \times 10^7 \text{ M}^{-1} \text{ s}^{-1}$
$\cdot\text{OH} + \text{BrO}_2^- \rightarrow \text{BrO}_2 + \text{OH}^-$	$1.9 \times 10^9 \text{ M}^{-1} \text{ s}^{-1}$
$\cdot\text{OH} + \text{BrO}_2 \rightarrow \text{BrO}_3^- + \text{H}^+$	$2 \times 10^9 \text{ M}^{-1} \text{ s}^{-1}$
$\text{BrO}_2 + \text{BrO}_2 \rightleftharpoons \text{Br}_2\text{O}_4$	$1.4 \times 10^9 \text{ M}^{-1} \text{ s}^{-1}, 7 \times 10^7 \text{ s}^{-1}$
$\text{Br}_2\text{O}_4 + \text{OH}^- \rightarrow \text{BrO}_3^- + \text{BrO}_2^- + \text{H}^+$	$7 \times 10^8 \text{ s}^{-1}$

Furthermore, the ozonation of water in the presence of the bromide ion can even lead to an increase in the concentration of chlorination DBPs. This happens on account of the reaction of chlorine with bromo-organic compounds upon final chlorination [6,77]. Moreover, the bromide ion can participate in the reaction between NOM and chlorine to form various by-products that contain a combination of chlorine and bromine. Chlorine in the form of hypochlorous

acid/hypochlorite ion ( $\text{HOCl}/\text{OCl}^-$ ), can react with the bromide ion and oxidize it to the hypobromous acid/hypobromite ion ( $\text{HOBr}/\text{OBr}^-$ ). Hypochlorous acid and hypobromite acid will react collectively with NOM to form chlorinated DBPs, including THMs, HAAs, haloketones, and chloropicrin [42].

So far, a brief summary regarding major disinfection by-products, their formation mechanisms and governing factors has been presented. In the following section, a brief review of the research that has been previously carried out on the chlorination and ozonation DBPs and the respective findings are presented.

### **1.3.3. Historical perspective**

Several researchers have investigated the ozonation process, pertinent disinfection by-products, and the influence of various parameters and operational conditions on the process. However, few studies on the hybrid ozonation/membrane filtration with the aim of DBPs analysis have been carried out.

Karnik et al., 2005 [10] developed a hybrid ozonation and ceramic membrane filtration system, for which they examined the removal of NOM and the formation of DBPs. They achieved up to 50% reduction in the dissolved organic carbon (DOC) concentration. Furthermore, they observed that humic substances, which are the main precursor of chlorination by-products, were transformed to non-humic substances, which are less reactive with chlorine. This resulted in the reduction of TTHM and HAA formation by up to 80% and 65%, respectively. They indicated that the hybrid ozonation/filtration system produced lower

concentrations of aldehydes, ketones, and ketoacids as compared to ozonation alone. It was also reported that pH reduction can decrease the concentration of TTHMs and HAAs formed following chlorination. Moreover, the concentration of aldehydes and ketones decreased by about 50% as pH was lowered from 8.2 to 7.0.

In another investigation, Karnik et al., 2005 [78,79] used ceramic membranes coated with iron oxide nanoparticles ( $\text{Fe}_2\text{O}_3$ ). By taking advantage of catalytic ozonation/membrane filtration, they were able to reduce the concentration of dissolved organic carbon by more than 85%. In addition, the concentration of chlorination by-products, including TTHMs and HAAs, were decreased by up to 90% and 85%, respectively. As compared to the results of their earlier work, catalytic ozonation considerably improved the elimination efficiency of these two harmful chlorination by-products. Furthermore, they reported that ozonation using coated membrane can reduce the concentration of ozonation by-products including aldehydes, ketones, and ketoacids by more than 50% as compared to results obtained with the uncoated membranes. This implies the important role of iron oxide in the removal of these compounds. They suggested that hydroxyl or other radicals formed on the iron oxide coated membrane surface due to ozone decomposition promoted the elimination of NOM, and therefore suppressed DBP formation.

Kusakabe et al., [80] used an advanced oxidation process (AOP) including ozonation/ultraviolet (UV) irradiation to study chlorination DBP formation. They

found that ozonation coupled with UV irradiation can more efficiently reduce the potential for chlorination by-product formation as compared to that of ozonation alone. This phenomenon was attributed to fast and non-selective oxidation of dissolved organic compounds by hydroxyl radicals, which are formed by the photochemical decomposition of ozone. These results were verified by other researchers [81].

In another investigation, Chin et al., 2005 [82] used an advanced oxidation process to remove precursors of chlorination DBPs from raw surface water. They observed that the hybrid system is more effective than either ozonation or UV treatment alone in terms of mineralization and removal of organic compounds. Their experimental results exhibited that the ozonation/UV irradiation system mineralized up to 50% of the total organic carbon (TOC) and also reduced the formation potential for THMs and HAAs by about 80% and 70%, respectively.

The review of the previously accomplished research and the obtained results reveals that, several investigations with the aim of control, suppression of the formation of or the removal of chlorination and ozonation organic DBPs in ozonation/membrane filtration configurations have been carried out and some recommendations and strategies regarding minimization of such by-products have been proposed. Among research conducted in this field, ceramic membrane owing to its catalytic nature has shown very promising results in terms of ozonation organic by-products and post chlorination by-product reduction. However, bromate formation and minimization in such hybrid systems has not been extensively

studied and very few investigations in this regard have been carried out. Hence, it is crucial to study DBP formation in hybrid membrane/ozonation systems.

#### **1.3.4. Strategies to Cope with $\text{BrO}_3^-$ Formation**

Bromate forms via a complicated and multistage mechanism, which is initiated by the direct reaction of ozone and bromide ion. The initial reaction is followed by hydroxyl radical participation [62]. Therefore, both direct and indirect pathways play roles. However, several researchers have pointed out that the contribution of  $\cdot\text{OH}$  is more profound compared to that of ozone. Referring to Tables 3 and 4 the reaction rate constants ( $K$ ) for the hydroxyl radical pathway are appreciably greater than that of those involving molecular ozone, therefore it is expected that the contribution of the indirect pathway is significant. It is reported that almost 70% of bromate formation is through  $\cdot\text{OH}$  mediated oxidation reactions (the indirect pathway) and the remaining 30% depends on the direct pathway [59,62].

The type and concentration of NOM present in the water, ozone dosage, pH, and temperature can influence ozone stability and decay, and can therefore, also affect the conversion of bromide to the bromate ion [65]. According to the scheme shown in Figure 3, every process that can retard or interrupt any of intermediate routes leading to bromate formation, can in fact assist to suppress its formation. Based on such theory, various approaches can be employed to cope with this water treatment side-product. These strategies can be classified into three main categories, including Prevention, Suppression and Removal techniques:

I- Prevention: In dealing with environmental pollution, the wisest method is to prevent environmental pollution from happening in the first place and to confine the pollutant source. In the case of bromate, the essential precursor is the bromide ion that can be introduced to drinking water supplies through salt water intrusion and anthropogenic activities, such as coal mining [6,62,65,77] and hydrofracking. This option, which leads to water resources quality management and control, is outside of the scope of this research.

Another alternative that one may consider is the elimination of bromide from target water before contacting with ozone. This can be accomplished by using suitable adsorbents such as activated carbon and or ion exchange filters [45]. However, these methods are essentially impractical for most drinking waters. Considering the very large volumes of water that are treated per day, a large amount of activated carbon or resin would be required, which would be costly. In addition, the competition among the ions present in water (including carbonate, and bicarbonate ions which are normally available in water at much greater concentrations than the bromide ion) for ion exchange sites reduces the efficiency of bromide removal by activated carbon. Additionally, the disposal of the sludge and brine that would be generated would add to this problem and cost. Moreover, natural water includes a variety of ions and organic matter that may sorb to reactive surfaces of adsorbents, and hence compete with bromide and interfere with the adsorption/removal process. Therefore, this method does not seem to provide an economical solution especially in the case of waters with a relatively

high bromide content, or with high concentrations of multivalent anions, which would preferentially compete for sites on ion exchange resins and decrease the efficacy of the process for bromide removal.

II- Suppression: In most cases, environmental engineers have to deal with situations in which the environmental medium of concern is already contaminated and aside from source control, actions have to be taken to rectify the existing situation. Once bromide has entered a water body, the next priority is to minimize and suppress bromate formation during ozonation practice. A brief summary of methods in this category has been presented below:

- pH depression: The  $pK_a$  of the reversible reaction between the hypobromite ion and its conjugate acid [  $\text{HOBr} \leftrightarrow \text{OBr}^-$  ] is 8.8 at  $20^\circ\text{C}$ . Therefore referring to Figure 3, at pHs lower than 8.8, equilibrium shifts toward left and the production of HOBr is favoured. Hence, due to lack of  $\text{OBr}^-$ , bromate formation will be slowed [68, 83].

In addition to this fact, as pH decreases, ozone stability in water increases and less  $\cdot\text{OH}$  is generated [33,75]. Given the fact that  $\cdot\text{OH}$  plays a significant role in the process of bromate formation, pH depression can effectively retard the process. For the time being, pH reduction is one of the most reliable strategies for controlling bromate formation, however this method is extremely costly, since pH has to be increased again before pumping water into the distribution system, and it is associated with the consumption of a large amount of acid and base. Moreover, high doses of acid and base will increase the total dissolved solid (TDS) concentration in the water [6].

-  $\cdot\text{OH}$  scavenging ( $\text{HCO}_3^-$ ,  $\text{CO}_3^{2-}$ ): By adding bicarbonate/carbonate to water, the half-life of ozone can be increased. At concentrations of a few millimoles per liter of bicarbonate, the decay rate of ozone can be decreased by about a factor of ten or more and the stability of ozone can be increased. Scavengers can react with hydroxyl radicals, eliminate them and thus slow down the bromate formation through suppression of the hydroxyl radical pathway [52,53,55]. However, this method requires high alkalinity, which limits its application.

- Ammonia dosing: As it is indicated in Figure 3,  $\text{NH}_3$  will act as a sink for  $\text{HOBr}$  and will transform it back to  $\text{Br}^-$ . By this mechanism, ammonia removes  $\text{HOBr}$  from the cycle and in turn hinders the formation of  $\text{OBr}^-$  and  $\text{BrO}^\cdot$ , which results in less  $\text{BrO}_3^-$  generation [70,73,75,84]. Tanaka et al. 2002 [69] showed that ammonia in fact induces a lag in bromate formation and as long as ammonia is still available, bromate formation will be suppressed, indicating that the reaction of ammonia with  $\text{HOBr}$  is very fast. This strategy also has a major drawback, which is the production of nitrite ( $\text{NO}_2^-$ ) that is formed as ozone reacts with ammonia. Nitrite can cause methemoglobinemia, which can be fatal especially to infants [1].

- Multistage ozonation: This method might reduce bromate concentration, but it brings about some additional troubles. Extra ozone contactors need to be built and more land space is required, which increases installation costs.

III- Removal: The last option is to remove bromate after it is formed. Such methods include:

- Activated carbon and ion exchange resin: Activated carbon and ion exchange filters can be used to remove ions such as bromate from water [85,65]. However, as explained earlier these methods have such drawbacks as high cost and competition between the target ion and background electrolytes. As such, these strategies are inefficient.

- Membrane filtration (RO / NF): Reverse osmosis and nanofiltration membranes can effectively exclude the bromate ion from finished water, however their application is unfavourable due to extensive membrane fouling and high costs associated with elevated operating pressure required with these types of membranes.

- Chemical reduction: Reducing agents such as ferrous ion ( $\text{Fe}^{2+}$ ) can be added to water to reduce bromate to bromide [33,42,86,87]. However, ferrous ion would promptly react with ozone and produce the insoluble ferric hydroxide,  $\text{Fe}(\text{OH})_3$ , which would deposit readily on the membrane surface and cause fouling problems. Moreover, some portion of the  $\text{Fe}^{2+}$  may pass through filtration process and cause aesthetic problems in the finished water.

### **1.3.5. Objectives & Scope of Research**

As already discussed, several methods have been suggested in the literature to cope with bromate formation during the ozonation process, however as a matter of fact none of them are efficient or economically practical for large-scale drinking water production. Therefore, the main objective of the proposed research project is to investigate the effects of important operating parameters including

inlet ozone mass injection rate, initial bromide concentration, membrane molecular weight cut off, membrane coating, hydroxyl radical scavenger, pH, and temperature on the formation of bromate, and organic by-products including TTHMs and HAAs. To achieve this goal, a hypothesis is suggested:

Ceramic membranes are made of a combination of metal oxides such as titanium dioxide ( $\text{TiO}_2$ ) and iron oxide ( $\text{Fe}_2\text{O}_3$ ), aluminum oxide ( $\text{Al}_2\text{O}_3$ ) and zirconium dioxide ( $\text{ZrO}_2$ ) that can act as catalysts to accelerate some chemical reactions in aqueous solutions. It has been shown that ozonation in conjunction with catalysts is more effective than ozonation or photocatalysis alone for decomposition and mineralization and thus elimination of several types of organic compounds [24,88]. A catalyst is defined as a substance which can act as a support for chemical reactions to happen. Catalysts can exert orienting effects to enable and accelerate the progress of a thermodynamically possible chemical reaction [24,110]. It is believed that these metal oxides can facilitate and promote ozone decomposition by catalytic reactions.

Catalytic decomposition of ozone occurs on the catalyst surface, and in case of ceramic membrane that is the membrane surface and pore walls. As the ozone decomposition rate increases, more hydroxyl radicals are produced. Hydroxyl radicals are very strong oxidants and will react rapidly with natural organic matter, which deposits on the membrane surface. By such mechanism, catalytic ozonation will lead to the quick destruction and removal of NOM, and subsequent elimination of foulants from membrane surfaces [79]. Due to greater efficiency of

the catalytic ozonation process, lower ozone dosages will solve fouling problems. By applying less ozone, exposure to ozone will decrease which in turn results in less bromate formation [62].

Another fact that is noteworthy is that  $\cdot\text{OH}$  is very short-lived. The second order rate constant for reaction of most of natural organic matter with  $\cdot\text{OH}$  is on the order of  $10^{10}$  L/mole $\cdot$ sec. For neutral to slightly basic pHs and typical  $\cdot\text{OH}$  concentrations found in ozonation processes, this yields a half-life for  $\cdot\text{OH}$  in the range of  $10^{-1}$  seconds [54,89]. Therefore, considering the diffusive and convective rates in water, hydroxyl radicals that are generated on the membrane surface are not expected to migrate very far from their origin. Therefore, they would react with the most available and reactive species in their vicinity, which are believed to be NOM attached to the membrane surface. Moreover, the catalyst will act as an adsorbent and organic compounds will adsorb onto its surface [24]. Therefore, due to the accumulation of NOM on the ceramic membrane surface (or catalyst surface), its high concentration would increase the reaction rate with  $\cdot\text{OH}$  as well as that with dissolved ozone.

Another point to make here is that the bromide ion, which is water-soluble, is likely to predominate in the bulk water, and not be sorbed to the membrane surface. Therefore compared to NOM it is relatively less available to  $\cdot\text{OH}$ , which is produced on the surface. Nevertheless, ozone that exists in the bulk water can react with coexisting bromide and produce bromate. However, as explained earlier, only 30% of bromate formation happens through the ozone pathway and

the remaining is by the hydroxyl radical pathway. In addition, at regular natural water pHs, the rate of ozone self-decomposition is much lower than the rate of catalytic ozone decomposition. This implies that the majority of ozone decomposition and  $\cdot\text{OH}$  formation would occur on the catalytic membrane surface rather than in the bulk water. Thereafter, the dominant portion of  $\cdot\text{OH}$  that is formed via catalytic decomposition will most likely react with NOM concentrated near the membrane surface. By such a mechanism,  $\cdot\text{OH}$  will be rapidly eliminated from water and will be mostly made inaccessible to bromide ions in the bulk water. This in all is believed to lead to a decrease in bromate formation in the hybrid ozonation/membrane filtration system.

## **Chapter 2: Ozone Mass Transfer in a Recirculating Loop Semibatch Reactor Operated at High Pressure**

### **2.1. Abstract**

The effects of water flow rate, mixing, gaseous ozone concentration, inlet gas flow rate, temperature, and pH on ozone hydrodynamics at high pressure were studied. Varying the cross flow rate had only a slight influence on the ozone mass transfer rates, indicating that sufficient mixing in the reactor was attained at the low flow rates used. The addition of an inline static mixer had a negligible effect on aqueous ozone concentrations in the reactor, suggesting that mixing was sufficient without the mixer. The dissolved ozone concentration increased with increasing gaseous ozone concentration and with the inlet gas flow rate. The dissolved ozone concentration decreased with increasing pH due to the greater rate of ozone decomposition at higher pH. Increasing the temperature resulted in a decrease in the ozone mass transfer. A model to describe the ozone mass transfer was developed. Good agreement between the model predictions and the experimental data was achieved.

**Keywords:** ozone, mass transfer, water treatment, ozonation, reactor design, gas transfer model

## 2.2. Introduction

The application of ozone for drinking water treatment began with the first full scale installation of an ozone system in Nice, France in 1906 and has increased dramatically over the last two decades as the costs for ozone generation have decreased and drinking water regulations have become more stringent (1-3). Ozone is a strong oxidant that can oxidize and decompose much of the natural organic matter present in surface waters (4, 5). This enables it to accomplish a number of treatment objectives (6-9), including, the:

- disinfection and reduction in disinfectant demand
- oxidation of organic compounds, and removal of taste, odour, and color compounds
- removal of the precursors of some chlorination by-products, including trihalomethanes (THMs)
- reduction in total organic carbon (TOC) levels by mineralization
- improved performance of coagulation through the transformation of natural organic matter (NOM) to smaller and more polar compounds, and
- oxidation of Fe(II) and Mn(II), allowing subsequent removal by precipitation.

In water treatment, ozone, commonly produced from air or oxygen gas, is introduced to the ozone contactors in the gas phase. The mass transfer of ozone gas to water plays a pivotal role in the effectiveness and performance of ozonation systems. Several researchers have studied ozone mass transfer and the effect of various operating parameters on the mass transfer coefficient of ozone (for

example, see (10-15)). Wu and Masten (16) developed a mathematical model for the mass transfer of ozone in a semibatch reactor, which was successfully employed to predict the ozone concentration profile in the reactor under various conditions. Chen et al. (17) studied the effect of reactor conditions on the ozone mass transfer coefficient for a hybrid ozonation-ceramic membrane system.

A number of researchers have combined ozonation with membrane filtration for drinking water treatment. They have reported that ozonation can be used in combination with membrane filtration in order to overcome fouling problems resulting from the deposition of natural organic matter present in natural waters on the membrane surface (18-22). In the hybrid ozonation-membrane system, aqueous ozone will react with organic material deposited on the membrane surface or attached to the pores walls, resulting in the degradation and removal of foulants from the membrane surface. This method allows continuous operation and eliminates the need for frequent membrane cleaning (5, 18-22). Karnik et al. (21), along with other researchers, including Schlichter et al. (20) and Mozia et al. (22), have demonstrated that maintaining a minimum aqueous ozone concentration in a hybrid ozonation-membrane system, enables continuous operation at relatively high permeate fluxes (more than 90% of the initial flux) and eliminates the need for other cleaning procedures. Karnik et al. (21) achieved nearly complete recovery of permeate flux using a hybrid ozonation/ceramic ultrafiltration membrane system, which was operated in a cross-flow configuration. Their experimental results suggest that flux enhancement is due

mainly to the oxidation of foulants by ozone and/or hydroxyl radicals (which are formed on the membrane surface due to ozone decomposition), and not the scouring effect of the gas bubbles.

Previous work on the hybrid ozonation-membrane system was conducted at pressures much lower than those typically used in ultrafiltration systems (19-22). In order to operate this system at pressures more typical of those used commercially, a high pressure ozone generator was developed in conjunction with Absolute Systems Inc., Canada. This is the first study of ozone mass transfer using static mixing at high pressure. In order to simplify the mass balance analysis, this study was conducted without the membrane filtration unit installed in the system; however, the employed configuration can be used in conjunction with membrane filtration in a cross-flow mode (21).

In the current study, the influence of operating parameters, including water flow rate, gaseous ozone concentration, inlet gas flow rate, temperature, and pH, on the ozone hydrodynamics were investigated. Moreover, the influence of inline static mixing on the ozone concentration profile was also examined. Static mixers can offer good mixing conditions with relatively low power demand. They are able to provide turbulent flow, which is desirable in terms of mass transfer efficiency at very low cross flow velocities (laminar flow regime). It has been shown by a number of researchers that the application of static mixers in systems operating at atmospheric pressures can enhance ozone dissolution in water and also improve the efficiency of water/wastewater disinfection using ozonation (23-26).

## **2.3. Materials and Methods**

### **2.3.1. Experimental Apparatus**

A schematic of the semibatch reactor used in these experiments is illustrated in Figure 1 (also see Fig. A1). The system was equipped with a high-pressure stainless steel tank with the maximum capacity of 5 L (Fig. A2). The tank was located in the recycle line to supply the system with the feed water. All tubing and connections were either Teflon® or 316-stainless steel, both of which are ozone resistant. Experiments were carried out at high pressure, and nitrogen gas was used to initially pressurize the system, which was designed to withstand pressures of up to 550 kPa (80 psi). A gear pump (Model 000-380, Micropump Inc., USA) was used to circulate the water in the loop. The water inside the tank was mixed as a result of the turbulence created by the jet of water recycled to the tank. The data showed that mixing conditions in the reactor were consistently reproduced.

Gaseous ozone was generated by a corona discharge ozone generator (Absolute Ozone AE15MC80P, Absolute System Inc., Canada) using pure oxygen gas (99.999%) from a pressurized cylinder. The pressure in the cylinder was sufficient to inject the ozone containing gas into the system. In all experiments, ozonated gas was first vented to a catalytic ozone destruction column until a constant ozone level in the inlet gas was obtained; afterwards, the gas was diverted into the system using a 3-way valve. The inlet gas flow rate was adjusted using a digital flow-controller (Model MC-500SCCM-D, Alicat Scientific Inc., USA) and ozone gas was introduced to the loop using a Swagelok

Tee fitting (Model SS-400-3, Swagelok, USA). The water flow mixed the injected gas and the feed water. A pressure regulator (Model KCB1F0A2A5P20000, Swagelok, USA) was mounted on the recycle tank for safety reasons and to regulate the pressure in the recirculation loop. Any off-gas from the system was destroyed either by passing the off-gas into the catalytic destruction column or by purging the off-gas through a potassium iodide (2% KI) solution.

A bleed line was installed in the recycle loop, which allowed for continuous sampling of the water. The bleed flow rate was regulated at 5.0 mL/min by a digital flow-controller (Model LC-50CCM-D, Alicat Scientific Inc., USA). To evaluate the effect of turbulent mixing of the gas and water phases on the ozone hydrodynamics, a number of experiments were carried out with and without a static mixer (1/4-34-SS Static Mixer, Koflo Co., USA), which was placed in line. A digital flow meter (Model L-5LPM-D, Alicat Scientific Inc., USA) and a digital pressure gauge (Model 2074, Ashcroft Inc., USA) were placed in the loop in order to monitor water flow rate and pressure within the system (see Figure 1).

### **2.3.2. Experimental Conditions**

In these studies, the effect of water flow rate (in the loop), inlet ozone gas concentration, temperature, pH, inlet gas flow rate, and mixing on the ozone hydrodynamics was examined. The initial water volume in the tank was 3 L. Distilled deionized water (DDI) was used in order to eliminate any interference exerted by impurities existing in the natural water. The pressure in the tank was set to 207 kPa (30 psi). In order to increase the stability of ozone, experiments were carried out

under acidic conditions (pH 3.0). To study the effect of pH on ozone mass transfer, experiments were also conducted at pH 6.0 and 8.0. The pH was adjusted by the addition of phosphoric acid ( $\text{H}_3\text{PO}_4$ ) and/or sodium hydroxide ( $\text{NaOH}$ ). Experiments were carried out at least in duplicate.

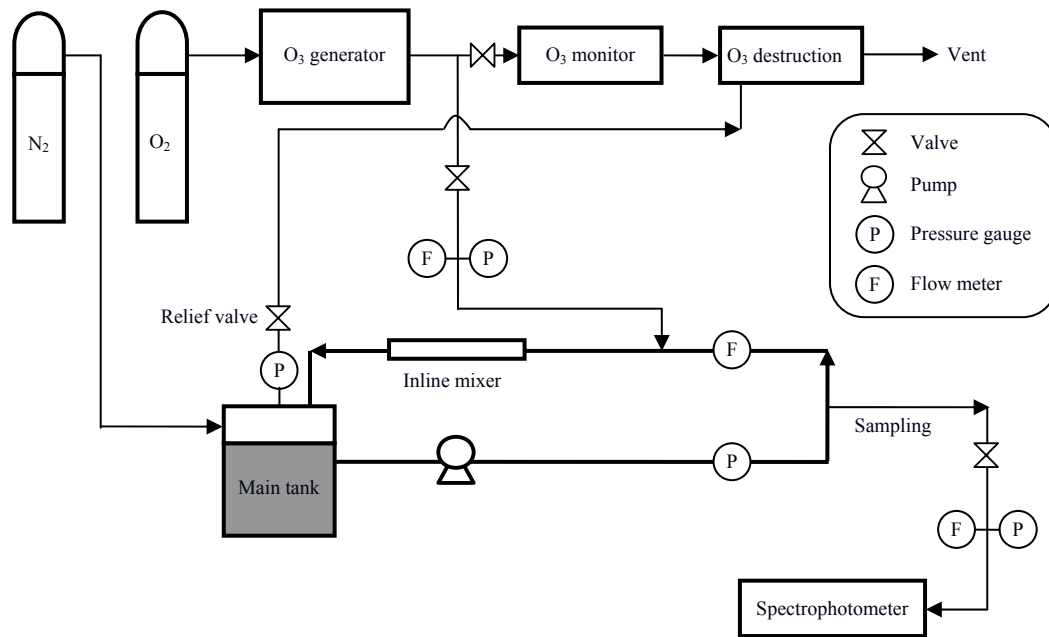


Fig. 1- Schematic of the experimental apparatus.

### 2.3.3. Analytical Methods

The aqueous ozone concentration in the bleed water was continuously measured using a UV/Vis spectrophotometer (Model 4054 LKB Biochrom, Pharmacia LKB Biochrom Ltd., UK) at a wavelength of 254 nm (3). The ozone concentration was calculated using Lambert-Beer's law, using an extinction coefficient of  $2950 \text{ M}^{-1}\text{cm}^{-1}$ , which was determined experimentally. The ozone concentration in the inlet gas was

continuously measured using a UV ozone monitor (Model 454H, Teledyne Instruments, USA). pH was measured using a pH meter.

## 2.4. Determination of the Ozone Mass Transfer Coefficient

To calculate the mass transfer coefficients using experimental data, a mathematical model was developed. Assuming that the system is a completely mixed semibatch reactor and considering the control volume depicted in Figure 2, the mass balance on ozone can be expressed as below:

$$\frac{d(CV)}{dt} = K_L a(C_s - C)V - CQ - kCV \quad (1)$$

where  $C = O_3$  concentration in the bulk water, mg/L;  $C_s =$  aqueous  $O_3$  concentration at equilibrium with the inlet  $O_3$  gas concentration ( $C_G$ ), mg/L;  $V =$  total volume of water in the system, L;  $t =$  time, min;  $K_L a =$  the overall mass transfer coefficient, 1/min;  $Q =$  sampling flow rate, L/min;  $k =$  first order rate constant for the loss of  $O_3$ , 1/min (27).

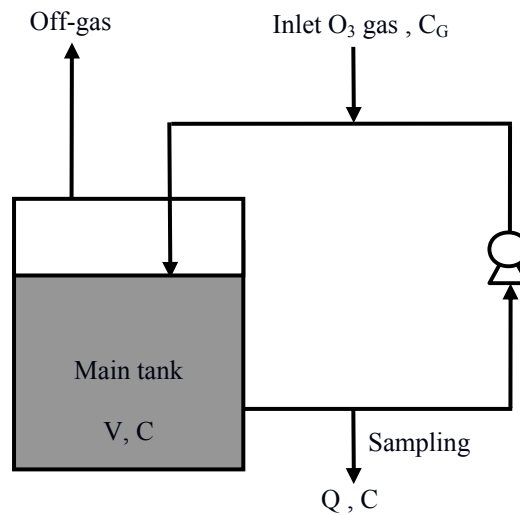


Fig. 2- Simplified control volume for modeling ozone mass transfer.

Since water is continuously leaving the system through the bleed line, the total volume of water gradually decreases with time. Considering that the bleed flow rate is constant throughout the experiments, the total volume of water at time,  $t$ , can be obtained by the following equation:

$$V = V_0 - Qt \quad (2)$$

where  $V_0$  = initial volume of water in the reactor, L. Taking the derivatives of both sides of Eq. 2 with respect to  $t$  yields:

$$\frac{dV}{dt} = -Q \quad (3)$$

It also can be written: 
$$\frac{d(CV)}{dt} = V \frac{dC}{dt} + C \frac{dV}{dt} \quad (4)$$

Substituting Eq. 3 into 4 results:

$$\frac{d(CV)}{dt} = V \frac{dC}{dt} - CQ \quad (5)$$

After substituting and rearranging, Eq. 1 can be expressed as:

$$\frac{dC}{dt} = K_L a (C_s - C) - kC \quad (6)$$

$$\frac{dC}{K_L a (C_s - C) - kC} = dt \quad (7)$$

Integrating from both sides of Eq. 7 from  $C=0$  to  $C$  and  $t=0$  to  $t$  yields the following mathematical model for the calculation of the dissolved ozone concentration in the system as a function of time.

$$C = \frac{K_L a C_s}{K_L a + k} (1 - e^{-(K_L a + k)t}) \quad (8)$$

At steady state, the ozone concentration in the system will not change with time, thus,  $dC/dt=0$ . Hence, after substitution into Eq. 6, the steady state ozone concentration in the reactor ( $C_{ss}$ ) is given by Eq. 9. It is noteworthy that  $C_{ss}$  is in fact the ozone concentration in the system when the ozone profile reaches a plateau (see Figures 3 to 8):

$$C_{ss} = \frac{K_L a C_s}{K_L a + k} \quad (9)$$

By combining Eq. 8 and 9 and after rearranging, the following expression is obtained:

$$\frac{C_{ss}}{C_s} \ln\left(\frac{C_{ss}}{C_{ss} - C}\right) = K_L a \cdot t \quad (10)$$

$C_s$  can be calculated using the Henry's law constant as a function of inlet ozone gas concentration ( $C_G$ ):

$$C_s = \frac{C_G}{H'} \quad (11)$$

where  $H'$  = dimensionless Henry's law constant. The Henry's law constants were estimated using the empirical model proposed by Roth et al. (27), which is valid over the temperature range of 3.5 to 60 °C and the pH range of 0.65 to 10.2.

$$H = 3.84 \times 10^7 [\text{OH}^-]^{0.035} \exp(-2428/T) \quad (12)$$

where  $H$  = Henry's law constant, atm/mole fraction;  $[\text{OH}^-]$  = hydroxide ion concentration, mole/L; and  $T$  = temperature, K. The Henry's law constant can be converted to a dimensionless constant using the following expression (28):

$$H' = \frac{V}{RT} H \quad (13)$$

where  $V$  = the molar volume of the water, L/mole, and  $R$  = the universal gas constant, 0.08205 (atm·L)/(mole·K). Table 1 shows the dimensionless Henry's law constants calculated using Eq. 12 and 13 for the various pH and temperature values investigated in this paper.

Table 1- Dimensionless Henry's law constants.

pH	3.0			6.0	8.0
Temperature (°C)	15	20	25	20	20
H'	2.63	2.98	3.37	3.80	4.46

According to Eq. 10,  $K_L a$  is the slope of the plot of  $\frac{C_{ss}}{C_s} \ln\left(\frac{C_{ss}}{C_{ss} - C}\right)$  against time. The analysis of our experimental results verifies the existence of a linear relationship as it is expressed by Eq. 10 (see  $R^2$  values in Tables 3 through 8).

## 2.5. Results and Discussion

### 2.5.1. Water Flow Rate

Experiments were conducted at water circulation flow rates of 0.17, 0.25, 0.5, and 1.0 L/min. The Reynolds numbers were calculated for different water flow rates. These were used to determine the flow regime in the membrane holder (see Table 2). As the cross flow velocity of water in the membrane holder increased, the flow regime changed from laminar to turbulent, which is expected to result in better mixing and contact between the liquid phase (water) and the gas bubbles in the system. Panda et al. (29) studied the impact of water flow rate on ozone mass

transfer in a tubular ozone reactor operated at relatively low pressure. They observed that for Reynolds numbers in the range of 55 to 166, mass transfer coefficients increase with increasing the circulation flow rate. Chen et al. (17) also found that mass transfer coefficient increases with increasing water flow rate inside a hybrid ozonation-membrane system operating at low pressure. However, it can be seen from Figure 3 that the influence of water flow rate on the ozone mass transfer rates within our experimental setup was relatively small. According to calculated mass transfer coefficients listed in Table 3, little improvement in the ozone mass transfer coefficients was obtained by increasing the circulation flow rate. Statistical analysis using the F test with  $\alpha=0.05$  (level of significance) also indicated that the mass transfer coefficients obtained at various water flow rates were not statistically different ( $F=2.66 < \text{critical value}=4.07$ ). This is consistent with the fact that even at low flow rates, the degree of mixing is sufficient to achieve optimal mass transfer.

Table 2- Water flow rates versus flow regime.

Q (L/min)	0.17	0.25	0.50	1.0
v (cm/sec)	10	15	30	60
Re	600	900	1800	3600
Flow regime	Laminar $\longleftrightarrow$ Turbulent			

Q: water flow rate ; v: cross flow velocity ; Re: Reynolds number

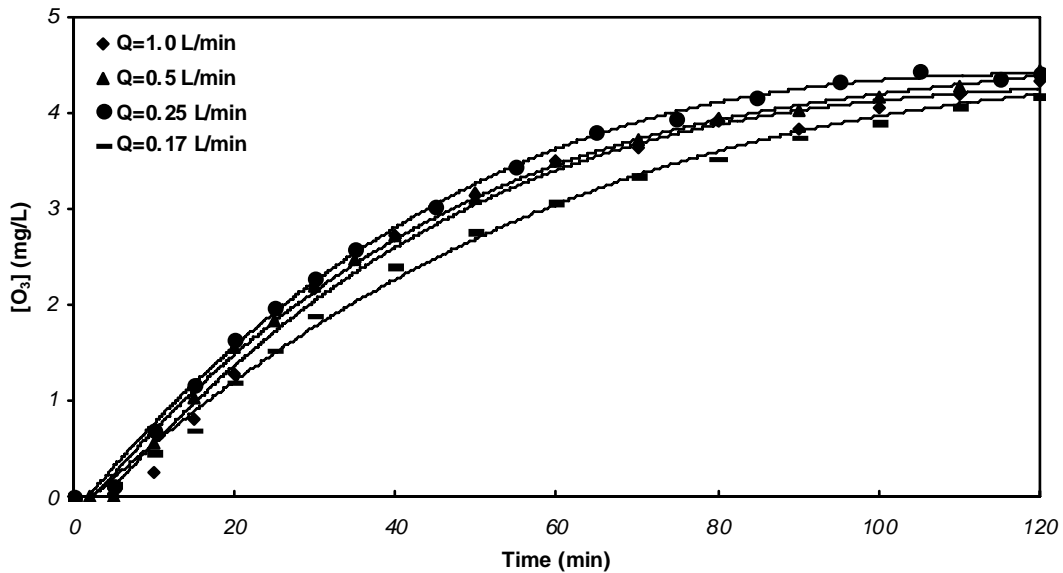


Fig. 3- Dissolved ozone concentration vs. time at various water flow rates. With mixer, gaseous ozone concentration 10 mg/L, inlet gas flow rate 75 mL/min, temperature 20 °C, pH 3.0, pressure 30 psi.

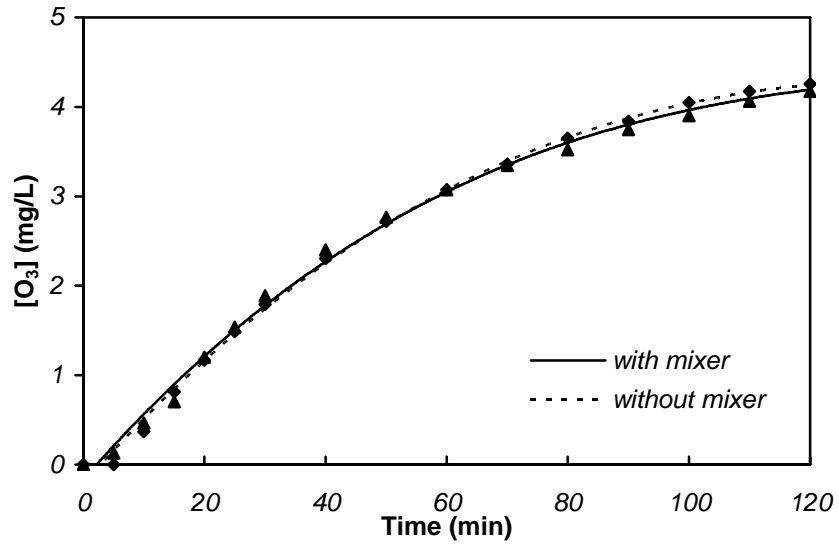
Table 3-  $K_{La}$  values calculated by modelling experimental results at various water flow rates.

Water flow rate (L/min)	0.17	0.25	0.50	1.00
$K_{La}$ (1/min)	0.0317	0.0354	0.0360	0.0357
$R^2$	0.97	0.98	0.99	0.98
Standard deviation	0.0019	0.0011	0.0018	0.0032

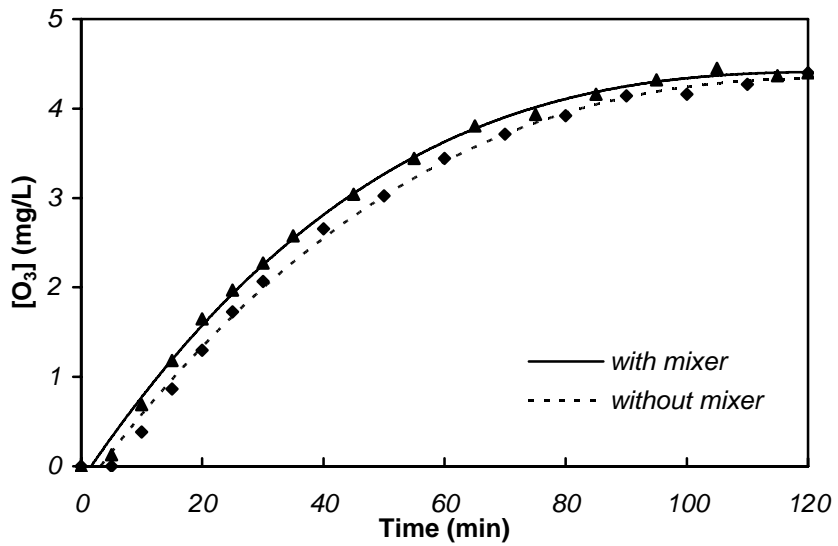
### 2.5.2. Inline Mixer

Inline static mixers have been shown to enhance gas transfer into water of ozone (30) and other gases (31). However, the energy dissipation in these system is significantly higher than in those without a mixer (31) resulting in higher

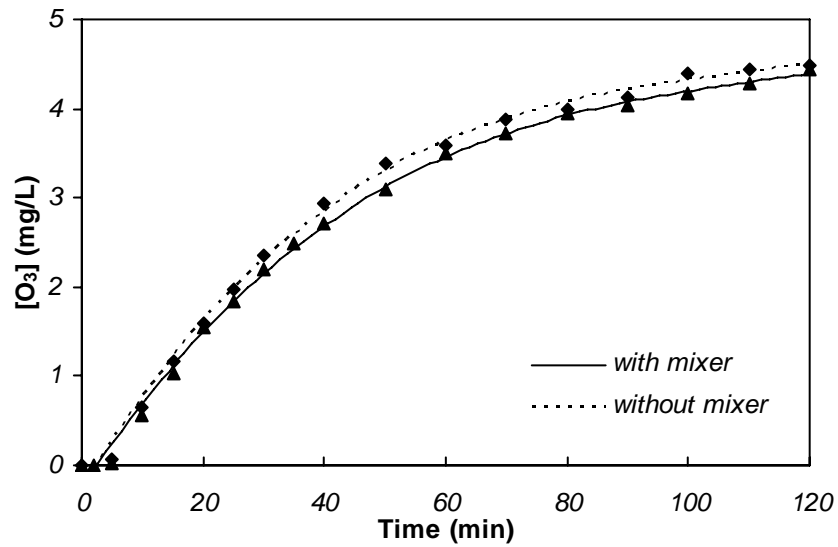
pumping costs. To assess the contribution of the inline tubular mixer to ozone mass transfer, a number of experiments were carried out with and without a static mixer. Figure 4 shows the effect of inline mixing on the mass transfer of ozone at various water flow rates. It is apparent from this figure that in this system, even at low water flow rates, there is little difference between the ozone profiles observed with and without the static mixer. As indicated in Table 4, for similar water flow rates, the  $K_L a$  values for the experiments with and without a mixer are very close. This suggests that, even when the static mixer was not installed, mixing in the system was sufficient and as a result, the additional turbulence created by the mixer did not significantly improve the mass transfer efficiency. Therefore, the installation of inline mixer is not advantageous, since it did not improve mass transfer of ozone in the system. On the contrary, the resistance to flow created by the mixer increases pumping costs. Similarly, according to a mass transfer study carried out at low pressure by Chen et al. (17), the  $K_L a$  values obtained using a high efficiency mixer were only slightly greater than those obtained using simple Y mixer. This implies that turbulence in the system is sufficient, so little enhancement is obtained by using high efficiency mixer.



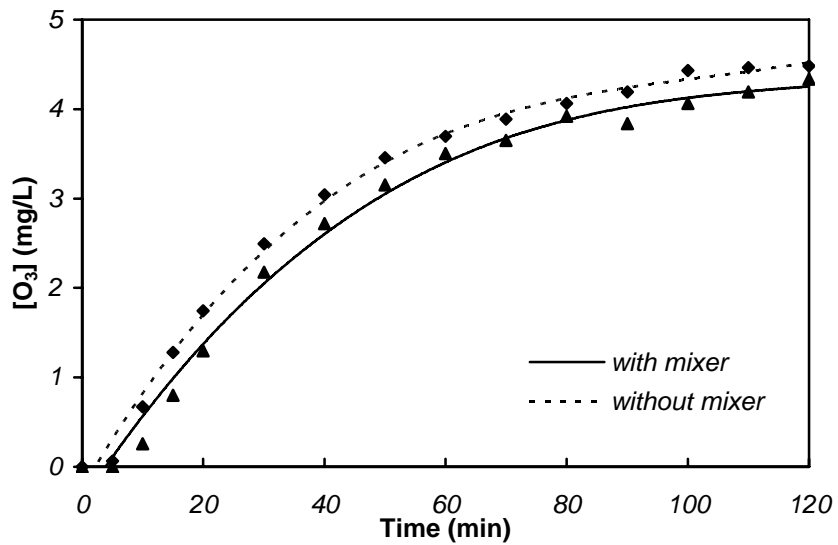
(a)



(b)



(c)



(d)

Fig. 4- Dissolved ozone concentration versus time - The effect of inline mixer. (a)  $Q=0.17$  L/min ; (b)  $Q=0.25$  L/min ; (c)  $Q=0.5$  L/min ; (d)  $Q=1.0$  L/min, gaseous ozone concentration 10 mg/L, inlet gas flow rate 75 mL/min, temperature 20 °C, pH 3.0, pressure 30 psi.

Table 4-  $K_{La}$  values calculated by modelling experimental results under various mixing conditions.

Water flow rate (L/min)	0.17		0.25		0.5		1.0	
Mixer	w	w/o	w	w/o	w	w/o	w	w/o
$K_{La}$ (1/min)	0.0317	0.0309	0.0354	0.0336	0.0360	0.0369	0.0357	0.0369
$R^2$	0.97	0.91	0.98	0.93	0.99	0.89	0.98	0.95
Standard deviation	0.0019	0.0017	0.0011	0.0035	0.0018	0.0028	0.0032	0.0022

### 2.5.3. Inlet Ozone Gas Concentration

The effect of the inlet ozone gas concentration on ozone mass transfer was determined at three gaseous ozone concentrations (2.5, 5.0 and 10.0 mg/L). As shown in Figure 5, as the inlet ozone concentration increased, a significant increase in the dissolved ozone concentration in the system was obtained. The steady state (final) aqueous ozone concentration ( $[O_3]_{lss}$ ) was found to be proportional to the gaseous ozone concentration ( $[O_3]_g$ , see inset in Figure 5). This finding is consistent with the experimental results presented by Chen et al. (17), which can be used to demonstrate a linear relationship between inlet ozone gas concentrations and dissolved ozone concentrations in the reservoir and the permeate. Chen et al. (17) used a hybrid ozonation-membrane setup, operated at low pressure. As shown in Table 5, variations in the inlet ozone concentration

over the range studied herein, does not exert a considerable effect on the ozone mass transfer coefficient. The F test results with  $\alpha=0.05$  (level of significance) also confirmed that the  $K_L a$  values obtained at various gaseous ozone concentrations were not statistically different ( $F=1.14 < \text{critical value}=5.14$ ). Hence, the improvement in the ozone dissolution as a result of increasing inlet ozone concentration can be attributed to the ozone deficit term ( $C_s - C$ ) of the mass transfer rate.

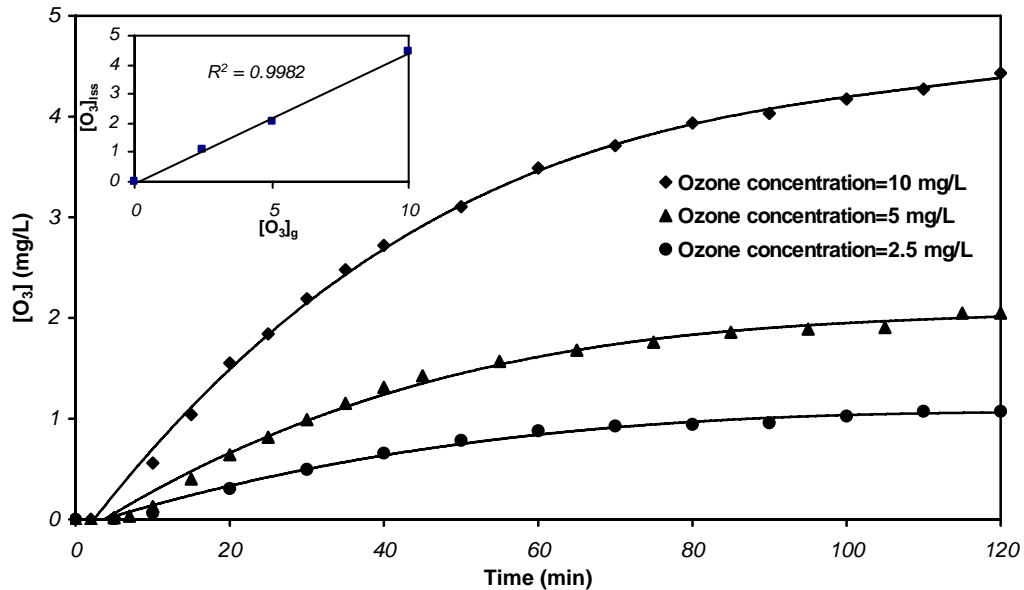


Fig. 5- Dissolved ozone concentration versus time at various gaseous ozone concentrations. Water flow rate 0.5 L/min, with mixer, inlet gas flow rate 75 mL/min, temperature 20 °C, pH 3.0, pressure 30 psi.

Table 5-  $K_{La}$  values calculated by modelling experimental results at various gaseous ozone concentrations.

Gaseous ozone concentration (mg/L)	2.5	5	10
$K_{La}$ (1/min)	0.0328	0.0353	0.0360
$R^2$	0.96	0.93	0.99
Standard deviation	0.0036	0.0025	0.0018

#### 2.5.4. Inlet Gas Flow Rate

The effect of inlet ozone gas flow rate (25, 50, 75 and 100 mL/min) on ozone mass transfer is presented in Figure 6. At higher gas flow rates, the resulting ozone concentrations are greater and the system reaches steady state more quickly. As it is shown by Table 6,  $K_{La}$  also increases with increasing gas flow rate, which is believed to be due to greater interfacial area between the gas bubbles and water along with increased turbulence in the loop and applied ozone dosage (for  $\alpha=0.05$ :  $F=18.53 > \text{critical value}=4.07$ , approving that  $K_{La}$  varies with changes in inlet gas flow rate). It has been shown by other researchers (13, 17, 29) that at low pressure, inlet gas flow rate impacts the mass transfer of ozone in the same way. However, as the inlet gas flow rate increases, ozone loss from the system also increases. For an ozone concentration of 10.0 mg/L, the experimental results indicate that the total ozone losses at gas flow rates of 25, 50, 75 and 100 mL/min are 83.5, 87.5, 90.0 and 91.0 %, respectively (Table 7). In addition,

considering the ultimate ozone concentrations indicated in Figure 6, for the given range of gas flow rates, it appears that little enhancement in the ozone mass transfer has been achieved when the gas flow rate was increased. Therefore, it is inferred that, for this system, the use of lower gas flow rates may be more favorable, since the associated expenses and the volume of off-gas are lower.

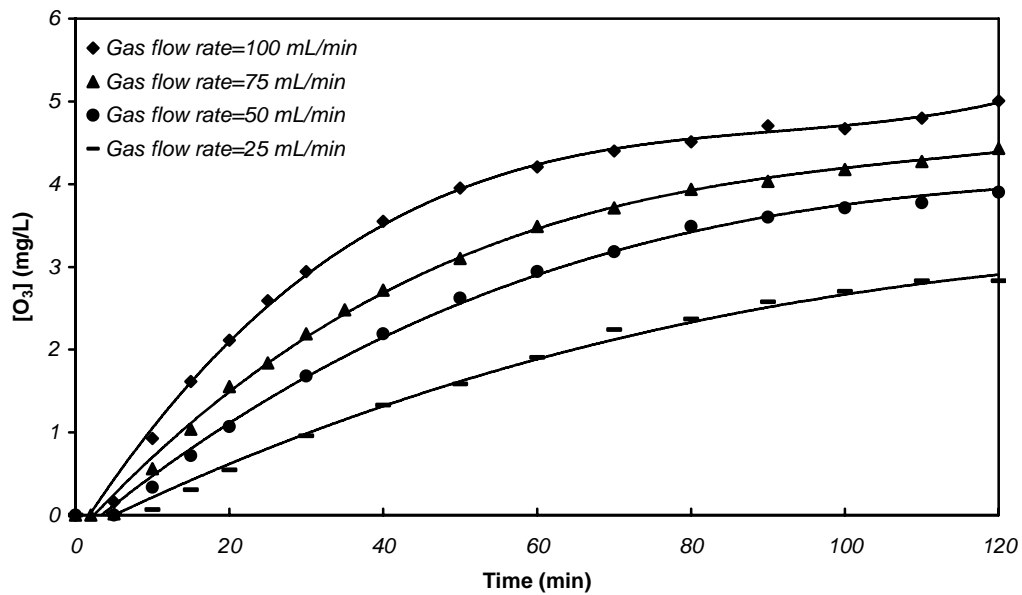


Fig. 6- Dissolved ozone concentration versus time at various inlet gas flow rates. Water flow rate 0.5 L/min, with mixer, gaseous ozone concentration 10 mg/L, temperature 20 °C, pH 3.0, pressure 30 psi.

Table 6-  $K_L a$  values calculated by modelling experimental results at various inlet gas flow rates.

Inlet gas flow rate (mg/L)	25	50	75	100
$K_L a$ (1/min)	0.0235	0.0306	0.0360	0.0396
$R^2$	0.97	0.99	0.99	0.95
Standard deviation	0.0021	0.0012	0.0018	0.0048

Table 7- Ozone uptake at various inlet gas flow rates.

Inlet gas flow rate (mL/min)	25	50	75	100
Gaseous ozone concentration (mg/L)	10	10	10	10
Total inlet ozone mass (mg) over the course of experiment (120 min)	30	60	90	120
Total ozone uptake (%)	16.5	12.5	10.0	9.1
Total ozone loss (%)	83.5	87.5	90.0	90.9

### 2.5.5. Temperature

The impact of temperature (15, 20 and 25 °C) on the dissolved ozone concentration is shown in Figure 7. The results obtained are consistent with the observations reported by other researchers (8, 32, 33); i.e., as temperature rises, the solubility of ozone in water decreases. Moreover, the ozone decomposition rate increases at higher temperatures (34). Therefore, as the temperature was increased, the aqueous ozone concentration declined. From Table 8, which lists the mass transfer coefficients calculated at different temperatures, it is evident that as temperature increases, the mass transfer coefficient increases as well (for  $\alpha=0.05$ :  $F=6.11 > \text{critical value}=5.14$ , approving that  $K_L a$  varies with changes in temperature). Chen et al (17) and Hsu et al. (35) have also carried out experiments at low pressure and have observed similar effects. This behaviour is believed to be due to greater diffusivity of ozone molecules at higher temperatures (35).

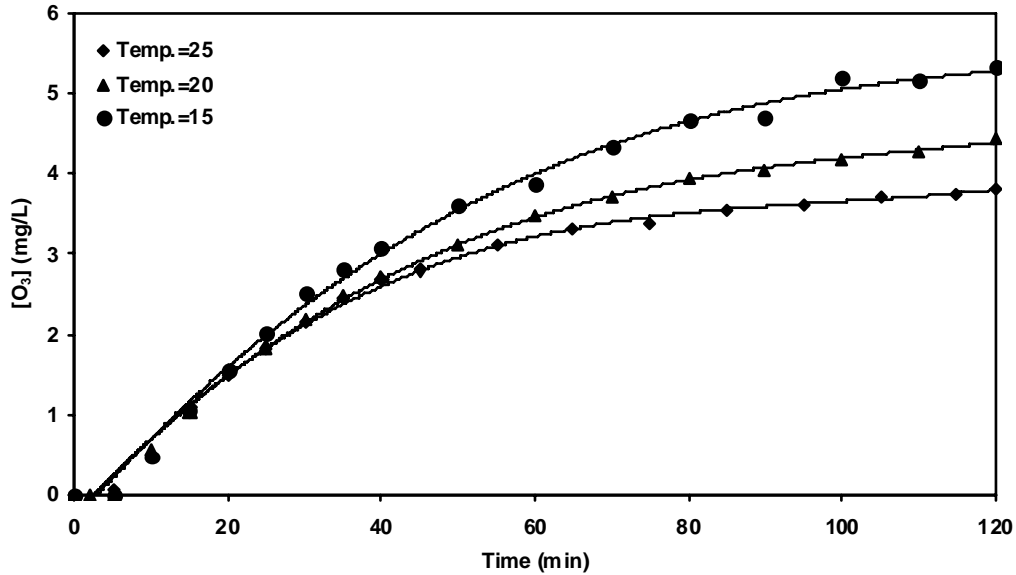


Fig. 7- Dissolved ozone concentration versus time at various temperatures. Water flow rate 0.5 L/min, with mixer, gaseous ozone concentration 10 mg/L, inlet gas flow rate 75 mL/min, pH 3.0, pressure 30 psi.

Table 8-  $K_{L,a}$  values calculated by modelling experimental results at various temperatures.

Temperature (°C)	15	20	25
$K_{L,a}$ (1/min)	0.0333	0.0360	0.0401
$R^2$	0.94	0.99	0.95
Standard deviation	0.0010	0.0018	0.0036

### 2.5.9. pH

The mechanism for the decomposition of ozone is pH dependent and, therefore, pH has a profound effect on ozone stability in aqueous solutions. Ozone self-decomposition proceeds through reactions with initiators such as hydroxide

ions (36, 37). As the pH increases, the  $\text{OH}^-$  concentration increases, which would result in a higher rate of ozone decomposition. As can be seen from Figure 8, the steady state dissolved ozone concentration decreases with pH, which is in agreement with the experimental results presented in the literature (29, 34).

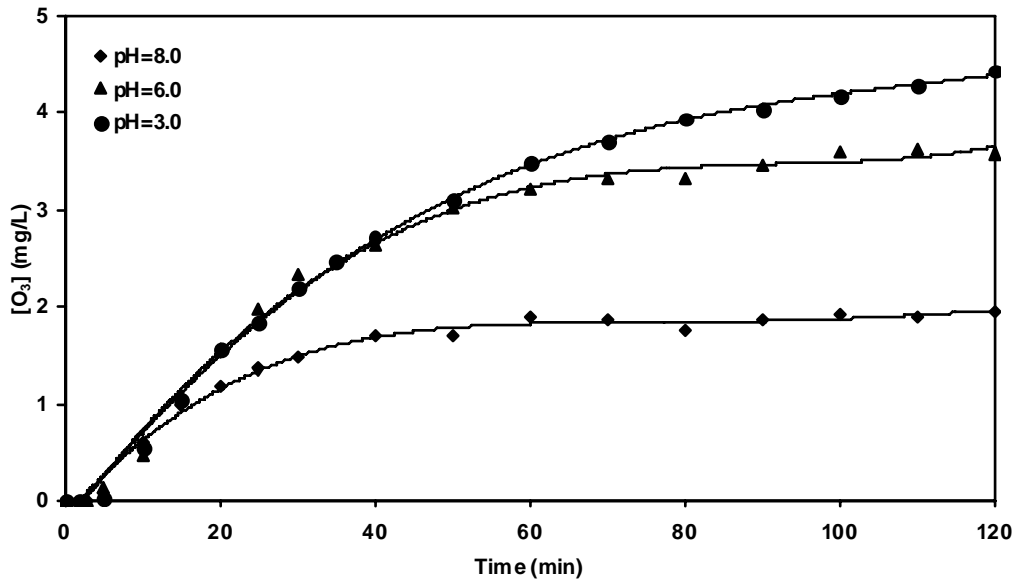


Fig. 8- Dissolved ozone concentration versus time at various pH vales. Water flow rate 0.5 L/min, with mixer, gaseous ozone concentration 10 mg/L, input gas flow rate 75 mL/min, temperature 20 °C, pressure 30 psi.

### 2.5.10. Mass Balance on Ozone

For the experiments at low pH, an analysis of the results shows that at the end of the experiment only about 10 to 15% of the total mass of injected ozone is dissolved in the water. The high ozone losses appear to be largely due to fugitive losses of ozone through the pressure relief valve. These losses are due to the degassing of oxygen as a result of its relatively low solubility in water. Also, during the course of the experiment the dissolved ozone approaches the solubility

limit. Consequently, ozone losses in the latter part of the experiment are high, as no additional ozone can dissolve in the water.

The overall mass transfer coefficient values found in this study are lower than those measured by Chen et al. (17) in a similar system that was operated at lower pressures. The fact that neither the use of a static inline mixer nor a higher cross flow rate to increase turbulence greatly improved ozone mass transfer coefficient suggests that mixing in the system is adequate. The low  $K_L a$  values found reflect the small size of the system, which is based upon the design used in our previous membrane filtration studies (38). In this system, the residence time of the gas bubbles in the injection loop is short (1- 4 s). This leads to poor mass transfer, since as the water in the reservoir is not mixed the gas bubbles and water separate in the reservoir. As discussed above, in the pressurized system, venting of the gas to maintain constant pressure leads to significant ozone losses due to degassing, thus reducing the overall mass transfer rate. Gas transfer would be expected to be better in a larger system, as more effective mass transfer would occur in a larger pressurization loop. Despite these limitations the study does show that, given the size of the system, adequate mixing and mass transfer can be achieved using the simple ozone injection technique employed in this study.

## **2.6. Conclusion**

Good agreement was achieved between predictions from the model developed to describe the mass transfer of ozone and the experimental results. Our results show that, despite, the small size of the system, adequate mass transfer can be achieved using a simple tee to inject the ozone gas into the pressurized water stream. Moreover, the use of an inline static mixer did not greatly improve the mass transfer of ozone. High cross flow rates also did not greatly improve ozone mass transfer. It is believed that the simple tee inlet along with the hydraulic mixing inside the system can achieve sufficient contact between ozone gas and the water phase. The mass transfer of ozone increased slightly with temperature, however, due to the lower solubility of ozone at higher temperature, the final ozone concentration achieved decreased with increasing temperature. The dissolved ozone concentration decreased with increasing pH. The final dissolved ozone concentration was found to be proportional to the inlet ozone concentration.

## **2.7. Acknowledgements**

The authors acknowledge the financial support of this work from the National Science Foundation (Research Grant CBET-056828), the Natural Sciences and Engineering Research Council of Canada (Discovery Grant 327560-2006 RGPIN) and the Department of Civil Engineering at McMaster University.

## 2.8. References

- (1) Gomella, C. J. *AWWA* 1972, 64, 39-46.
- (2) Masschelein, W. J. *Ozonization manual for water and wastewater treatment*; Wiley: New York, USA, 1982.
- (3) Gottschalk, C.; Libra, J. A.; Saupe, A. *Ozonation of water and waste water: A practical guide to understanding ozone and its application*; Wiley-VCH: New York, USA, 2000.
- (4) Rice, R. G.; Robson, C. M.; Miller, G. W.; Hill, A. G. *J. AWWA* 1981, 73, 44-57.
- (5) You, S. H.; Tseng, D. H.; Hsu, W. C. *Desalination* 2007, 202, 224-230.
- (6) Glaze, W. H. *Environ. Sci. Technol.* 1987, 21, 224-230.
- (7) Chandrakanth, M. S.; Honeyman, B. D.; Amy, G. L. *Colloids Surf. A: Physiochem. Eng. Aspects* 1996, 107, 321-342.
- (8) Camel, V.; Bermond, A. *Wat. Res.* 1998, 32, 3208-3222.
- (9) Peter, A.; von Gunten, U. *Environ. Sci. Technol.* 2007, 41, 626-631.
- (10) Roustan, M.; Mallevialle, J.; Roques, H.; Jones, J. P. *Ozone Sci. Eng.* 1981, 2, 337-344.
- (11) Ouederni, A.; Mora, J. C.; Bes, R. S. *Ozone Sci. Eng.* 1987, 9, 1-12.
- (12) Laplanche, A.; Le Sauze, N.; Martin, G.; Langlais, B. *Ozone Sci. Eng.* 1991, 13, 535-558.
- (13) Zhou, H.; Smith, D. W. *Wat. Res.* 2000, 34, 909-921.
- (14) Kuosa, M.; Laari, A.; Kallas, J. *Ozone Sci. Eng.* 2004, 26, 277-286.

- (15) Mitani, M. M.; Keller, A. A.; Sandall, O. C.; Rinker, R. G. *Ozone Sci. Eng.* 2005, 27, 45-51.
- (16) Wu, J. J.; Masten, S. J. *J. Environ. Eng.* 2001, 127, 1089-1099.
- (17) Chen, K. C.; Davies, S. H.; Masten, S. J. *J. Adv. Oxid. Technol.* 2007, 10, 287-296.
- (18) Park, Y. G. *Desalination* 2002, 147, 43-48.
- (19) Schlichter, B.; Mavrov, V.; Chmiel, H. *Desalination* 2003, 156, 257-265.
- (20) Schlichter, B.; Mavrov, V.; Chmiel, H. *Desalination* 2004, 168, 307-317.
- (21) Karnik, B. S.; Davies, S. H. R.; Chen, K. C.; Jaglowski, D. R.; Baumann, M. J.; Masten, S. J. *Wat. Res.* 2005, 39, 728-734.
- (22) Mozia, S.; Tomaszewska, M.; Morawski, A. W. *Desalination* 2006, 190, 308-314.
- (23) Grosz-Röll, F.; Bättig, J.; Moser, F. *Fourth Eur. Conf. Mixing* 1982, 225.
- (24) Zhu, Q. *Ozone Sci. Eng.* 1991, 13, 313-328.
- (25) Martin, N.; Benezet-Toulze, M.; Laplace, C.; Faivre, M.; Langlais, B. *Ozone Sci. Eng.* 1992, 14, 391-405.
- (26) Craik, S. A.; Smith, D. W.; Chandrakanth, M.; Belosevic, M. *Wat. Res.* 2003, 37, 3622-3631.
- (27) Roth, J. A.; Sullivan, D. E. *Ind. Eng. Chem. Fundam.* 1981, 20, 137-140.
- (28) Schwarzenbach, R. P.; Gschwend, P. M.; Imboden, D. M. *Environmental organic chemistry*; Wiley: New Jersey, USA, 2003.
- (29) Panda, K. K.; Mathews, A. P. *J. Environ. Eng.* 2008, 134, 860-869.
- (30) Mysore, C.; Leparc, J.; Lake, R.; Agutter, P.; Prévost, M. *Ozone Sci. Eng.* 2004, 26, 207-215.

- (31) Heyouni, A.; Roustan, M.; Do-Quang, Z. *Chem. Eng. Sci.* 2002, 57, 3325-3333.
- (32) Rischbieter, E.; Stein, H.; Schumpe, A. *J. Chem. Eng. Data.* 2000, 45, 338-340.
- (33) Guiza, M.; Ouederni, A.; Ratel, A. *Ozone Sci. Eng.* 2004, 26, 299-307.
- (34) Sotelo, J. L.; Beltran, F. J.; Benitez, F. J.; Heredia, J. B. *Wat. Res.* 1989, 23, 1239-1246.
- (35) Hsu, Y. C.; Chen, T. Y.; Chen, J. H.; Lay, C. W. *Ind. Eng. Chem. Res.* 2002, 41, 120-127.
- (36) Tomiyasu, H.; Fukutomi, H.; Gordon, G. *Inorg. Chem.* 1985, 24, 2962-2966.
- (37) Staehelin, J.; Hoigné, J. *Environ. Sci. Technol.* 1982, 16, 676-681.
- (38) Kim, J.; Davies, S. H. R.; Baumann, M. J.; Tarabara, V. V.; Masten, S. J. *J. Membr. Sci.* 2007, 311, 165-172.

## **Chapter 3: Bromate Formation in a Hybrid Ozonation – Ceramic Membrane Filtration System**

### **3.1. Abstract**

The effect of pH, inlet ozone mass injection rate, initial bromide concentration, and membrane molecular weight cut off (MWCO) on bromate formation in a hybrid membrane filtration–ozonation reactor was studied. Decreasing the pH, significantly reduced bromate formation. Bromate formation increased with increasing inlet gaseous ozone mass injection rate, due to increase in dissolved ozone concentrations. Greater initial bromide concentrations resulted in higher bromate concentrations. An increase in the bromate concentration was observed by reducing MWCO, which resulted in a concomitant increase in the retention time in the system. A model to estimate the rate of bromate formation was developed. Good correlation between the model simulation and the experimental data was achieved.

**Keywords:** bromide, bromate, ozonation, ceramic membrane, water treatment, modeling

### **3.2. Introduction**

Ozonation has gained widespread use in drinking water treatment over the past few decades (Gottschalk et al., 2000). Recently, a number of researchers have shown that when ozonation is used in combination with membrane filtration,

problems of fouling resulting from the deposition of natural organic matter on the membrane surface or within the membrane pores can be overcome (Van Geluwe et al., 2011, Kim et al., 2010, Mozia et al., 2006; Karnik et al., 2005). In such hybrid systems, aqueous ozone reacts with and degrades organic foulants accumulated on the membrane surface, thereby decreasing fouling. In this innovative method, ensuring a minimum dissolved ozone concentration enables the continuous treatment of drinking water and eliminates or greatly reduces the need for membrane cleaning procedures (Kim et al., 2009, You et al., 2007, Mozia et al., 2006, Schlichter et al., 2003).

A major concern in the treatment of bromide-containing waters using ozonation is the formation of brominated by-products (Siddiqui et al., 1995). Bromate ( $\text{BrO}_3^-$ ), an inorganic by-product of ozonation, is a human carcinogen, and the United States Environmental Protection Agency (USEPA), the Ontario (Canada) Safe Drinking Water Act, and the European Union have set the maximum contaminant level (MCL) for bromate at  $10 \mu\text{g/L}$  (Ontario drinking-water quality standards, 2002; European Union, 1998; USEPA, 1998).

Bromate is formed by the reaction of molecular ozone with the bromide ion ( $\text{Br}^-$ ), which is naturally present in many waters. The reactions involved are complex and involve both molecular ozone and OH radicals, as shown in Figure 1 (Crittenden and Harza, 2005; Leqube et al., 2004; Pinkernell and von Gunten, 2001; Haag and Hoigné, 1983). Bromide ion reacts with molecular ozone to form hypobromous acid (HOBr), which is at equilibrium with the hypobromite ion

( $\text{OBr}^-$ ). Subsequently, the hypobromite ion reacts with ozone to form the bromite ion, which further reacts with molecular ozone to form bromate. Bromide can also react with the hydroxyl radical ( $\cdot\text{OH}$ ) to form the bromine radical, which then reacts with molecular ozone in a complex set of reactions to form bromate. As such, both direct and indirect pathways play a role in bromate formation; however the rate constants for the reaction of hydroxyl radical with bromide are appreciably greater than that of those involving molecular ozone and it has been also shown that the contribution of  $\cdot\text{OH}$  to bromate formation is more significant compared to that of molecular ozone (Mizuno et al., 2004; von Gunten and Oliveras, 1998). It is reported that in Milli-Q water, almost 70% of bromate formation occurs through  $\cdot\text{OH}$  mediated oxidation reactions and the remaining 30% depends on the molecular ozone reactions (Ozegin et al., 1998).

While the formation of various bromine containing by-products in conventional ozonation systems has been studied (Haag and Hoigne, 1983; Krasner et al., 1993; von Gunten and Pinkernell, 2000), the formation of such disinfection by-products in a hybrid ozonation-membrane filtration has not been previously investigated. Hence, it is crucial to study bromate formation under various operating conditions in such hybrid systems. In this study, the effect of pH, inlet ozone mass injection rate, initial bromide concentration, and membrane molecular weight cut off on bromate formation in a membrane filtration–ozonation system were investigated.

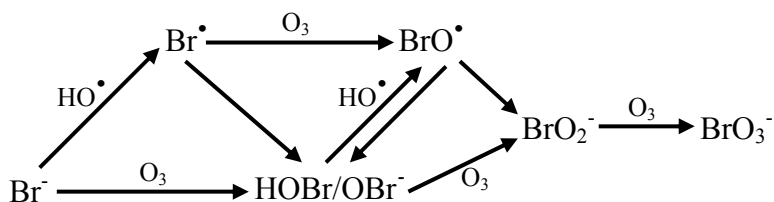


Fig. 1- Bromate formation - Molecular ozone and hydroxyl radical pathways. Adapted from Pinkernell and von Gunten (2001).

### 3.3. Materials and Methods

#### 3.3.1. Experimental Setup

Figure 2 illustrates the schematic of the reactor that was used in this study (also Fig. A1). The system was designed to withstand pressures of up to 550 kPa (80 psi) and pressurized using nitrogen gas. The experimental apparatus was equipped with two high-pressure stainless steel tanks with capacities of 5 and 8 liters (Fig. A2). The smaller tank was located in the recycle line to supply the system with the feed water. The second tank operated as reserve raw water supply to replace the water lost from the system through permeation and bleeding and was connected to the main tank through a solenoid valve (Type 6013, Bürkert Corp., USA ), which was programmed to maintain a constant water level in the main tank. The total water volume and the pressure inside the reactor were maintained at 1.5 L and 138 kPa (20 psi), respectively, throughout the experiments. All equipment, tubing and connections were made of ozone resistant materials and were either Teflon® or 316-stainless steel. Water was circulated in the loop at a flow rate of 200 mL/min using a gear pump (Model 000-380, Micropump Inc.,

USA). The water inside the tank was mixed as a result of the turbulence produced by the jet of water as it was returned to the tank.

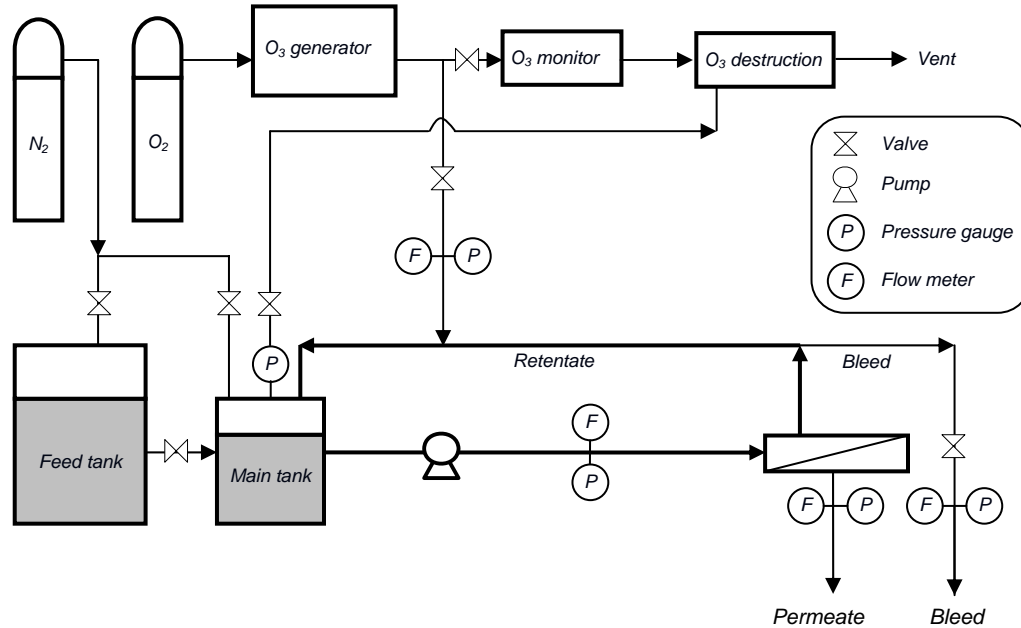


Fig. 2- Schematic of the experimental setup.

Gaseous ozone was generated from pressurized oxygen gas (having a purity of 99.999%) using a corona discharge ozone generator (Absolute Ozone AE15MC80P, Absolute System Inc., Edmonton, AB, Canada). The gaseous ozone concentration was adjusted by varying the ozone generator's voltage. Ozone gas was injected into the water stream flowing in the recirculation loop through a Swagelok Tee fitting (Model SS-400-3, Swagelok, USA). Ozone was transferred from the gas phase to the aqueous phase, as a result of the hydraulic mixing inside the reactor. The inlet gas flow rate was adjusted to the desired values using a digital flow-controller (Model MC-500SCCM-D, Alicat Scientific Inc., USA). Any gas exhausted from the system was destroyed by purging the gas

through a potassium iodide (2% KI) solution. A pressure regulator (Model KCB1F0A2A5P20000, Swagelok, USA) was employed to monitor and regulate the pressure in the recirculation loop. The water temperature was kept at  $20 \pm 0.1$  °C by recycling water through a water coil which was installed inside the main tank (Fig. A3). The temperature of the chilled water was controlled using a refrigerated circulator bath (NESLAB RTE-10, Thermo Fisher Scientific, USA).

In these experiments, tubular ultrafiltration (UF) ceramic membranes (TAMI North America, QC, Canada) with nominal molecular weight cut offs of 5, 8 and 15 kilodaltons (kD) were used (Fig. A4). UF membranes, rather than nanofiltration (NF) membranes, were chosen because the desired flux can be achieved at a lower operating pressure with a UF membrane, than with an NF membrane. Ceramic membranes were used as they are ozone resistant. The active length and the external diameter of the employed membranes were 25 cm and 10 mm, respectively. A stainless steel housing (TAMI North America, QC, Canada) was used to hold the membrane.

A bleed line was installed in the recycle loop to allow the retentate to be sampled. The bleed flow rate was set to 5.0 mL/min using a digital flow-controller (Model LC-50CCM-D, Alicat Scientific Inc., USA). A digital flow meter (Model L-5LPM-D, Alicat Scientific Inc., USA) and a digital pressure gauge (Model 2074, Ashcroft Inc., USA) were mounted in the loop to monitor the water flow rate and pressure within the system. The permeate flux was continuously measured using a balance (Adventurer Pro, Ohaus Corporation,

USA). Temperature, pressure, and cross flow rate were continuously recorded using a data acquisition system (LabView, National Instruments, USA).

### 3.3.2. Analytical Methods

The concentrations of ozone in the permeate and the retentate were continuously monitored by measuring the absorbance at a wavelength of 258 nm using flow-through cells mounted in a UV/Vis spectrophotometer (Model 4054, Pharmacia LKB, Biochrom Ltd., UK). The aqueous ozone concentration was then determined using an extinction coefficient of  $2900 \text{ M}^{-1}\text{cm}^{-1}$  (Hoigne and Bader, 1976). The inlet ozone gas concentration was also continuously measured using a UV ozone monitor (Model 454H, Teledyne Instruments, USA). To quench further ozone reactions, the residual dissolved ozone in the samples for bromide and bromate analysis were purged by bubbling nitrogen gas through the sample for 2 minutes. Bromide and bromate concentrations in the samples were measured in triplicate using an ion chromatograph, consisting of a high performance liquid chromatography system (Model 230, Varian ProStar, USA) with an anion-exchange column (IonPac AS23, Dionex Corp., USA) a guard column (IonPac AG23, Dionex Corp., USA), an anion micromembrane suppressor (AMMS III - 4mm, Dionex Corp., USA) and a conductivity detector (CD25A, Dionex Corp., USA). The analysis was carried out in accordance with the method proposed by Dionex (Application Note 184, Dionex Corp., USA). A solution of 4.5 mM sodium carbonate ( $\text{NaCO}_3$ ) (99.5%, EMD, USA) and 0.8 mM sodium bicarbonate ( $\text{NaHCO}_3$ ) (99.7%, Sigma-Aldrich, Germany) was used as the mobile phase. The

column flow rate was 1 mL/min. pH was measured using a pH meter (pHTestr 30, Eutech Instruments, Illinois, USA).

#### **3.3.4. Reagents**

Ultrapure water (Milli-Q water with resistivity greater than 18 M $\Omega$ ) was used to prepare all reagents and solutions. Milli-Q water was spiked with sodium bromide (NaBr) to obtain the desired concentrations. Subsequently, the pH of water was adjusted to the desired value by adding phosphoric acid (H<sub>3</sub>PO<sub>4</sub>) (99.99%, Sigma-Aldrich, USA) and/or sodium hydroxide (NaOH) (98.0+%, Fluka, Germany). The water was not buffered, since our experimental results showed that the pH did not vary over the course of the experiment. Tertiary butyl alcohol (Fisher Scientific, Germany) was used as hydroxyl radical scavenger. Bromide and bromate standards were prepared using sodium bromide (99.995% (metals basis), Fluka, Germany) and sodium bromate (NaBrO<sub>3</sub>) (99.7+%, Fisher Scientific, USA).

### **3.4. Results and Discussion**

The effects of pH, inlet ozone gas concentration, inlet ozone gas flow rate, initial bromide concentration, and membrane molecular weight cut off (MWCO) on bromate formation were investigated. Steady state bromate concentrations observed under various operating conditions are presented in Table 1. Experiments were carried out at least in duplicate. All bromate concentrations

reported are averages of triplicate analyses within replicate experiments. In all cases, the relative standard deviation for the measurement was less than 3.6%.

Table 1- Steady state bromate concentration in the permeate under various operating conditions

pH	Inlet O <sub>3</sub> mass injection rate (mg/min)	Initial [Br <sup>-</sup> ] (mg/L)	MWCO (kD)	Temperature (°C)	Steady state [BrO <sub>3</sub> <sup>-</sup> ] (µM)
3	1.5	1.00	5	20	0.58
6	1.5	1.00	5	20	4.13
8	1.5	1.00	5	20	8.03
6	0.5	1.00	5	20	1.57
6	1.0	1.00	5	20	2.86
6	0.75	1.00	5	20	2.55
6	2.25	1.00	5	20	4.67
6	1.5	0.05	5	20	0.055
6	1.5	0.25	5	20	0.72
6	1.5	0.50	5	20	1.75

### 3.4.1. Effect of pH

As shown in Figure 3, the steady state concentration of bromate ion measured in the permeate line at a reactor pH of 3.0 is significantly less than that observed at pH 6.0 or 8.0. This is not surprising since the hydroxyl radical ( $\cdot\text{OH}$ ) is more reactive with bromide than is the ozone molecule (von Gunten and Oliveras, 1998) and at low pH, the ozone molecule is more stable and the concentration of hydroxyl radicals in the reactor would be expected to be less than that found at higher pH (Pinkernell and von Gunten, 2001; von Gunten, 2003). Furthermore, HOBr is much less reactive with ozone than is OBr<sup>-</sup> (Mizuno et al., 2004). The pK<sub>a</sub>

for the dissociation of hypobromous acid to hypobromite ( $\text{HOBr} \leftrightarrow \text{OBr}^- + \text{H}^+$ ) is 8.8, so (Haag and Hoigne, 1983; Siddiqui and Amy, 1993) the concentration of  $\text{OBr}^-$  is low at low pH, hence the rate of formation of bromate is slower at low pH. While pH reduction is an effective way to control bromate formation, doing so is neither cost effective nor practical in terms of full scale drinking water treatment (Crittenden and Harza, 2005).

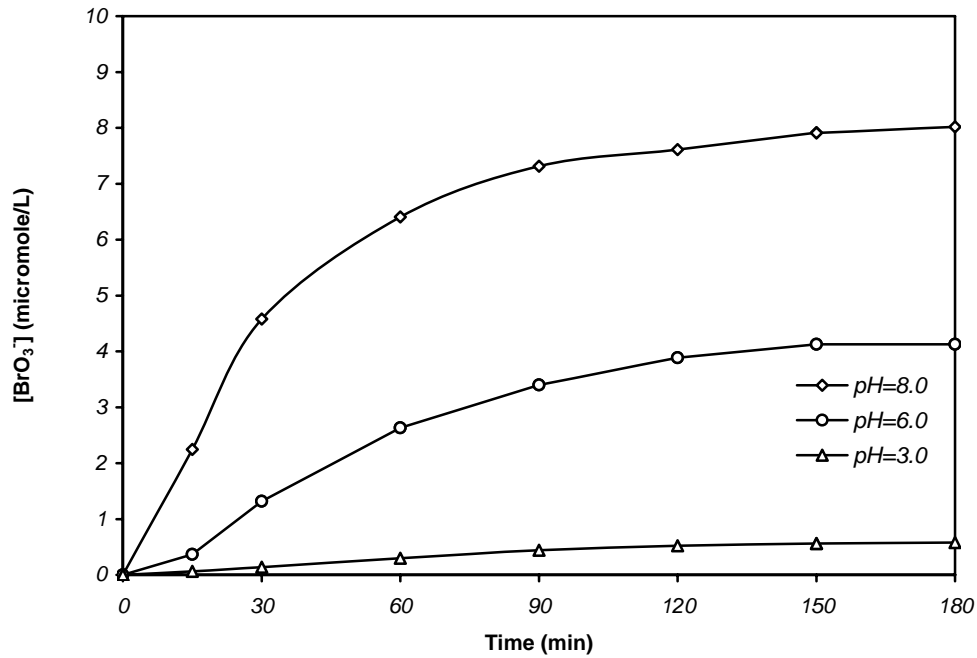


Fig. 3- Bromate concentration in the permeate vs. time at various pH values. Membrane: 7 channel – 5 kD, inlet  $\text{O}_3$  mass injection rate: 1.5 mg/min, initial  $[\text{Br}^-]$ : 1 mg/L, temperature: 20°C, ionic strength: 512.5, 13.0 and 12.5  $\mu\text{M}$  corresponding to pH 3, 6 and 8, respectively.

### 3.4.2. Effect of Inlet Ozone Mass Injection Rate

The effects of the inlet ozone mass injection rate (0.50, 0.75, 1.00, 1.50, 2.25 mg/min) on the dissolved ozone and bromate concentration are shown in Figures

4 and 5, respectively. Aqueous ozone concentrations increased with time until steady state conditions were attained. The steady state aqueous ozone concentration ( $[O_3]_{ss}$ ) was found to be proportional to the inlet ozone mass injection rate (see inset in Figure 4), which is also consistent with the experimental results presented by Moslemi et al. (2010). Higher inlet ozone mass injection rates resulted in greater bromate concentrations in the permeate. As shown in Figure 6, there is a strong linear relationship between the steady state bromate concentration in the permeate and the steady state dissolved ozone concentration ( $R^2 = 0.996$ ). This result shows the importance of developing processes that effectively minimize DBP formation by operating at the lowest possible dissolved ozone concentrations.

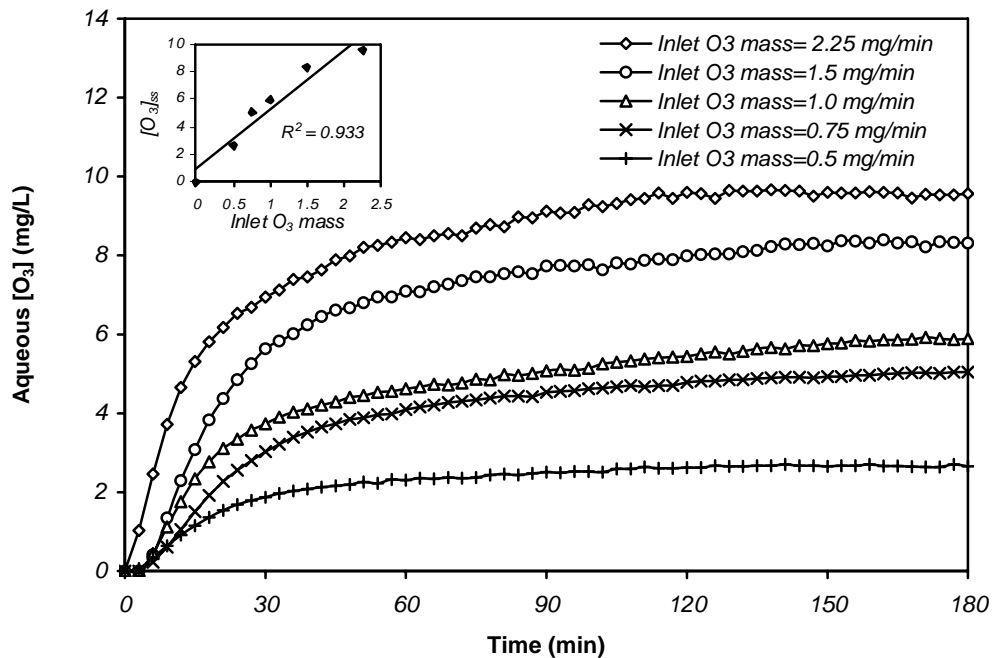


Fig. 4- Dissolved ozone concentration in the permeate vs. time at various inlet O<sub>3</sub> mass rates. Membrane: 7 channel – 5 kD, initial [Br<sup>-</sup>]: 1 mg/L, temperature: 20°C, pH: 6.0, ionic strength: 13.0 μM

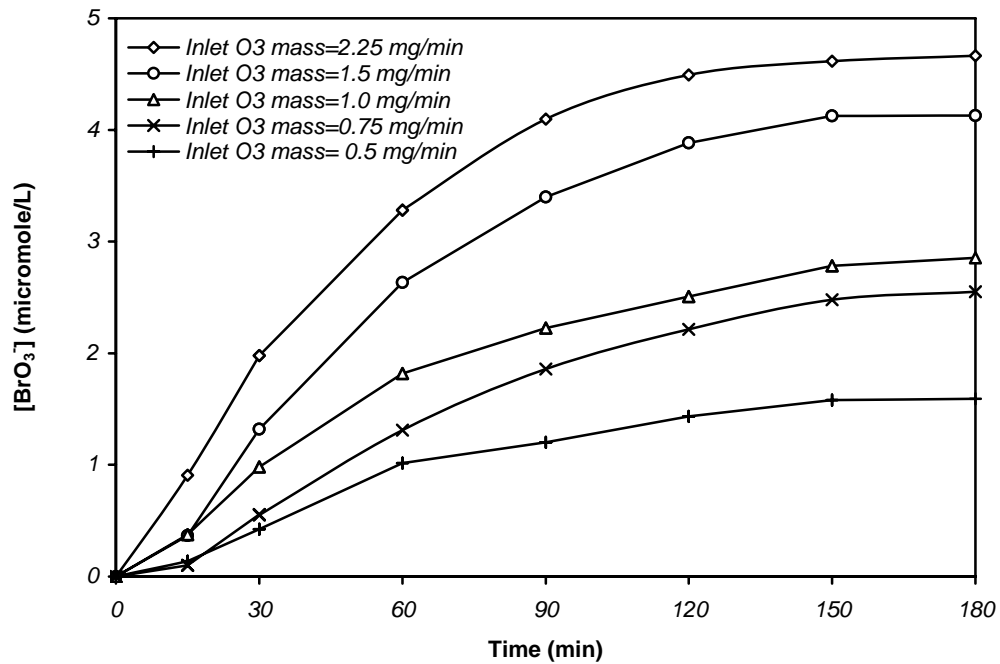


Fig. 5- Bromate concentration in the permeate vs. time at various inlet O<sub>3</sub> mass rates. Membrane: 7 channel – 5 kD, initial [Br<sup>-</sup>]: 1 mg/L, temperature: 20°C, pH: 6.0, ionic strength: 13.0 μM

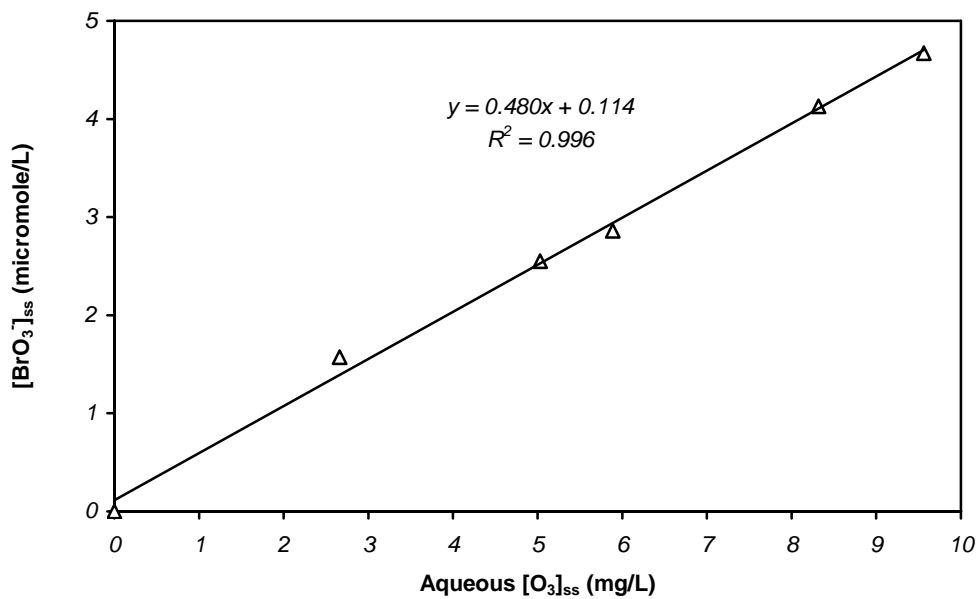


Fig. 6- Steady state bromate concentration in the permeate vs. steady state aqueous O<sub>3</sub> concentration. Membrane: 7 channel – 5 kD, initial [Br<sup>-</sup>]: 1 mg/L, temperature: 20°C, pH: 6.0, ionic strength: 13.0 μM

### 3.4.3. Initial Bromide Concentration

In another set of experiments, the initial bromide concentration was varied (0.05, 0.25, 0.5 or 1.0 mg/L) (see Figure S1). As it is shown in Figure 7, there is a strong correlation between the steady state bromate concentration in the permeate and the initial bromide concentration in the feed solution ( $R^2=0.992$ ) indicating that as more bromide ion was available to react with molecular ozone and/or hydroxyl radicals, more bromate was produced.

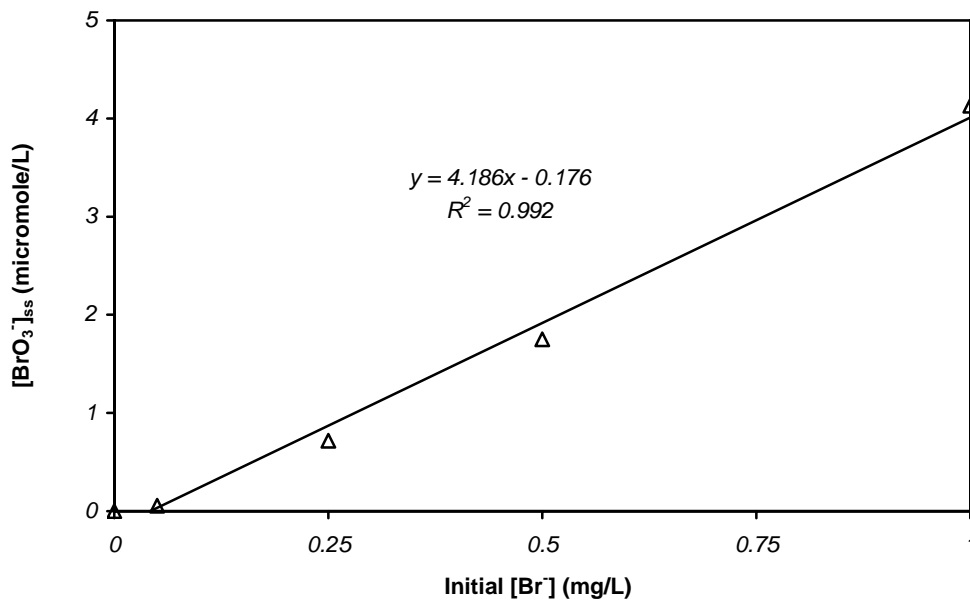


Fig. 7- Steady state bromate concentration in the permeate vs. initial bromide concentration. Membrane: 7 channel – 5 kD, inlet O<sub>3</sub> mass injection rate: 1.5 mg/min, temperature: 20°C, pH: 6.0

### 3.4.5. Effect of MWCO

As presented in Table 2, lower bromate concentrations were observed with membranes having higher MWCOs (also see Figure S2). The permeability of the membranes tested increases with MWCO, so at a constant operating pressure, as

the MWCO of the membrane increases, the permeate flux also increases, and the residence time inside the reactor decreases. Therefore, for membranes with greater MWCOs, the ozone exposure (the dissolved ozone concentration multiplied by retention time) is reduced. The retention times for each system and the three different membranes were calculated (see Supporting Documentation for details). The retention times for the membranes with MWCOs of 5, 8, and 15 kD were 34, 23, and 18 seconds, respectively (Table 3). As can be seen in Figure 8 there is a strong linear correlation between the steady state bromate concentration and the retention times in the membrane ( $R^2=0.999$ ) and the entire system ( $R^2=0.993$ ). This implies that in hybrid systems, bromate formation is significantly affected by the contact times in the membrane and the entire system, although the latter likely predominates simply because of its greater magnitude. These results suggest that bromate formation can be minimized by employing membranes with the largest MWCO feasible for the particular operation.

Table 2- Steady state  $[\text{BrO}_3^-]$  at various MWCOs

MWCO (kD)	pH	Inlet $\text{O}_3$ mass injection rate (mg/min)	Initial $[\text{Br}^-]$ (mg/L)	Steady state $[\text{BrO}_3^-]$ ( $\mu\text{M}$ )
5	6.0	1.5	1.00	4.13
8	6.0	1.5	1.00	3.18
15	6.0	1.5	1.00	2.67

Table 3- Retention time in the membrane for various MWCOs

MWCO (kD)	$V_{mp}$ (mL)	$W_m$ (g)	$V_{md}$ (mL)	$V_p$ (mL)	$J$ (mL/s)	$\theta$ (s)
5	14.1	38.7	10.2	3.96	0.116	34
8	14.1	38.8	10.2	3.93	0.169	23
15	14.1	40.2	10.6	3.57	0.198	18

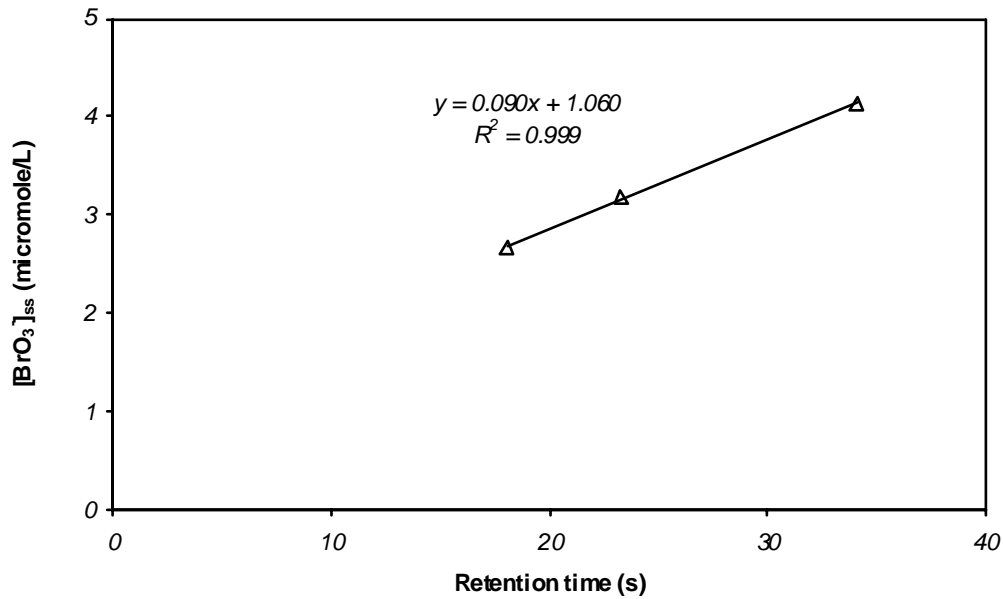


Fig. 8- Steady state bromate concentration in the permeate vs. retention time in the membrane. Membrane: 7 channel, inlet O<sub>3</sub> mass injection rate: 1.5 mg/min, initial [Br<sup>-</sup>]: 1 mg/L, temperature: 20°C, pH: 6.0, ionic strength: 13.0 μM

### 3.5. Bromate Formation Model

A kinetic-based model was developed to predict the rate of bromate formation in the hybrid ozone-membrane system. Experimental results reported herein were used to calculate the reaction rate constant. Bromate formation in the employed reactor can be expressed using the following mass balance equation:

$$V \frac{dC_R}{dt} = Q_{in} C_{in} - Q_P C_P - Q_B C_R + k C_R V \quad (1)$$

where,

V: total volume of water in the system (1500 mL)

t: time (min)

$C_R$ : concentration of bromate in the system (retentate) ( $\mu\text{M}$ )

$C_{in}$ : concentration of bromate in the inflow into the system ( $\mu\text{M}$ )

$C_P$ : concentration of bromate in the permeate ( $\mu\text{M}$ )

$Q_{in}$ : inlet flow rate (mL/min)

$Q_P$ : permeate flow rate (mL/min)

$Q_B$ : bleed flow rate (mL/min)

k: rate constant of bromate formation (1/min)

At steady state, the bromate concentration in the system will not vary with time ( $dC/dt=0$ ). Moreover, the feed water was free of bromate ion ( $C_{in}=0$ ). Hence, after substitution into Equation 1, the rate constant of bromate formation can be obtained using the following equation.

$$k = \frac{Q_P C_P + Q_B C_R}{C_R V} \quad (2)$$

Using Equation 2, the rate constants for the experiments with inlet ozone mass injection rate were calculated (see Table 4). According to the results, rate constants do not vary significantly as a result of variations in ozone mass injection rate. Hence, one can assume similar bromate formation mechanism for all conditions tested herein.

Table 4- Rate constants for the formation of bromate in the hybrid ozonation-membrane system

Inlet O <sub>3</sub> mass (mg/min)	Rate constant (min <sup>-1</sup> )	Relative Standard deviation (%)
0.5	0.0061	4.8
0.75	0.0063	6.7
1.0	0.0064	2.4
1.5	0.0067	4.3
2.25	0.0068	5.6

### 3.6. Acknowledgements

The authors acknowledge financial support of this work from the National Science Foundation Research (Grant No. CBET-0506828) and from the Natural Sciences and Engineering Research Council of Canada Discovery Grant Program.

### 3.7. Supplemental Data

Figures S1 and S2 indicate bromate concentration in the permeate versus time for the experiments with various initial bromide concentrations (0.05, 0.25, 0.50, and 1.00 mg/L) and membrane MWCOs (5, 8, and 15 kD), respectively. According to the figures, bromate concentration increases by time and depending on the experimental conditions after approximately 150min it reaches a steady state value.

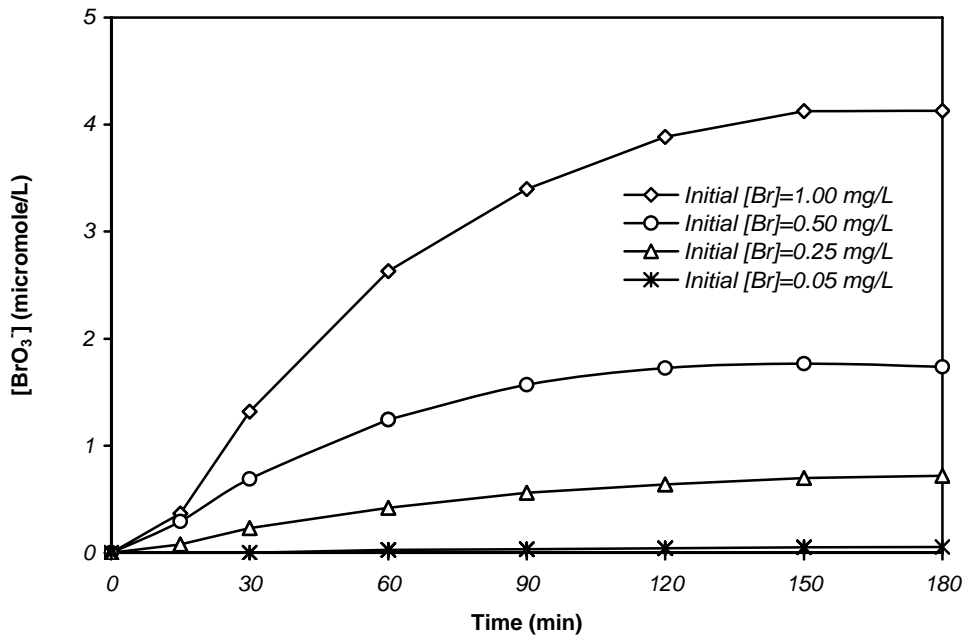


Fig. S1- Bromate concentration in the permeate vs. time at various initial bromide concentrations. Membrane: 7 channel – 5 kD, inlet O<sub>3</sub> mass injection rate: 1.5 mg/min, temperature: 20°C, pH: 6.0

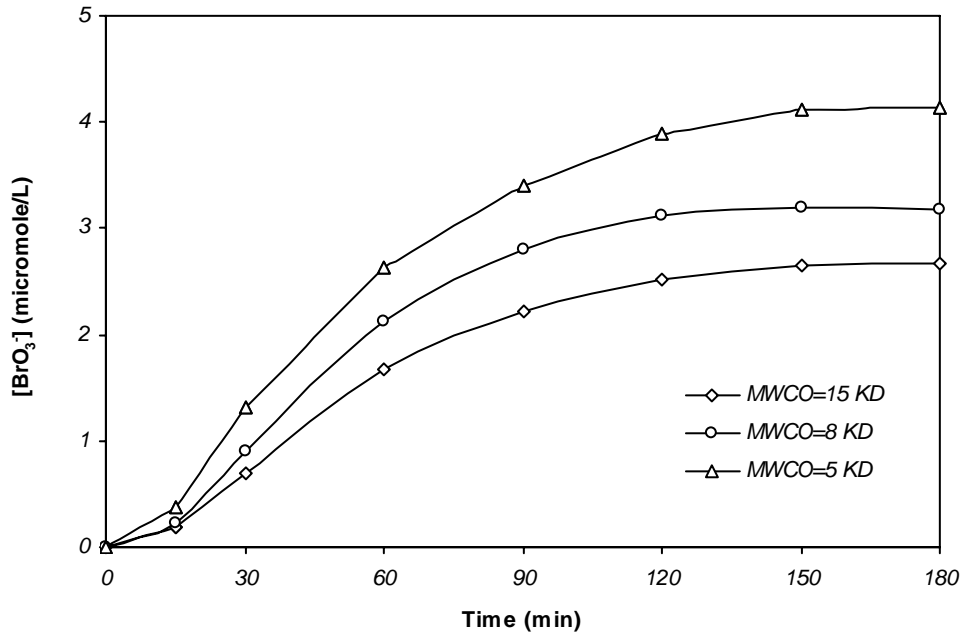


Fig. S2- Bromate concentration in the permeate vs. time at various MWCOs. Membrane: 7 channel, inlet O<sub>3</sub> mass injection rate: 1.5 mg/min, initial [Br<sup>-</sup>]: 1 mg/L, temperature: 20°C, pH: 6.0, ionic strength: 13.0 μM

### 3.8. Supporting Documentation

The retention time in the membrane can be calculated by dividing the total volume of the membrane pores by the permeate flux.

$$\theta = \frac{V_p}{J} \quad (1)$$

where,

$\theta$ : the retention time in the membrane (s)

$V_p$ : the total volume of the membrane pores (mL)

$J$ : the steady state permeate flux (mL/s)

To obtain  $V_p$ , the dense volume of the membrane material ( $V_{md}$ ) has to be subtracted from its porous volume ( $V_{mp}$ ).

$$V_p = V_{mp} - V_{md} \quad (2)$$

$V_{mp}$  is equal to the total volume of the membrane (including channels), minus the volume of the channels. The length ( $L$ ) and the external diameter of the tubular ceramic membranes ( $D$ ) utilized in this research were 25cm and 1cm, respectively. Membranes were composed of 7 channels with equivalent diameters ( $d$ ) of 0.2cm. Hence,  $V_{mp}$  can be obtained from the following formula:

$$V_{mp} = \pi L \frac{D^2}{4} - 7\pi L \frac{d^2}{4} \quad (3)$$

$V_{md}$  can be estimated using the following formula:

$$V_{md} = \frac{W_m}{\rho} \quad (4)$$

where,

$W_m$ : the weight of the membrane (g)

$\rho$ : the density of the ceramic membrane material, 3.8 g/mL

Values for the above terms are presented in Table 3.

The retention time in the entire system can be obtained from the following formula:

$$\tau = \frac{V}{J + F} \quad (5)$$

where,

$\tau$ : the retention time in the entire system (s)

$V$ : the total volume of water in the reactor (mL)

F: the bleed flow rate (mL/s)

The total volume of water in the system and the bleed flow rate for the experiments carried out in this study were maintained at 1500 mL and 5 mL/min, respectively. Thus, the retention times in the entire system for the membranes with MWCOs of 5, 8, and 15 kD were equal to 126, 99, and 89 minutes, respectively.

### 3.9. References

Crittenden, J., Harza, M.W. (2005) *Water treatment: Principles and design*. 2<sup>nd</sup> ed.

MWH, John Wiley, New Jersey.

European Union (1998) *Official Journal of the European Communities*, L 330,

Council Directive 98/83/EC.

Gottschalk, C., Libra, J.A., Saupe, A. (2000) *Ozonation of water and waste water:*

*A practical guide to understanding ozone and its application*. Wiley-VCH:  
New York.

Haag, W.R., Hoigne, J. (1983) *Ozonation of bromide-containing waters: Kinetics of*

*formation of hypobromous acid and bromate*. *Environ. Sci. Technol.* 17, 261-267.

Hoigne, J., Bader, H. (1976) *The role of hydroxyl radical reactions in ozonation*

*processes in aqueous solutions*. *Water Res.* 10, 377-386.

Karnik, B.S., Davies, S.H.R., Chen, K.C., Jaglowski, D.R., Baumann, M.J.,

Masten, S.J. (2005) *Effects of ozonation on the permeate flux of nanocrystalline ceramic membranes*. *Water Res.* 39, 728-734.

- Kim, J., Van der Bruggen, B. (2010) The use of nanoparticles in polymeric and ceramic membrane structures: Review of manufacturing procedures and performance improvement for water treatment. *Environmental Pollution* 158, 2335-2349.
- Kim, J., Shan, W., Daview, S.R., Baumann, M.J., Masten, S.J., Tarabara, V. (2009) Interactions of aqueous NOM with nanoscale TiO<sub>2</sub>: Implications for ceramic membrane filtration-ozonation hybrid process. *Environ. Sci. Technol.* 43, 5488-5494.
- Krasner, S.W., Glaze, W.H., Weinberg, H.S., Daniel, P.A., Najm, I.N. (1993) Formation and control of bromate during ozonation of waters containing bromide. *J. AWWA* 85, 73-81.
- Legube, B., Parinet, B., Gelinet, K., Berne, F., Croue, J.P. (2004) Modeling of bromate formation by ozonation of surface waters in drinking water treatment. *Water Res.* 38, 2185-2195.
- Mizuno, T., Yamada, H., Tsuno, H. (2004) Formation of bromate ion through a radical pathway in a continuous flow reactor. *Ozone Sci. Eng.* 26, 573-584.
- Moslemi, M., Davies, S.H., Masten, S.J. (2010) Ozone mass transfer in a recirculating loop semibatch reactor operated at high pressure. *Advanced Oxidation Technol.* 13, 79-88.
- Mozaia, S., Tomaszewska, M., Morawski, A.W. (2006) Application of an ozonation-adsorption-ultrafiltration system for surface water treatment. *Desalination* 190, 308-314.

- Ontario drinking-water quality standards (2002) Safe Drinking Water Act, Ontario regulation 169/03.
- Ozekin, K., Westerhoff, P., Amy, G.L., Siqqiqui, M. (1998) Molecular ozone and radical pathways of bromate formation during ozonation. *J. Environ. Eng.* 124, 456-462.
- Pinkernell, U., von Gunten, U. (2001) Bromate minimization during ozonation: Mechanistic considerations. *Environ. Sci. Technol.* 35, 2525-2531.
- Schlichter, B., Mavrov, V., Chmiel, H. (2003) Study of a hybrid process combining ozonation and membrane filtration - filtration of model solutions. *Desalination* 156, 257-265.
- Siddiqui, M.S., Amy, G.L. (1993) Factors affecting DBP formation during ozone-bromide reactions. *J. AWWA* 85, 63-72.
- Siddiqui, M.S., Amy, G.L., Rice, R.G. (1995) Bromate ion formation: A critical review, *J. AWWA* 87, 58-70.
- USEPA (1998) National primary drinking water regulations: Disinfection and disinfection byproducts. *Federal Register* 63, 69390-69476
- Van Geluwe, S., Braeken, L., Van der Bruggen, B. (2011) Ozone oxidation for the alleviation of membrane fouling by natural organic matter: A review. *Water Res.* 45, 3551-3570.
- von Gunten, U., Oliveras, Y. (1998) Advanced oxidation of bromide-containing waters: Bromate formation mechanisms. *Environ. Sci. Technol.* 32, 63-70.

von Gunten, U., Pinkernell, U. (2000) Ozonation of bromide-containing drinking waters: a delicate balance between disinfection and bromate formation. *Water Sci. Technol.* 41, 53-59.

von Gunten, U. (2003) Ozonation of drinking water: Part II. Disinfection and by-product formation in presence of bromide, iodide or chlorine. *Water Res.* 37, 1469-1487.

You, S.H., Tseng, D.H., Hsu, W.C. (2007) Effect and mechanism of ultrafiltration membrane fouling removal by ozonation. *Desalination* 202, 224-230.

## **Chapter 4: Empirical Modeling of Bromate Formation during Drinking Water Treatment Using a Hybrid Membrane Filtration–Ozonation**

### **4.1. Abstract**

The effect of the nature of the membrane surface, hydroxyl radical scavengers, and temperature, on bromate formation in a hybrid membrane filtration–ozonation reactor was studied. The presence of hydroxyl radical scavengers (tertiary butyl alcohol, t-BuOH) suppressed the indirect bromate formation pathway and less bromate was formed. The bromate concentration that resulted with the Mn oxide coated membrane was less than that formed with the uncoated TiO<sub>2</sub> membrane. As the temperature was increased, bromate formation was enhanced, which was attributed to greater reaction rates. An empirical model was also developed to predict bromate formation in a hybrid ozone-ceramic membrane filtration system. The model, which takes into account the effects of important experimental variables including initial bromide concentration, inlet ozone mass injection rate, pH, temperature, and reaction time, was generated using multiple linear regression method with logarithmic transformations. The model indicated that bromate formation was favoured at high bromide concentration, ozone dose, pH, and temperature. Good correlation was achieved between the model predictions and the experimental data.

**Keywords:** modeling, bromate, ozonation, ceramic membrane, water treatment

## 4.2. Introduction

Ozone is a more powerful disinfectant than chlorine or chlorine dioxide and it is capable of inactivating resistant pathogens including *Cryptosporidium* oocysts [1]. Ozone can oxidize many organic compounds; including those responsible for taste, odour, and color, and the precursors of chlorination by-products, such as chloroform. It can also reduce the concentration of total organic carbon (TOC) through mineralization and aid in coagulation through the transformation of NOM to smaller and more polar compounds [2]. Ozone can also effectively oxidize Fe (II) and Mn (II) [2-6]. As a result, the application of ozone in the water industry has increased dramatically since the first full scale installation of ozone for the treatment of potable water in Nice, France in 1906 [7-10].

Recently, a number of researchers have combined ozonation with membrane filtration to overcome fouling problems resulting from the deposition of natural organic matter on the membrane surface or within the pores of membrane [11-15]. In such a hybrid process, dissolved ozone reacts with organic foulants blocking membrane pores, thereby reducing the extent of membrane fouling. This greatly reduces the need for membrane cleaning procedures and allows for continuous operation of the treatment system [13,16,17].

Despite all of the advantages offered by ozonation processes, they have a major drawback: the formation of bromate. Bromate ion ( $\text{BrO}_3^-$ ) is formed during the ozonation of bromide ( $\text{Br}^-$ ) containing waters. Bromate is a potential human carcinogen and is regulated in drinking water [18-20]. The United States

Environmental Protection Agency (US EPA) has set a maximum contaminant level (MCL) of 10  $\mu\text{g/L}$  for the bromate ion [20].

The concentration of bromide in natural waters is highly variable, ranging from 10 to 1000  $\mu\text{g/L}$  [1]. Amy et al. [21] indicated that, under typical conditions, ozonation can transform nearly 20% of the bromide ion to bromate. It is reported that, low levels of bromide ( $<20 \mu\text{g/L}$ ) are not likely to result in bromate concentrations that exceed the regulatory limit. However, it is generally accepted that when bromide concentrations exceed 50  $\mu\text{g/L}$ , the concentration of bromate formed during ozonation may exceed the allowable concentration of 10  $\mu\text{g/L}$  [1].

The mechanism for the formation of bromate in the presence of ozone is illustrated in Figure 1. The reaction is initiated by the reaction of the molecular ozone with the bromide ion, resulting in the formation of hypobromous acid (HOBr) and the hypobromite ion ( $\text{OBr}^-$ ) [10,22,23]. The reaction is followed by a series of hydroxyl radical ( $\cdot\text{OH}$ ) and ozone initiated reactions that lead to the eventual formation of bromate. As such, both direct and indirect ( $\cdot\text{OH}$ ) pathways play significant roles in bromate formation [24,25].

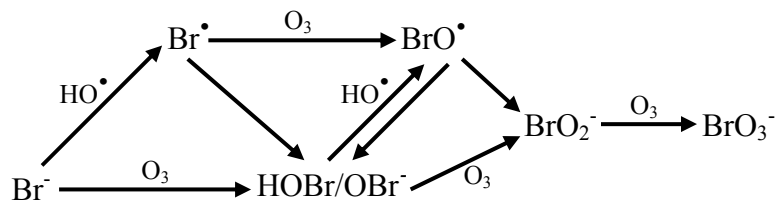


Fig. 1- Formation of bromate in aquatic systems. Adapted from Pinkernell and von Gunten [23].

Modeling can provide insight into the rate of bromate formation under various operating conditions. Despite of their simplicity, empirical models have been reported to yield accurate predictions of bromate formation and therefore, have been used widely [26]. Various empirical models have been proposed to predict the formation of bromate and other ozonation disinfection by-products in conventional ozonation processes including both batch and semi-batch reactor configurations [27-30].

It has been shown that bromate formation is influenced by a number of factors, including the concentration of bromide ion present in water, ozone dose, pH, contact time, and temperature [19,27,31,32]. The rate of formation of  $\cdot\text{OH}$  in ozone systems is strongly pH dependent as the hydroxide ion initiates the formation of  $\cdot\text{OH}$  in water [33], so pH can also influence bromate formation. The  $\text{pK}_a$  of  $\text{HOBr}$  is 8.8 at  $20^\circ\text{C}$ . Therefore, referring to Figure 1, at pHs greater than 8.8, the equilibrium between  $\text{HOBr}$  and  $\text{OBr}^-$  shifts towards the right (formation of the hypobromite ion). As  $\text{OBr}^-$  is much more reactive with ozone than is  $\text{HOBr}$ , more bromate is formed at higher pH [22,34]. Temperature has a considerable influence on bromate formation [1,18,34]. However, temperature is incorporated in few empirical bromate models [26].

We have developed a model that predicts simulation of the extent of bromate formation in hybrid ozonation-filtration systems. The model developed herein considers the effect of pH, initial bromide concentration, temperature, ozone dosing rate and reaction time on bromate formation in a membrane filtration–

ozonation system. The influence of the type of membrane on bromate formation was also investigated by comparing bromate formation using a commercial ceramic membrane with a titanium oxide filtration layer and a membrane coated manganese oxide (which catalyzes the decomposition of ozone). The importance of hydroxyl radical formation in the system was investigated by adding the  $\cdot\text{OH}$  scavenger, tertiary butyl alcohol, to the system.

### **4.3. Materials and Methods**

A recirculating loop semibatch reactor operated at high pressure was used to carry out the experiments. Moslemi et al. [35] provides a complete description of the experimental apparatus and methods used in this study. Experiments were carried out to develop a database that documents the amount of bromate formed as a function of initial bromide concentration, inlet ozone mass flow rate, pH, temperature, and reaction time. To observe the influence of the operating parameters on bromate formation and also in order to simplify the modeling effort, only one parameter was varied at a time while other parameters were kept constant.

The effects of t-butyl alcohol, a hydroxyl radical scavenger, membrane coating, and temperature on bromate formation were investigated. Experiments were carried out at least in duplicate. All bromate concentrations reported are the average of triplicate analyses within experiments and the error bars in Figures 2 and 3 represent the standard deviations of the triplicate measurements.

## 4.4. Results and Discussion

### 4.4.1. The Role of the Hydroxyl Radical

To assess the contribution of hydroxyl radicals to bromate formation, a number of experiments were carried out in the presence of t-BuOH, a hydroxyl radical scavenger. t-BuOH is highly reactive towards hydroxyl radicals, but is essentially unreactive with molecular ozone. As mentioned earlier, both direct and indirect pathways play a role in bromate formation, however the rate constants for the reaction of  $\cdot\text{OH}$  with bromide are considerably greater than that of those involving ozone. It has been reported that, as compared to the contribution of molecular ozone, the contribution of  $\cdot\text{OH}$  to bromate formation is more significant [24,25].

As shown in Figure 2, at pH 3.0, the addition of t-BuOH did not affect the steady state dissolved ozone concentration in the permeate. However, at higher pH values (6.0 and 8.0), the addition of t-BuOH considerably increased the dissolved ozone concentration. This is not surprising, since at pH 3.0 ozone is quite stable and the presence of t-BuOH has little effect on ozone stability and subsequently on the dissolved ozone and OH radical concentrations [1,23]. At pH 6 and 8, the presence of t-BuOH has a pronounced effect on ozone concentration. This is because the  $\cdot\text{OH}$  is involved in the radical chain reaction which propagates the ozone decomposition reaction initiated by the hydroxide ion. Figure 2 also shows the effect of t-BuOH on the steady state bromate formation at pH values of 3.0, 6.0 and 8.0. It is apparent that regardless of pH, the addition of t-BuOH suppresses bromate formation. This suggests that, the hydroxyl radical pathway

plays a significant role in bromate formation, even at pH 3. In acidified water, one would expect neither much ozone decomposition nor the formation of OH radicals. However, the influence of t-BuOH suggests that with the hybrid ozone-ceramic membrane system, OH radicals play a role in bromate formation even at pH 3. This is believed to be due to the catalytic decomposition of ozone on the ceramic membrane surface resulting in the formation of bromate. This is consistent with the findings of Karnik et al. [36] who showed that radical reactions play a significant role in the degradation of organic compounds, such as salicylic acid, in hybrid ozonation-ceramic membrane systems.

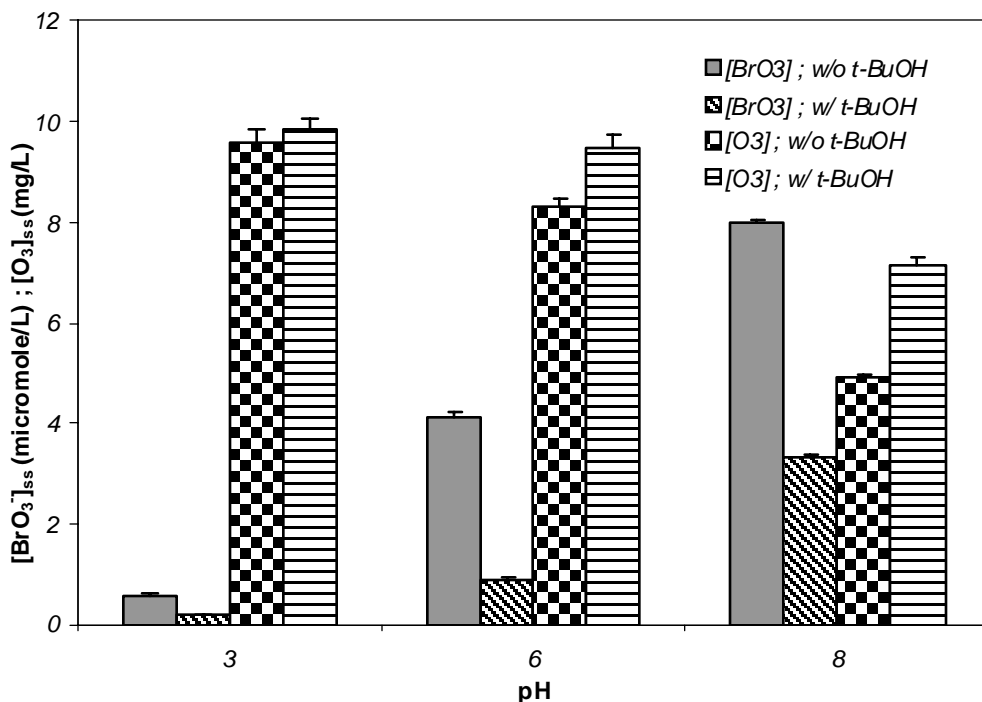


Fig. 2- The effect of  $\cdot\text{OH}$  scavenger on the steady state bromate and ozone concentrations in the permeate at various pHs. Membrane: 7 channel – 5 kD, O<sub>3</sub> mass injection rate: 1.5 mg/min, initial [Br<sup>-</sup>]: 1 mg/L, temperature: 20°C. The time dependent concentrations of dissolved ozone and bromate are shown in Figures S1 and S2.

#### 4.4.2. Membrane Coating

To study the effect of coating the membrane with manganese oxide on bromate formation, the performance of a 5 kD ceramic membrane, Inside Ceram (TAMI North America, Saint-Laurent, Quebec), coated with 30 layers of manganese oxide was compared with that of an uncoated membrane (see Corneal et al. [37] for the membrane preparation method). Manganese oxide is a more efficient catalyst of ozone decomposition than is titanium oxide (which is used in the filtration layer of the Inside Ceram membranes) and, in the presence of ozone, the Mn oxide coated membrane is more effective at controlling fouling on the membrane surface than is the uncoated membrane [38]. As can be seen in Figure 3, regardless of the operating pH, the steady-state bromate concentration that resulted with the coated membrane is less than that observed with the uncoated membrane. This is consistent with the work of Camel and Bermond [6] who showed that ozonation in the presence of heterogeneous catalysts reduced bromate formation.

As shown in Table 1, at pH 3, the steady state dissolved ozone concentration (the dissolved ozone concentration when it reaches a plateau, which was estimated from the experimental data) that resulted when the coated membrane was employed was 8% less than that observed with the uncoated membrane. At pH values of 6.0 and 8.0, the corresponding reductions in dissolved ozone concentrations were 23 and 25%, respectively. Thus, the coated membrane enhanced ozone decomposition, which resulted in lower concentrations of

dissolved ozone. As it is shown in Figure 1, four reactions in the bromate formation mechanism are dependent on the ozone concentration. Hence, the lower concentration of bromate ion formed when the coated membrane was used in the hybrid ozonation-membrane system may be a result of the lower ozone concentration present in the system.

Figure 3 also shows that the presence of t-BuOH suppresses bromate formation with both the coated and uncoated membranes. As t-BuOH scavenges hydroxyl radicals, it will suppress the initial and intermediate steps of the bromate formation mechanism (see Figure 1) and less bromate is formed.

Table 1- Steady state aqueous  $[O_3]$  at various pH values.

pH	Steady state aqueous $[O_3]$ , (mg/L)	
	uncoated	coated
3.0	9.6	8.8
6.0	8.3	6.4
8.0	4.9	3.7

Membrane: 7 channel – 5 kD,  $O_3$  mass injection rate: 1.5 mg/min, initial  $[Br^-]$ : 1 mg/L, temperature: 20°C.

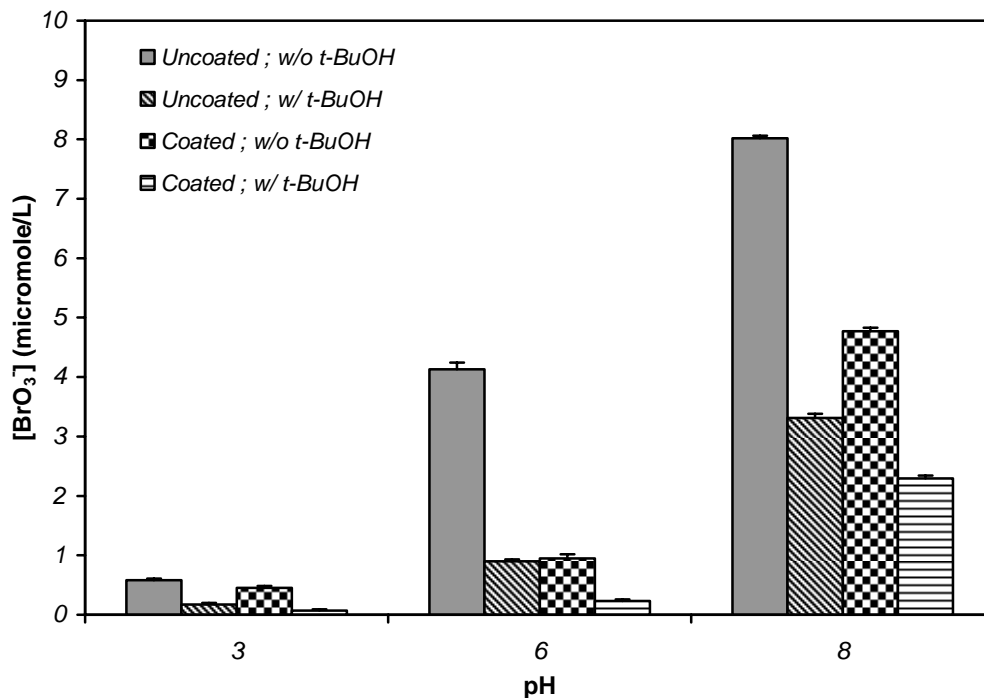


Fig. 3- Steady state bromate concentration in the permeate vs. pH. Membrane: 7 channel – 5 kD, O<sub>3</sub> mass injection rate: 1.5 mg/min, initial [Br<sup>-</sup>]: 1 mg/L, temperature: 20°C, [t-BuOH]: 0.01M. The time dependent concentration of bromate is shown in Figures S3 and S4.

#### 4.4.3. Temperature

The impact of temperature (15, 20 and 25°C) on the bromate concentration is shown in Figure 4. As temperature increases, the solubility of ozone in water decreases and the ozone decomposition rate increases [6,39-41]. Our finding that the bromate concentration increased with increasing temperature is consistent with the results reported elsewhere [1,18,42]. As shown in the inset in Figure 4, there is a linear correlation between the logarithm of the steady state aqueous ozone concentration and the operating temperature ( $R^2 = 0.917$ ). The logarithmic

relationship that resulted is consistent with the Arrhenius equation, suggesting that temperature influences the rate constant of various reactions.

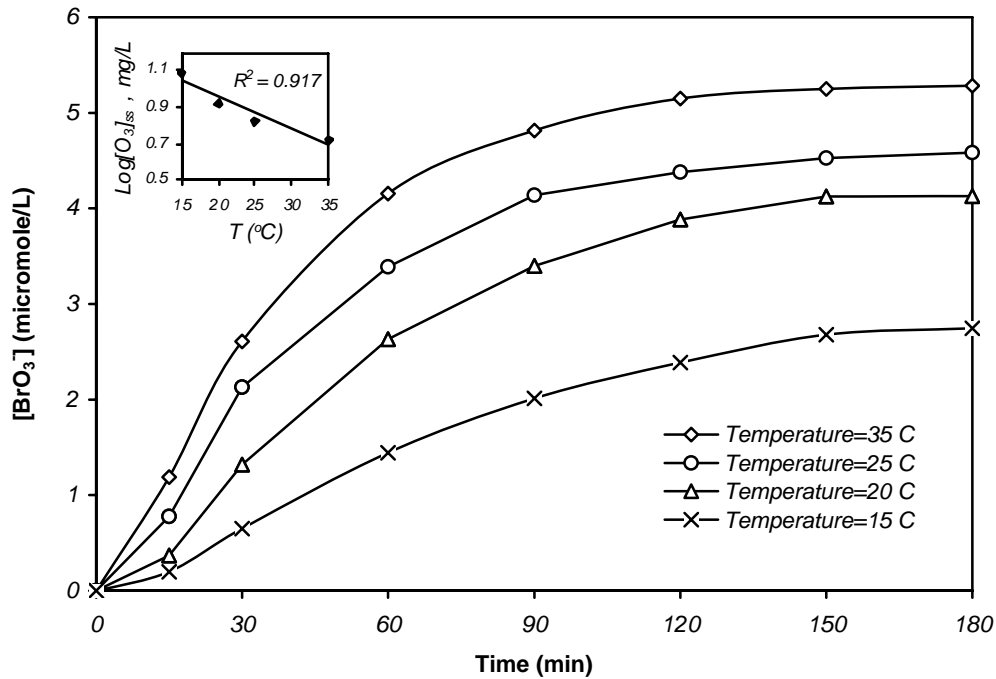


Fig. 4- Bromate concentration in the permeate vs. time at various temperatures. Membrane: 7 channel – 5 kD, O<sub>3</sub> mass injection rate: 1.5 mg/min, initial [Br<sup>-</sup>]: 1 mg/L, pH: 6.0, ionic strength: 13.0 μM

#### 4.5. Empirical Model for Bromate Formation

In an earlier work [35], the effect of pH, inlet ozone concentration, inlet gas flow rate, initial bromide concentration, and membrane molecular weight cut off (MWCO) on bromate formation was described. The data from this study has been used in this modeling effort (see Table S1). Empirical models using power functions have proved to be promising tools for simulating bromate formation during conventional ozonation systems [29,43]. As such, a power function with the following general form was used:

$$[\text{BrO}_3^-] = 10^{b_0} [\text{Br}^-]^{b_1} (\text{O}_3 \text{ mass rate})^{b_2} (\text{pH})^{b_3} (\text{T})^{b_4} (\text{t})^{b_5} \quad (1)$$

where,

$[\text{BrO}_3^-]$  = bromate concentration ( $\mu\text{g/L}$ ) in the permeate at time  $t$

$[\text{Br}^-]$  = initial bromide concentration ( $\mu\text{g/L}$ ) in the feed water,  $50 \leq [\text{Br}^-] \leq 1000$

$\text{O}_3$  mass rate = inlet gaseous ozone dose ( $\text{mg/min}$ ),  $0.5 \leq \text{O}_3 \text{ mass rate} \leq 2.25$

$\text{pH}$  = aqueous  $\text{pH}$ ,  $3.0 \leq \text{pH} \leq 8.0$

$T$  = water temperature ( $^\circ\text{C}$ ),  $15 \leq T \leq 35$

$t$  = reaction time ( $\text{min}$ ),  $0 \leq t \leq 180$

$b_i$  = regression coefficients

It should be noted that the coefficients in the model equation will vary depending upon the water composition [44] and the reactor design and that the empirical model developed is reactor specific and should only be used within the boundary conditions stated herein. In order to use the linear regression method to estimate model parameters, the power function was linearized using logarithmic transformation. After logarithmic transformation, equation 1 can be written as:

$$\log[\text{BrO}_3^-] = b_0 + b_1 \log[\text{Br}^-] + b_2 \log(\text{O}_3 \text{ mass rate}) + b_3 \log(\text{pH}) + b_4 \log(T) + b_5 \log(t) \quad (2)$$

Two hundred and sixty three (263) data points were used to perform the regression. Regression coefficients were determined by multiple linear regression analysis of the experimental data using Excel. After substitution the following empirical model is obtained. The standard error values for the coefficients  $[\text{Br}^-]$ ,  $\text{O}_3$  mass injection rate,  $\text{pH}$ ,  $T$ , and  $t$  were determined to be 0.023, 0.050, 0.088, 0.113, and 0.022. The standard error of estimation was 0.129.

$$[\text{BrO}_3^-] = 3.855 \times 10^{-8} [\text{Br}^-]^{1.430} (\text{O}_3 \text{ mass rate})^{0.927} (\text{pH})^{3.005} (\text{T})^{1.195} (\text{t})^{0.831} \quad (3)$$

#### 4.6. Model Validation

In order to validate the ability of the above model to predict bromate formation in the hybrid system, the bromate concentrations predicted by the model for various operating conditions were calculated using Equation 3. The sign of the coefficient in Equation 3 indicates whether a particular variable exerts a positive or negative influence on bromate formation. Hence, according to the model, bromate formation is favoured at high bromide concentration, ozone dose, pH, and temperature. This is consistent with the trends reported by Moslemi et al. [35].

Figure 5 shows the relationship between the observed bromate concentrations and the predicted values. The dotted lines in this figure indicate the 95% confidence intervals. Good agreement between the model predictions and experimental results was achieved ( $R^2=0.903$ ). The slope of the regression line was nearly one, which is indicative of a very good fit between the experimental and predicted bromate concentrations. However, since the slope is greater than 1, the model tends to slightly over-predict the bromate concentration at high concentration and under predict at low concentration. Similarly, the model proposed by Sohn et al. [32] overpredicted the bromate concentrations.

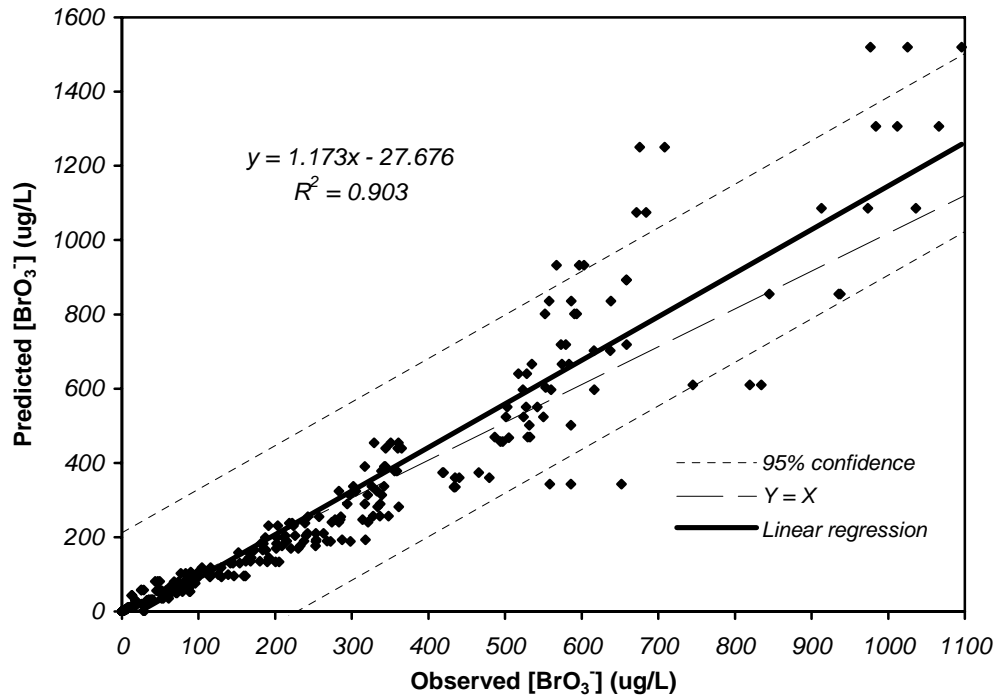


Fig. 5- Predicted bromate concentration vs. observed values.

Figures 6 to 9 indicate model results versus observed values as a function of time for sample sets of experiments. As it can also be seen from the plots, good agreement between the measured bromate concentrations and predicted values was achieved and the  $R^2$  and slope of the trendline is close to 1. Hence, the empirical bromate model can be favourably employed to predict bromate formation under various operating conditions. This enables the operators and engineers to manipulate the ozonation system in order to meet the standards for bromate ion.

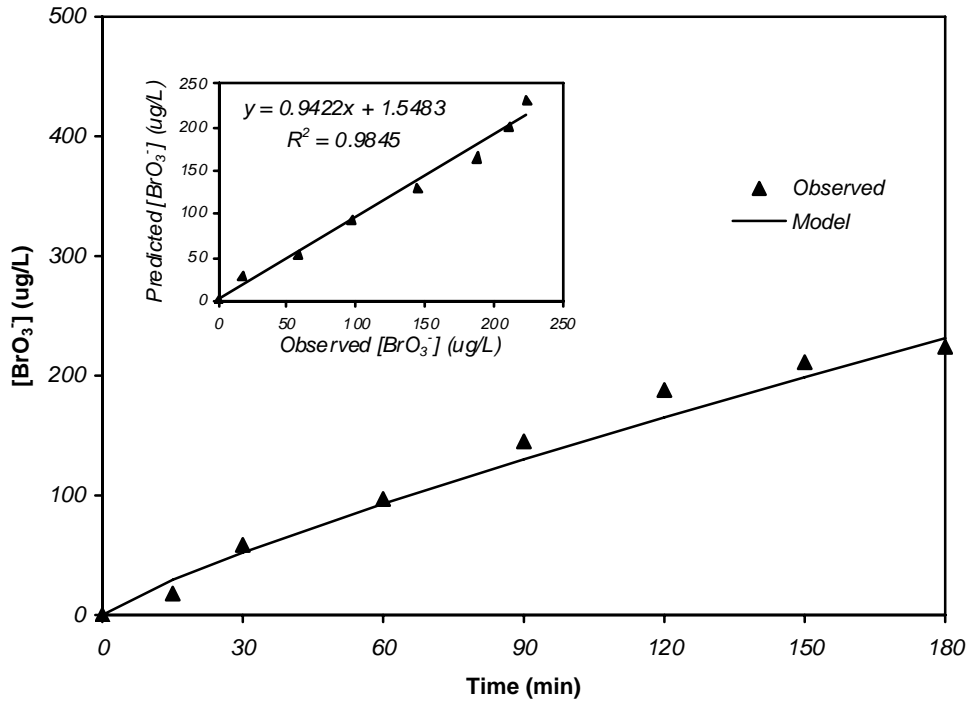


Fig. 6- Measured and simulated bromate concentrations vs. contact time. [Br<sup>-</sup>]: 1000 µg/L, O<sub>3</sub> mass injection rate: 0.5 mg/min, pH: 6.0, T: 20°C

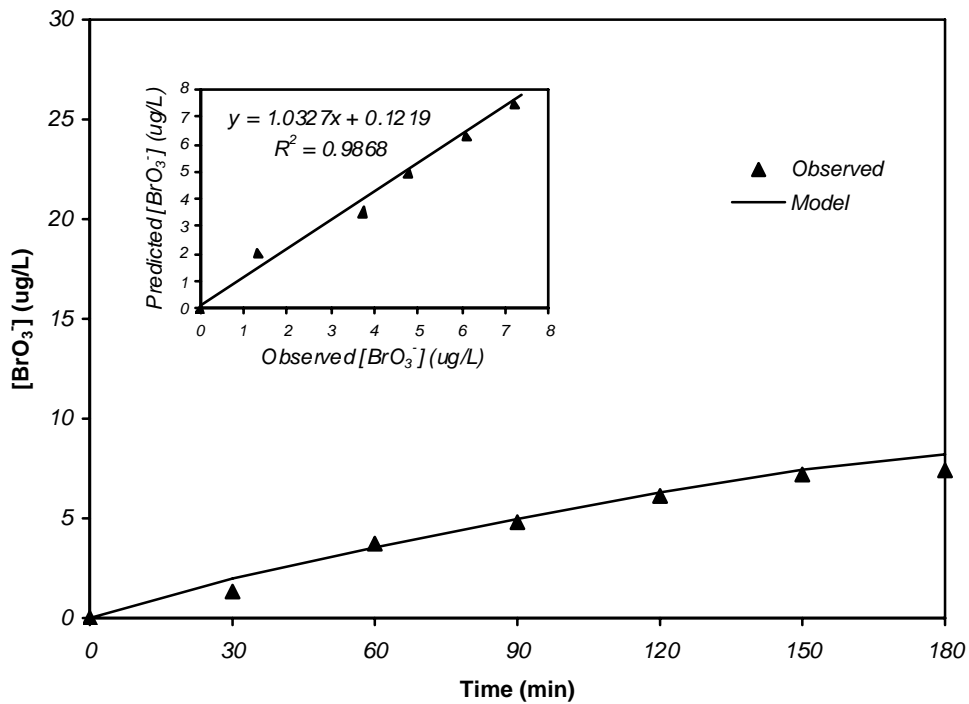


Fig. 7- Measured and simulated bromate concentrations vs. contact time. [Br<sup>-</sup>]: 50 µg/L, O<sub>3</sub> mass injection rate: 1.5 mg/min, pH: 6.0, T: 20°C

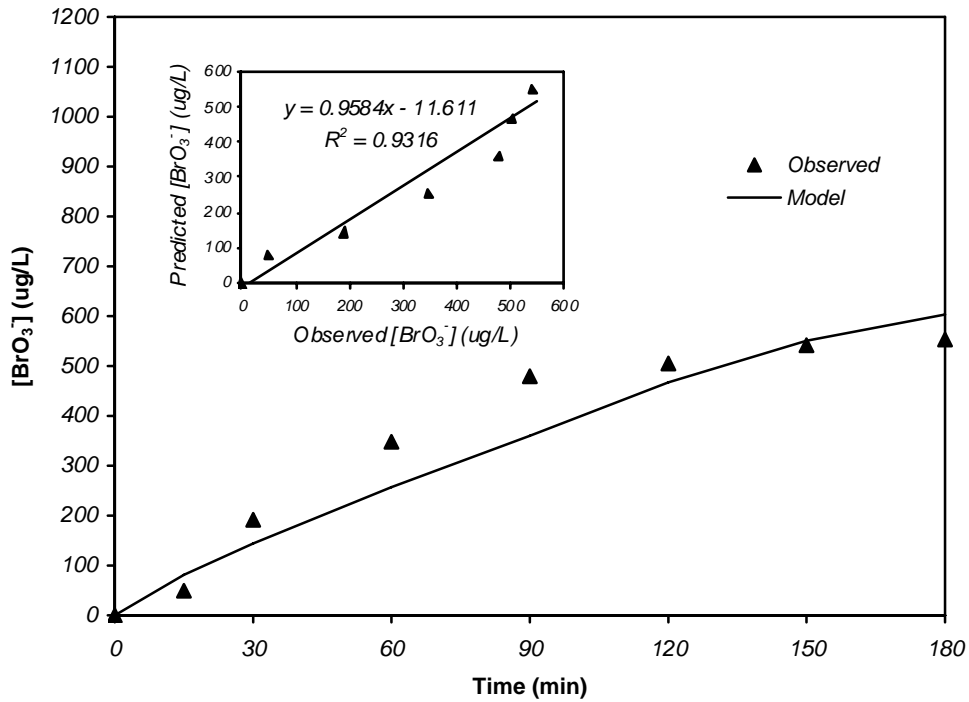


Fig. 8- Measured and simulated bromate concentrations vs. contact time. [Br<sup>-</sup>]: 1000 µg/L, O<sub>3</sub> mass injection rate: 1.5 mg/min, pH: 6.0, T: 20°C

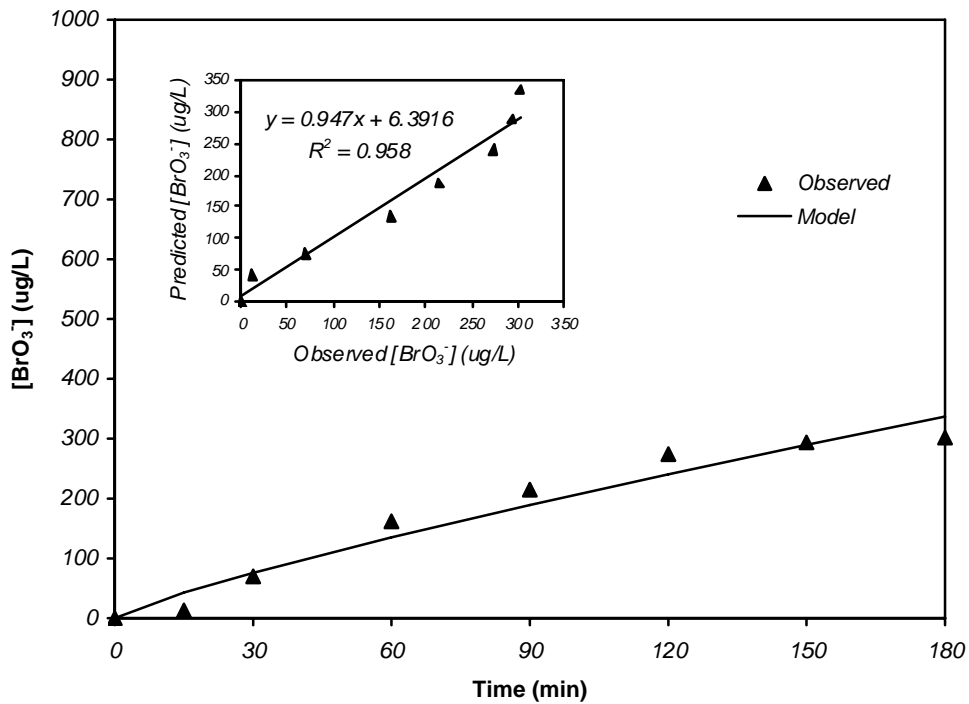


Fig. 9- Measured and simulated bromate concentrations vs. contact time. [Br<sup>-</sup>]: 1000 µg/L, O<sub>3</sub> mass injection rate: 0.75 mg/min, pH: 6.0, T: 20°C

## 4.7. Conclusion

Unlike empirical bromate models developed for conventional ozonation processes [26,43], the model described herein demonstrates that the initial bromide concentration plays a more significant role than does the ozone dose, although increasing the ozone dose resulted in an increase in the steady state bromate concentration [35].

The reduction in pH, ozone dose, and contact time can be used as strategies to suppress bromate formation. However, the most practical bromate control strategies would be to reduce the ozone dose or contact time. The contact time may be decreased by increasing the operating pressure or by using coarser membranes, which will also result in lower transmembrane pressures, decreased energy costs, and increased the permeate flux. The choice of ozone dose and contact time will be a compromise between the control of both fouling and bromate concentrations. Karnik et al. [14], along with other researchers [13,16], have shown that very low dissolved ozone concentrations ( $<0.3$  mg/L) are needed to maintain continuous operation of the hybrid ozonation-filtration system at a relatively high permeate flux (more than 90% of the initial flux) without the need for membrane cleaning. As mentioned earlier, ceramic membrane surfaces appear to enhance ozone decomposition and hydroxyl radical formation. Hydroxyl radicals are more efficient in terms of oxidation and the removal of ozone resistant compounds and chlorination disinfection by-products precursors [5,6]. Therefore, besides fouling control, such hybrid processes can be effective in

reducing the concentration of final chlorination by-products and also inactivating resistant pathogens.

#### **4.8. Supporting Documentation**

Dissolved ozone and bromate concentrations versus time for the experiments carried out in the presence of hydroxyl radical scavenger (t-BuOH) are presented in Figures S1 and S2, respectively. Figures S3 indicate the effect of membrane coating on bromate formation at various pHs. The effect of hydroxyl radical scavenger on bromate formation using coated and uncoated membranes is shown in Figure S4. The following plots are representative of the data generated in the replicate experiments. Table S1 summarizes the results of an earlier work [35] including the effect of pH, inlet ozone concentration, inlet gas flow rate, initial bromide concentration, and membrane molecular weight cut off on bromate formation.

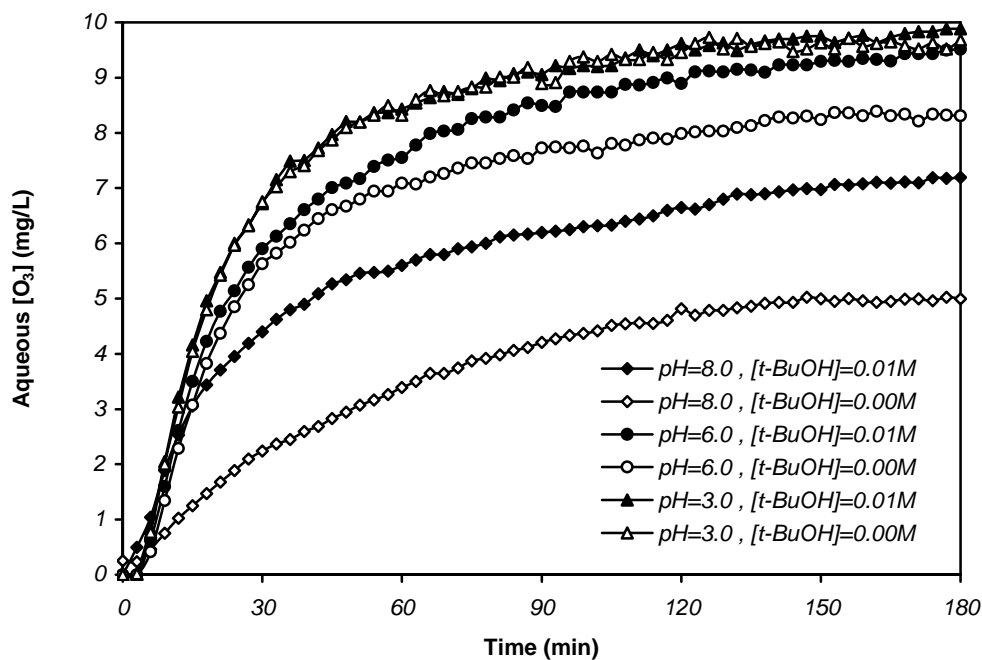


Fig. S1- The effect of  $\cdot\text{OH}$  scavenger on the dissolved ozone concentration in the permeate vs. time at various pHs. Membrane: 7 channel – 5 kD,  $\text{O}_3$  mass injection rate: 1.5 mg/min, initial  $[\text{Br}^-]$ : 1 mg/L, temperature: 20°C

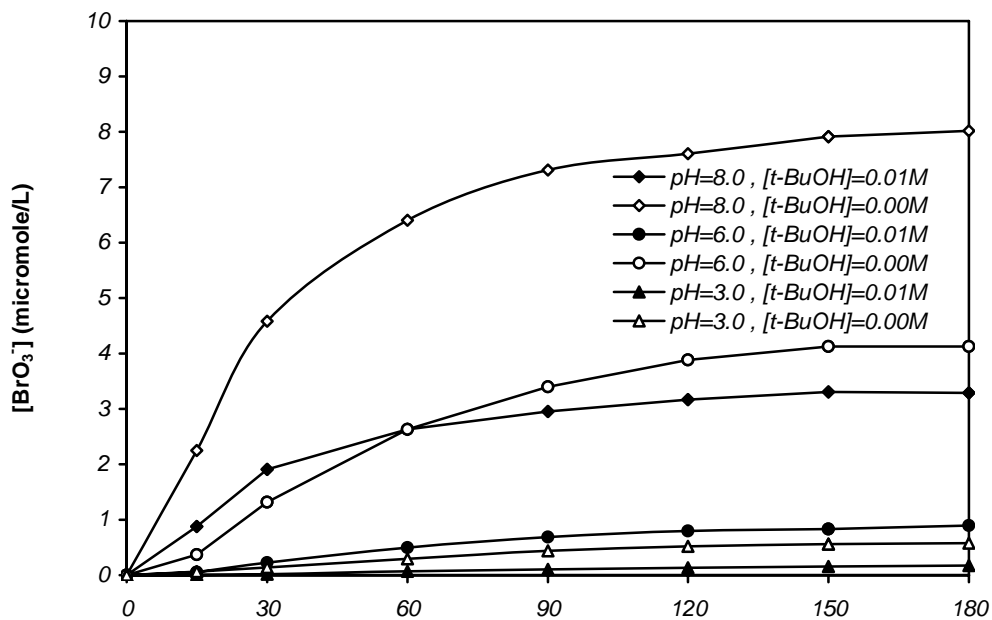


Fig. S2- The effect of  $\cdot\text{OH}$  scavenger on the bromate concentration in the permeate vs. time at various pHs. Membrane: 7 channel – 5 kD,  $\text{O}_3$  mass injection rate: 1.5 mg/min, initial  $[\text{Br}^-]$ : 1 mg/L, temperature: 20°C

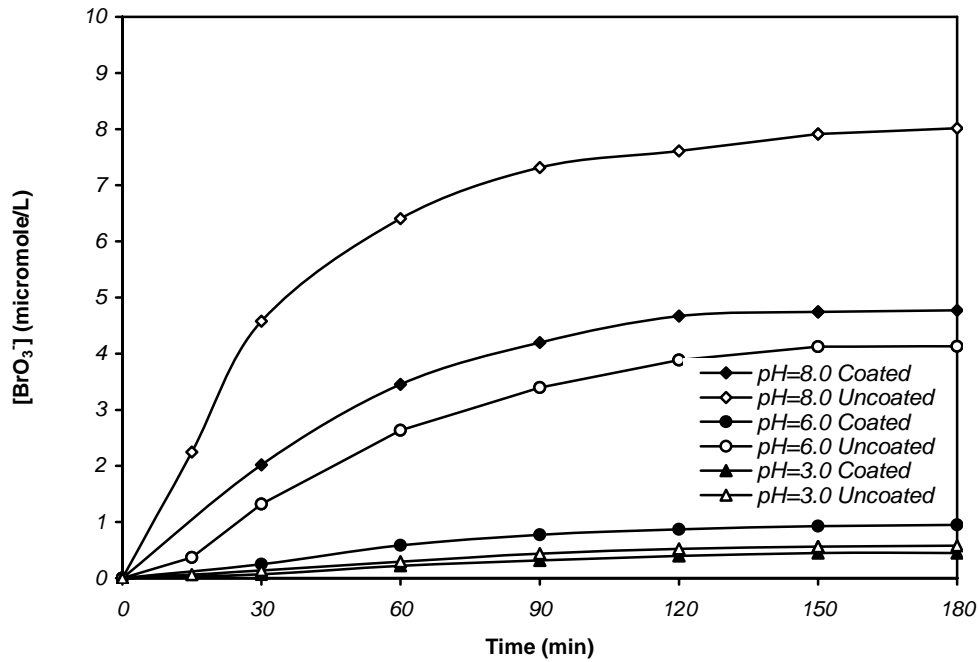


Fig. S3- Bromate concentration in permeate vs. time at various pH values. The effect of membrane coating. Membrane: 7 channel – 5 kD, O<sub>3</sub> mass injection rate: 1.5 mg/min, initial [Br<sup>-</sup>]: 1 mg/L, temperature: 20°C, ionic strength: 512.5, 13.0 and 12.5 μM corresponding to pH 3, 6 and 8, respectively.

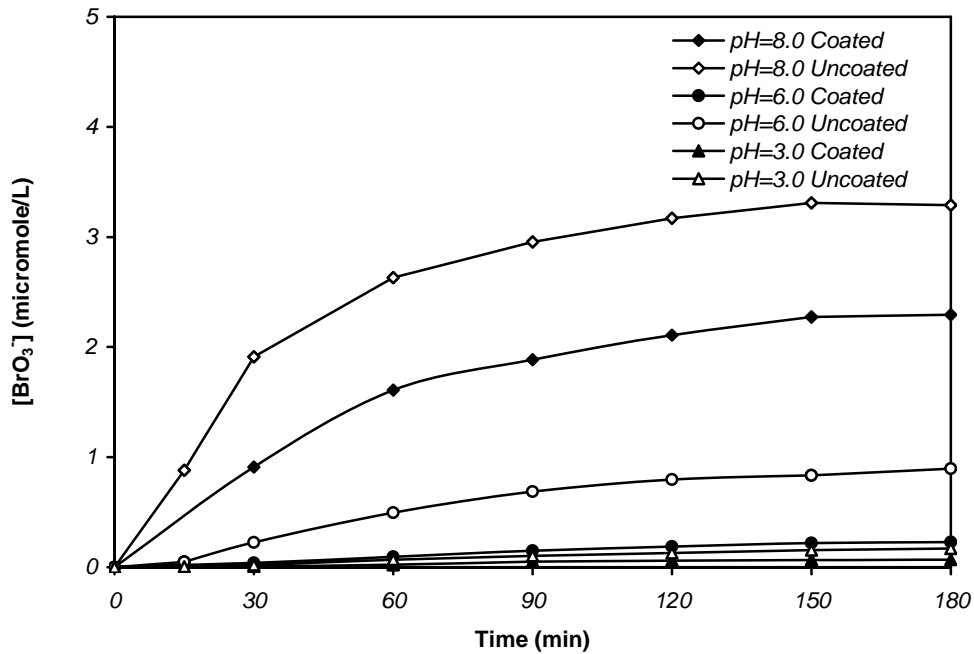


Fig. S4 - Bromate concentration in the permeate vs. time in the presence of t-BuOH. The effect of membrane coating. Membrane: 7 channel – 5 kD, O<sub>3</sub> mass injection rate: 1.5 mg/min, initial [Br<sup>-</sup>]: 1 mg/L, temperature: 20°C, [t-BuOH]: 0.01M

Table S1- Steady state bromate concentration in the permeate under various operating conditions

pH	O <sub>3</sub> mass injection rate (mg/min)	Initial [Br <sup>-</sup> ] (mg/L)	MWCO (kD)	Temperature (°C)	Steady state [BrO <sub>3</sub> <sup>-</sup> ] (µM)
3	1.5	1.00	5	20	0.579
6	1.5	1.00	5	20	4.129
8	1.5	1.00	5	20	8.018
6	0.5	1.00	5	20	1.573
6	1.0	1.00	5	20	2.860
6	0.75	1.00	5	20	2.549
6	2.25	1.00	5	20	4.666
6	1.5	0.05	5	20	0.055
6	1.5	0.25	5	20	0.718
6	1.5	0.50	5	20	1.751
6	1.5	1.00	8	20	3.184
6	1.5	1.00	15	20	2.667

#### 4.9. References

- [1] U. von Gunten, Ozonation of drinking water: Part II. Disinfection and by-product formation in presence of bromide, iodide or chlorine, *Wat. Res.* 37 (2003) 1469-1487.
- [2] M.S. Chandrakanth, B.D. Honeyman, G.L. Amy, Modeling the interactions between ozone, natural organic matter, and particles in water treatment, *Colloids Surf. A: Physiochem. Eng. Aspects* 107 (1996) 321-342.
- [3] R.G. Rice, C.M. Robson, G.W. Miller, A.G. Hill, Use of ozone in drinking water treatment., *J. AWWA* 73 (1981) 44-57.

- [4] W.H. Glaze, Drinking water treatment with ozone, *Environ. Sci. Technol.* 21 (1987) 224-230.
- [5] A. Peter, U. von Gunten, Oxidation kinetics of selected taste and odour compounds during ozonation of drinking water, *Environ. Sci. Technol.* 41 (2007) 626-631.
- [6] V. Camel, A. Bermond, The use of ozone and associated oxidation processes in drinking water treatment, *Wat. Res.* 32 (1998) 3208-3222.
- [7] C. Gottschalk, J.A. Libra, A. Saupe, *Ozonation of water and waste water: A practical guide to understanding ozone and its application*, Wiley-VCH, New York, 2000.
- [8] B. Langlais, D.A. Reckhow, D.R. Brink, *Ozone in water treatment: Application and engineering: Cooperative research report*, AWWA Research Foundation, Lewis Publishers, Michigan, 1991.
- [9] C. Gomella, Ozone practice in France, *J. AWWA* 64 (1972) 39-46.
- [10] J. Crittenden, M.W. Harza, *Water treatment: Principles and design*, second ed. MWH, John Wiley, New Jersey, 2005.
- [11] S. van Geluwe, L. Braeken, B. van der Bruggen, Ozone oxidation for the alleviation of membrane fouling by natural organic matter: A review, *Wat. Res.* 45 (2011) 3551-3570.
- [12] J.W. Kim, W.Q. Shan, H.R. Davies, S.J. Masten, V.B. Tarabara, Interactions of Aqueous NOM with Nanoscale TiO<sub>2</sub>: Implications for Ceramic

- Membrane Filtration-Ozonation Hybrid Process, *Environ. Sci. Technol* 43 (2009) 5488-5494.
- [13] S. Mozia, M. Tomaszewska, A.W. Morawski, Application of an ozonation-adsorption-ultrafiltration system for surface water treatment, *Desalination* 190 (2006) 308-314.
- [14] B.S. Karnik, S.H.R. Davies, K.C. Chen, D.R. Jaglowski, M.J. Baumann, S.J. Masten, Effects of ozonation on the permeate flux of nanocrystalline ceramic membranes, *Wat. Res.* 39 (2005) 728-734.
- [15] Y.G. Park, Effect of ozonation for reducing membrane-fouling in the UF membrane, *Desalination* 147 (2002) 43-48.
- [16] B. Schlichter, V. Mavrov, H. Chmiel, Study of a hybrid process combining ozonation and membrane filtration - filtration of model solutions, *Desalination* 156 (2003) 257-265.
- [17] S.H. You, D.H. Tseng, W.C. Hsu, Effect and mechanism of ultrafiltration membrane fouling removal by ozonation, *Desalination* 202 (2007) 224-230.
- [18] U. von Gunten, U. Pinkernell, Ozonation of bromide-containing drinking waters: a delicate balance between disinfection and bromate formation, *Wat. Sci. Technol.* 41 (2000) 53-59.
- [19] S.W. Krasner, W.H. Glaze, H.S. Weinberg, P.A. Daniel, I.N. Najm, Formation and control of bromate during ozonation of waters containing bromide, *J. AWWA* 85 (1993) 73-81.

- [20] USEPA, National primary drinking water regulations: Disinfection and disinfection byproducts, Federal Register 63 (1998) 69390-69476.
- [21] G.L. Amy et al., Bromate occurrence: National bromide survey, AWWARF Report, Denver, 1993.
- [22] W.R. Haag, J. Hoigne, Ozonation of bromide-containing waters: Kinetics of formation of hypobromous acid and bromate, Environ. Sci. Technol. 17 (1983) 261-267.
- [23] U. Pinkernell, U. von Gunten, Bromate minimization during ozonation: Mechanistic considerations, Environ. Sci. Technol. 35 (2001) 2525-2531.
- [24] U. von Gunten, Y. Oliveras, Advanced oxidation of bromide-containing waters: Bromate formation mechanisms, Environ. Sci. Technol. 32 (1998) 63-70.
- [25] T. Mizuno, H. Yamada, H. Tsuno, Formation of bromate ion through a radical pathway in a continuous flow reactor, Ozone Sci. Eng. 26 (2004) 573-584.
- [26] P. Jarvis, S.A. Parsons, R. Smith, Modeling bromate formation during ozonation, Ozone Sci. Eng. 29 (2007) 429-442.
- [27] R. Song, C. Donohoe, R. Minear, P. Westerhoff, K. Ozekin, G. Amy, Empirical modeling of bromate formation during ozonation of bromide-containing water, Wat. Res. 30 (1996) 1161-1168.

- [28] M. Siddiqui, G. Amy, K. Ozekin, P. Westerhoff, Empirically and theoretically-based models for predicting brominated ozonated by-products, *Ozone Sci. Eng.* 16 (1994) 157-178.
- [29] P. Jarvis, R. Smith, S.A. Parsons, A robust analysis of bromate formation models, *Water Practice Technol.* 4 (2006) Vol 1.
- [30] T. Mizuno, H. Tsuno, H. Yamada, A simple model to predict formation of bromate ion and hypobromous acid/hypobromite ion through hydroxyl radical pathway during ozonation, *Ozone Sci. Eng.* 29 (2007) 3-11.
- [31] U. von Gunten, J. Hoigne, Factors controlling the formation of bromate during ozonation of bromide containing waters, *J. Water SRT-Aqua* 41 (1992) 299–304.
- [32] J. Sohn, G. Amy, J. Cho, Y. Lee, Y. Yoon, Disinfectant decay and disinfection by-products formation model development: chlorination and ozonation by-products, *Wat. Res.* 38 (2004) 2461–2478.
- [33] J. Staehelin, J. Hoigne, Decomposition of ozone in water: Rate of initiation by hydroxide ions and hydrogen peroxide, *Environ. Sci. Technol.* 16 (1982) 676-681.
- [34] M.S. Siddiqui, G.L. Amy, Factors affecting DBP formation during ozone-bromide reactions, *J. AWWA* 85 (1993) 63-72.
- [35] M. Moslemi, S.H. Davies, S.J. Masten, Bromate Formation in a Hybrid Ozonation – Ceramic Membrane Filtration System, *Wat. Res.* 45 (2011) 5529-5534.

- [36] B.S. Karnik, S.H. Davies, M.J. Baumann, S.J. Masten, Use of salicylic acid as a model compound to investigate hydroxyl radical reaction in ozonation-membrane filtration hybrid process, *Environ. Eng. Sci.* 24 (2007) 852-860.
- [37] L.M. Corneal, S.J. Masten, S.H.R. Davies, V.V. Tarabara, S. Byun, M.J. Baumann, AFM, SEM and EDS characterization of manganese oxide coated ceramic water filtration membranes, *J. Mem. Sci.* 360 (2010) 292-302.
- [38] S. Byun, S.H. Davies, A.L. Alpatova, L.M. Corneal, M.J. Baumann, V.V. Tarabara, S.J. Masten, Mn oxide coated catalytic membranes for a hybrid ozonation-membrane filtration: Comparison of Ti, Fe and Mn oxide coated membranes for water quality, *Wat. Res.* 45 (2011) 163-170.
- [39] E. Rischbieter, H. Stein, A. Schumpe, Ozone solubilities in water and aqueous salt solutions, *J. Chem. Eng. Data.* 45 (2000) 338-340.
- [40] M. Guiza, A. Ouederni, A. Ratel, Decomposition of dissolved ozone in the presence of activated carbon: An experimental study, *Ozone Sci. Eng.* 26 (2004) 299-307.
- [41] J.L. Sotelo, F.J. Beltran, F.J. Benitez, J.B. Heredia, Henry's law constant for the ozone-water system, *Wat. Res.* 23 (1989) 1239-1246.
- [42] A. Driedger, E. Staub, U. Pinkernell, B. Marinas, W. Koster, U. von Gunten, Inactivation of *Bacillus Subtilis* spores and formation of bromate during ozonation, *Wat. Res.* 37 (2001) 2950-2960.

- [43] R. Song, R. Minear, P. Westerhoff, G. Amy, Modeling and risk analysis of bromate formation from ozonation of bromide-containing waters, *Water Sci. Technol.* 34 (1996) 79-85.
- [44] J.H. Kim, U. von Gunten, B.J. Marinas, Simultaneous prediction of *Cryptosporidium parvum* oocyst inactivation and bromate formation during ozonation of synthetic waters, *Environ. Sci. Technol.* 38 (2004) 2232-2241.

## **Chapter 5: Disinfection By-products Formation in the Presence of NOM in a Hybrid Ceramic Membrane Filtration – Ozonation**

### **5.1. Abstract**

The effect of pH, inlet ozone mass injection rate, natural organic matter (NOM) concentration, initial bromide concentration, membrane coating, hydroxyl radical scavenger, and membrane molecular weight cut off (MWCO) on the formation of disinfection by-products (including bromate ( $\text{BrO}_3^-$ ), chloroform ( $\text{CHCl}_3$ ), bromoform ( $\text{CHBr}_3$ ), dichlorobromomethane ( $\text{CHBrCl}_2$ ), dibromochloromethane ( $\text{CHBr}_2\text{Cl}$ ), and also the effect of inlet ozone mass injection rate on the formation of halo acetic acids (HAAs) in a hybrid membrane filtration–ozonation reactor treating bromide containing water was studied. Furthermore, variations in the TOC,  $\text{UV}_{254}$ , SUVA (specific UV absorbance), color and turbidity of water as function of these parameters were investigated. Bromate formation increased with increasing inlet gaseous ozone mass injection rate, and initial bromide concentration. TTHMs (total trihalomethanes) formation favoured at high initial bromide concentration. In the presence of NOM less bromate was formed. The extent of bromate formation decreased with decreasing pH. The presence of hydroxyl radical scavengers (tertiary butyl alcohol (t-BuOH)) significantly reduced bromate and TTHM formation. The bromate and TTHM concentrations that were observed with the Mn oxide coated membrane were less than that formed with the

uncoated TiO<sub>2</sub> membrane. An increase in the bromate concentration was observed with decreasing MWCO of the filtration membrane. Consistent with earlier work, experimental results indicated that ozonation can be used to overcome membrane fouling problem by maintaining a minimum dissolved ozone concentration in the system. This allows for continuous operation of the hybrid ozonation-membrane filtration system at a relatively high permeate flux as compared to the original permeate flux obtained with pure water. An empirical model was also developed using multiple linear regression method to estimate bromate formation in the system as a function of bromide concentration, dissolved organic carbon (DOC) concentration, inlet ozone mass injection rate, pH, and reaction time. Good correlation was achieved between the model predictions and the experimental data. According to the model, bromate formation was favoured as bromide concentration, ozone mass injection rate, and pH increased. However, increase in DOC exerted reverse effect on bromate formation.

**Keywords:** bromide, bromate, THMs, ozonation, ceramic membrane, modeling

## 5.2. Introduction

Pressure driven membrane filtration has recently gained increasing application in drinking water treatment (Gottschalk et al., 2000, Schlichter et al., 2003). However, such systems have a major disadvantage which is the fouling of the membrane due to the deposition of organic material on the membrane and inside the membrane. A solution to the fouling problem is to inject ozone into the

membrane filtration system. It has been shown that ozone is able to decompose NOM species and remove them from the membrane surface and, as such, prevent fouling (Van Geluwe et al., 2011, Kim et al., 2010, Mozia et al., 2006; Karnik et al., 2005).

The incorporation of a strong oxidizer such as ozone into the water treatment system can lead to the formation of disinfection by-products, some of which could be of health concern to humans. For instance, the bromide ion ( $\text{Br}^-$ ) in drinking water does not exert adverse health effects on human beings (Siddiqui et al., 1995); however, the ozonation of bromide containing waters can result in the formation of organic and inorganic by-products such as bromate, trihalomethanes (THMs), and haloacetic acids (HAAs), which are potential carcinogens (Morris et al., 1992) and are regulated in drinking water. The United States Environmental Protection Agency (USEPA), the Ministry of the Environment (Ontario Safe Drinking Water Act, Canada), and the European Union have set the maximum contaminant level (MCL) for bromate at 0.01 mg/L. The MCL for TTHMs is 0.08, 0.1, and 0.1 as set by USEPA, the Ontario Ministry of the Environment, and the European Union, respectively (Ontario drinking-water quality standards, 2002; European Union, 1998; USEPA, 1998). Although ozone is a much stronger disinfectant than conventional disinfectants such as chlorine, it is very short-lived (Evans, 1972). Therefore, in order to maintain residual disinfectant in the distribution system a secondary and long-lasting disinfectant such as chlorine

needs to be eventually added to water, leading to the potential formation of TTHMs and HAAs.

Bromate is formed through multistage reactions of molecular ozone and OH radicals with the bromide ion (Leqube et al., 2004; Pinkernell and von Gunten, 2001) OH radicals are generated as a result of ozone decomposition in the aqueous phase or on the solid surface. Both direct (involving molecular ozone) and indirect (involving OH radicals) pathways play a role in bromate formation; however the rate constants for the reaction of OH radicals with bromide are considerably greater than that of ozone molecule and according to literature (Mizuno et al., 2004; von Gunten and Oliveras, 1998) OH radicals contribute more significantly to bromate formation than molecular ozone does. Bromide and brominated compounds present in the ozonation system can react with NOM and form bromo-organic by-products such as bromoform. Furthermore, in the post chlorination step, chlorine can also react with NOM and brominated organic by-products present in the ozonation system and contribute to the formation of various forms of THMs and HAAs (Camel and Bermond, 1998).

Hence, it is crucial to study DBP formation during drinking water treatment of bromide containing waters using ozonation systems. This study focuses on DBP formation in hybrid ozonation-membrane filtration systems in the presence of NOM and investigates the influence of important operating parameters including pH, inlet ozone mass injection rate, NOM concentration, initial bromide

concentration, membrane coating, hydroxyl radical scavenger, and membrane MWCO on DBP concentrations.

Moreover, an empirical model was generated to predict bromate formation in hybrid ozonation-filtration systems. Power function with multiple linear regression was used for the modeling purpose. This method has been widely used by researchers (Mizuno et al., 2007; Jarvis et al., 2007; Sohn et al., 2004, Song et al., 1996) for the modeling of DBPs formation in conventional ozonation systems and satisfactory results have been reported. The independent variables used in the model included bromide concentration, dissolved organic carbon concentration, ozone mass injection rate, pH, and reaction time.

### **5.3. Materials and Methods**

#### **5.3.1. Experimental Setup**

Figure 1 shows the schematic of the experimental apparatus used in this study (also Fig. A1). The system was designed to withstand pressures of up to 550 kPa (80 psi) and pressurized using nitrogen gas. The experimental apparatus was equipped with two high-pressure stainless steel tanks with capacities of 5 and 8 liters (Fig. A2). The smaller tank was located in the recycle line to supply the system with the feed water. The second tank operated as reserve raw water supply to replace the water lost from the system through permeation and bleeding and was connected to the main tank through a solenoid valve (Type 6013, Bürkert Corp., USA ), which was programmed to maintain a constant water level in the

main tank. The total water volume and the pressure inside the reactor were maintained at 1.5 L and 138 kPa (20 psi), respectively, throughout the experiments. All equipment, tubing and connections were made of ozone resistant materials and were either Teflon® or 316-stainless steel. Water was circulated in the loop at a flow rate of 200 mL/min using a gear pump (Model 000-380, Micropump Inc., USA). The water inside the tank was mixed as a result of the turbulence produced by the jet of water as it was returned to the tank.

Gaseous ozone was generated from pressurized oxygen gas (having a purity of 99.999%) using a corona discharge ozone generator (Absolute Ozone AE15MC80P, Absolute System Inc., Edmonton, AB, Canada). The gaseous ozone concentration was adjusted by varying the ozone generator's voltage. Ozone gas was injected into the water stream flowing in the recirculation loop through a Swagelok Tee fitting (Model SS-400-3, Swagelok, USA). Ozone was transferred from the gas phase to the aqueous phase, as a result of the hydraulic mixing inside the reactor. The inlet gas flow rate was adjusted to the desired values using a digital flow-controller (Model MC-500SCCM-D, Alicat Scientific Inc., USA). Any gas exhausted from the system was destroyed by purging the gas through a potassium iodide (2% KI) solution. A pressure regulator (Model KCB1F0A2A5P20000, Swagelok, USA) was employed to monitor and regulate the pressure in the recirculation loop. The water temperature was kept at  $20 \pm 0.1$  °C by recycling water through a water coil which was installed inside the main tank

(Fig. A3). The temperature of the chilled water was controlled using a refrigerated circulator bath (NESLAB RTE-10, Thermo Fisher Scientific, USA).

In these experiments, tubular ultrafiltration (UF) ceramic membranes (TAMI North America, QC, Canada) with nominal molecular weight cut offs of 5, 8 and 15 kilodaltons (kD) were used (Fig. A4). UF membranes, rather than nanofiltration (NF) membranes, were chosen because the desired flux can be achieved at a lower operating pressure with a UF membrane than with an NF membrane. Ceramic membranes were used as they are ozone resistant. The active length and the external diameter of the employed membranes were 25 cm and 10 mm, respectively. A stainless steel housing (TAMI North America, QC, Canada) was used to hold the membrane.

A bleed line was installed in the recycle loop to allow the retentate to be sampled. The bleed flow rate was set to 5.0 mL/min using a digital flow-controller (Model LC-50CCM-D, Alicat Scientific Inc., USA). A digital flow meter (Model L-5LPM-D, Alicat Scientific Inc., USA) and a digital pressure gauge (Model 2074, Ashcroft Inc., USA) were mounted in the loop to monitor the water flow rate and pressure within the system. The permeate flux was continuously measured using a balance (Adventurer Pro, Ohaus Corporation, USA). Temperature, pressure, and cross flow rate were continuously recorded using a data acquisition system (LabView, National Instruments, USA).

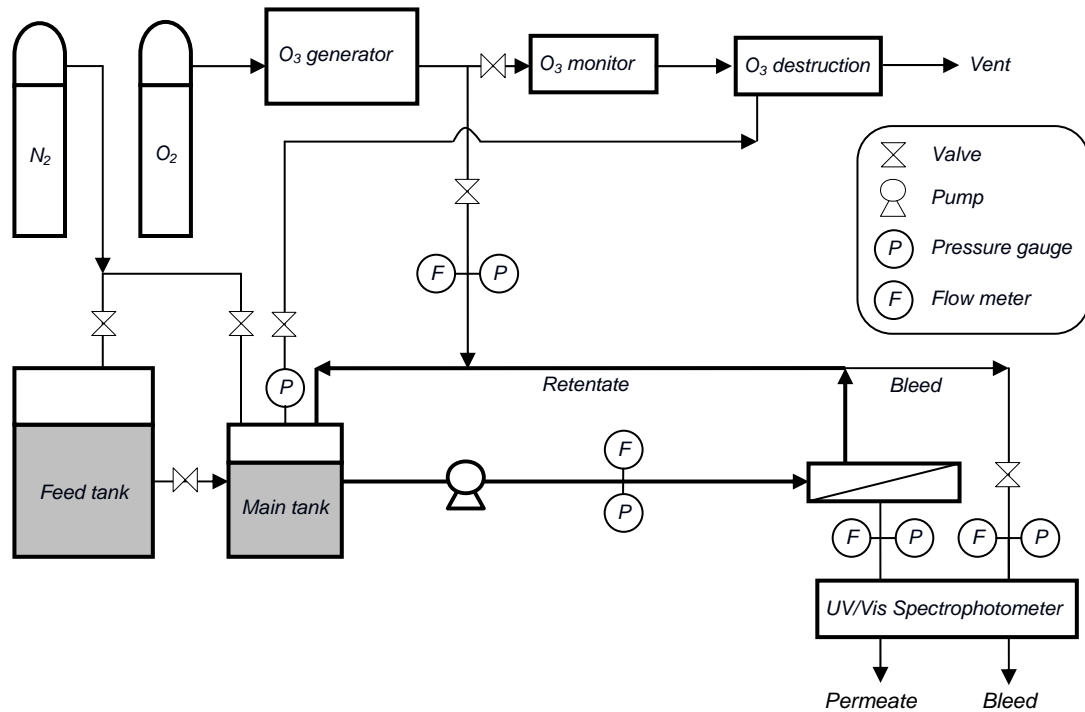


Fig. 1- Schematic of the experimental setup.

### 5.3.2. Analytical Methods

The experiments were continued for 180 min, and samples were taken from both permeate and retentate lines during the experiments. The concentrations of aqueous ozone in the permeate and the retentate were measured using the indigo colorimetric method 4500- $O_3$  (Standard Methods, APHA). To quench further ozone reactions, the residual dissolved ozone in the samples were immediately purged by bubbling nitrogen gas through the sample for 2 minutes. Prior to analysis, water samples were filtered through a  $0.45\ \mu\text{m}$  microfilter (Millipore). A

UV/Vis spectrophotometer (Model 4054, Pharmacia LKB, Biochrom Ltd., UK) was used to measure the  $UV_{254}$  of the samples at a wavelength of 254 nm.

The TOC of the water samples was measured in triplicate using a TOC analyzer (Model 1010 Analyzer, OI Analytical, College Station, TX). Color and turbidity of the water samples were measured using a spectrophotometer (DR 2000, Hach Company, USA). pH was measured using a pH meter (pHTestr 30, Eutech Instruments, Illinois, USA). The inlet ozone gas concentration was also continuously measured using a UV ozone monitor (Model 454H, Teledyne Instruments, USA).

Bromide and bromate concentrations in the samples were measured in triplicate using an ion chromatograph, consisting of a high performance liquid chromatography system (Model 230, Varian ProStar, USA) with an anion-exchange column (IonPac AS23, Dionex Corp., USA) a guard column (IonPac AG23, Dionex Corp., USA), an anion micromembrane suppressor (AMMS III - 4mm, Dionex Corp., USA) and a conductivity detector (CD25A, Dionex Corp., USA). The analysis was carried out in accordance with the method proposed by Dionex (Application Note 184, Dionex Corp., USA). The solution of 4.5 mM sodium carbonate ( $NaCO_3$ ) (99.5%, EMD, USA) and 0.8 mM sodium bicarbonate ( $NaHCO_3$ ) (99.7%, Sigma-Aldrich, Germany) was used as the mobile phase. The column flow rate was 1 mL/min.

Following the experiments, the simulated distribution system (SDS) THMs and SDS HAAs was measured in order to simulate the formation of THMs and HAAs

in the drinking water distribution system. To this end, water samples were dosed with chlorine at a concentration to achieve a residual chlorine in the range of 0.5-2 mg/L after 48 hr incubation at room temperature. SDS THMs and SDS HAAs were measured in triplicate in accordance with the oxidant demand method 2350 (Standard Methods, APHA) and EPA method 552.3 (USEPA, 2003), respectively.

A Perkin Elmer Autosystem gas chromatography machine (Perkin Elmer Instruments, Shelton, CT) with an electron capture detector (ECD) and a 30 m long  $\times$  0.25 mm ID, 1  $\mu$ m DB-5ms column (J&W Scientific, Folsom, CA) was employed to measure the concentration of chloroform, dichlorobromomethane, dibromochloromethane, and bromoform in accordance with the method 5710 (Standard Methods, APHA). Hexane was used to extract these compounds from water. An autosampler was used to inject 1 mL of sample onto the column. Nitrogen at a flow rate of 12 mL/min was used as the carrier gas. The temperatures of the injector and the detector were set to 275 °C and 350 °C, respectively. The temperature of the oven was increased from 50 to 150 °C at a rate of 10 °C/min.

The concentrations of monobromoacetic acid, monochloroacetic acid, dichloroacetic acid, trichloroacetic acid, and dibromoacetic acid were measured using the gas chromatography machine with a 30 m long  $\times$  0.32 mm ID, 3  $\mu$ m DB-1 column (J & W Scientific, Folsom, CA). The volume of the sample injected onto the column was 5 mL. Nitrogen at a flow rate of 10 mL/min was used as the carrier gas. The temperatures of the injector and the detector were set

to 200 °C and 260 °C, respectively. The temperature of the oven was set to 40 °C for 15 min following which it was increased to 75 °C at a rate of 5 °C/min and maintained at that temperature for 5 min.

### 5.3.3. Reagents

Ultrapure water (Milli-Q water with resistivity greater than 18 MΩ) was used to prepare all reagents and solutions. Raw water was prepared by spiking Milli-Q water with sodium bromide (NaBr) to obtain the desired concentrations. To attain the desirable NOM concentration, Suwannee River NOM (1R101N RO isolation, 48.8% C (w/w), International Humic Substances Society, MN, USA) was added to the raw water. Subsequently, the pH of the water was adjusted to the desired value by adding phosphoric acid (H<sub>3</sub>PO<sub>4</sub>) (99.99%, Sigma-Aldrich, USA) and/or sodium hydroxide (NaOH) (98.0+%, Fluka, Germany). The water was not buffered, since our experimental results showed that the pH did not vary over the course of the experiment. Tertiary butyl alcohol (Fisher Scientific, Germany) was used as hydroxyl radical scavenger. Following preparation, the raw water was stirred with a magnetic stirrer for 15 min. Bromide and bromate standards were prepared using sodium bromide (99.995% (metals basis), Fluka, Germany) and sodium bromate (NaBrO<sub>3</sub>) (99.7+%, Fisher Scientific, USA).

## 5.4. Results and Discussion

Experimental results presented herein indicate percent reduction in disinfection by-products concentration and also TOC,  $UV_{254}$ , SUVA, color and turbidity as a result of treating the raw water in the hybrid ozonation-ceramic membrane filtration system for 180 min as compared to the data obtained for raw water. In all figures and tables the steady state concentrations in the permeate line were used to calculate the percent reductions in various parameters. Experiments were carried out at least in duplicate. Data reported are averages of triplicate analyses within replicate experiments. Table 1 summarizes the TTHMs concentrations observed in the permeate under various operating conditions.

Table 1- TTHMs concentrations in the permeate under various operating conditions.

MWCO (kD)	[NOM] (mgC/L)	pH	Inlet O <sub>3</sub> mass injection rate (mg/min)	[Br <sup>-</sup> ] <sub>0</sub> (mg/L)	[CaCl <sub>2</sub> ] <sub>0</sub> (mM)	[t-BuOH] <sub>0</sub> (mM)	TTHMs t=0 min (ppb)	TTHMs t=180 min (ppb)
5	10	6	1.5	1	1	0	379	204
5	10	6	1.0	1	1	0	315	256
5	10	6	0.5	1	1	0	329	251
5	10	6	0.25	1	1	0	314	257
5	10	6	0.5	0.25	1	0	234	126
5	10	8	0.5	1	1	0	527	411
5	10	6	0.5	1	1	1	462	266
5	10	6	1.5	1	1	1	479	184
5-coated	10	6	0.5	1	1	0	359	211
15	10	6	0.5	1	1	0	410	275
1	10	6	0.5	1	1	0	400	243

#### 5.4.1. Effect of inlet ozone mass injection rate

The effects of the inlet ozone mass injection rate (0.25, 0.50, 1.00, 1.50 mg/min) on bromate concentrations are shown in Figure 2. The steady state aqueous ozone concentration was found to be directly proportional to the inlet ozone mass injection rate (see Chapter 3). As observed, increases in inlet ozone mass injection rate resulted in greater bromate concentrations in the permeate. In the presence of NOM a large portion of the dissolved ozone and hydroxyl radicals present in water can be expected to react with NOM. Hence, less ozone and hydroxyl radicals would be available to transform the bromide ion to bromate and therefore in the presence of NOM, bromate formation is suppressed. Our experimental results which verify this (see Figure 2), are consistent with the findings of Siddiqui et al., 2005 who showed that in homogeneous systems the presence of NOM suppressed bromate formation.

As shown in Figure 3, as a result of an increase in the inlet ozone mass injection rate, only minor variations in the percent reductions in the concentrations of  $\text{CHCl}_3$ ,  $\text{CHBrCl}_2$ , and  $\text{CHBr}_2\text{Cl}$  were observed. Unlike the other DBPs studied, ozonation resulted in an increase in the concentration of bromoform. However, increasing the inlet ozone mass injection rate resulted in lower steady state concentrations of bromoform, although there was always an increase in concentration with ozonation. This is believed to be due to the fact that at greater inlet ozone mass injection rates, the majority of bromide ions present in the water are transformed to bromate and hence fewer bromide ions are available

to react with NOM to form  $\text{CHBr}_3$ . Our experimental results also indicate that ozonation reduced the potential for HAA formation. The percent reduction in HAA concentrations at the inlet ozone mass injection rates of 0.25, 0.5, 1.0, and 1.5 were 65, 64, 59, and 55, respectively. Figure 4 shows the percent reduction in TOC,  $\text{UV}_{254}$ , SUVA, color, and turbidity.

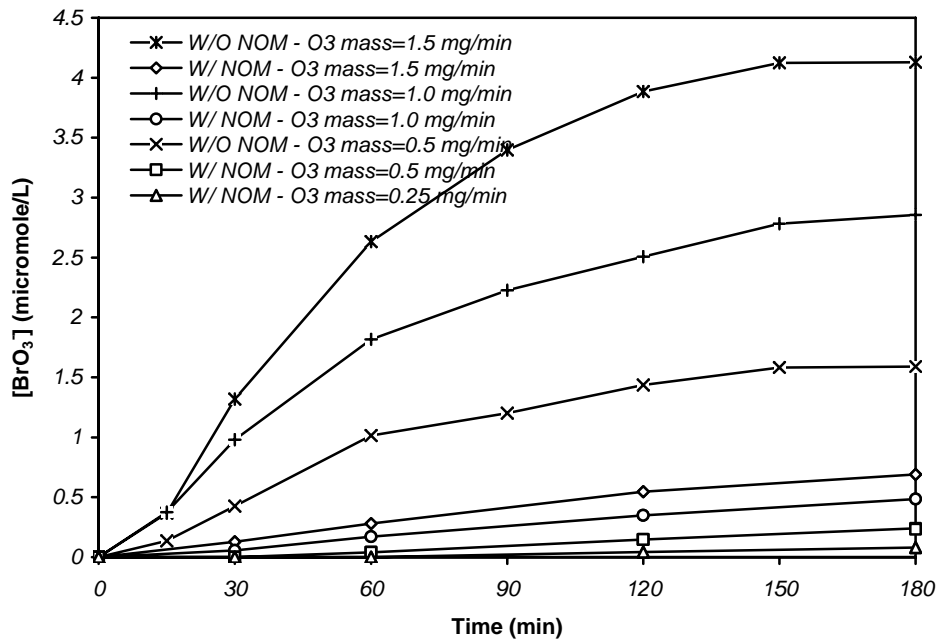


Fig. 2- Bromate concentration in the permeate vs. time at various inlet ozone mass injection rates. Membrane: 7 channel – 5 kD,  $[\text{Br}]_0$ : 1 mg/L,  $[\text{NOM}]_0$ : 10 mg C/L,  $[\text{CaCl}_2]_0$ : 1 mM,  $[\text{t-BuOH}]_0$ : 0 mM, pH: 6.0.

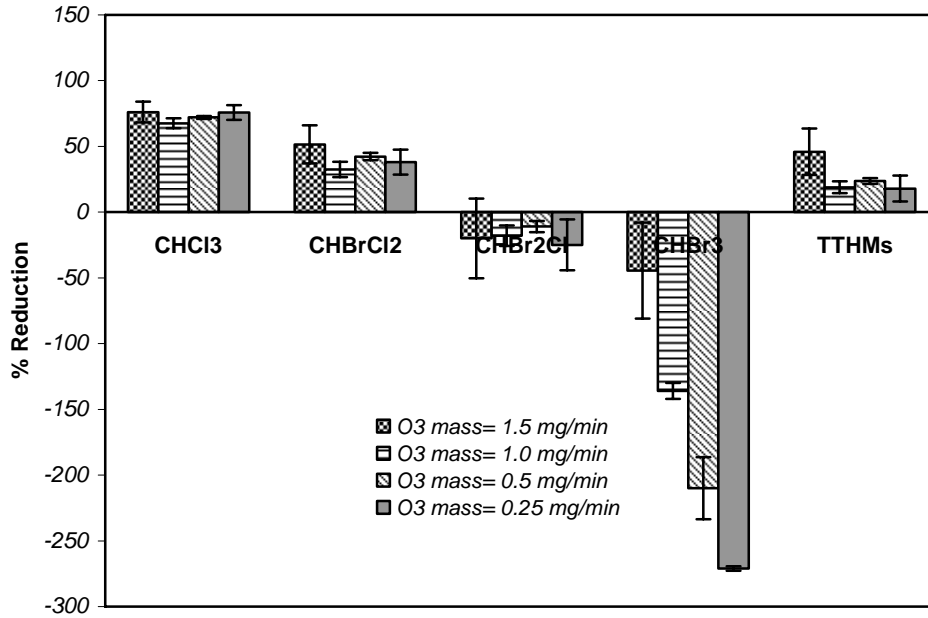


Fig. 3- Percent reduction in the steady state DBPs concentration at various inlet ozone mass injection rates. Membrane: 7 channel – 5 kD, [Br<sup>-</sup>]<sub>0</sub>: 1 mg/L, [NOM]<sub>0</sub>: 10 mg C/L, [CaCl<sub>2</sub>]<sub>0</sub>: 1 mM, [t-BuOH]<sub>0</sub>: 0 mM, pH: 6.0.

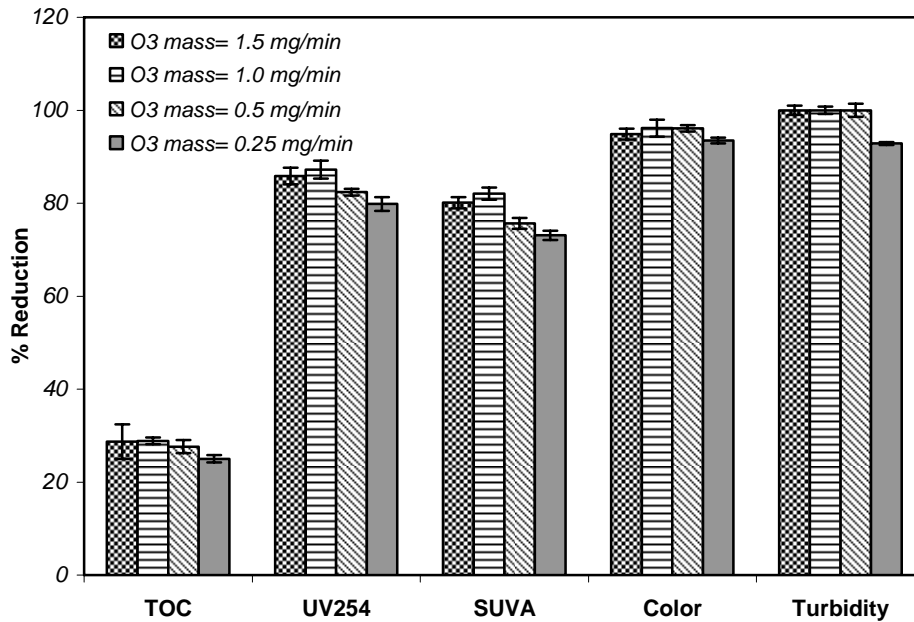


Fig. 4- Percent reduction at various inlet ozone mass rates. Membrane: 7 channel – 5 kD, [Br<sup>-</sup>]<sub>0</sub>: 1 mg/L, [NOM]<sub>0</sub>: 10 mg C/L, [CaCl<sub>2</sub>]<sub>0</sub>: 1 mM, [t-BuOH]<sub>0</sub>: 0 mM, pH: 6.0.

#### **5.4.2. Effect of Initial Bromide Concentration**

In another set of experiments, the influence of the initial bromide concentration on DBP formation was studied. As it is shown in Figure 5, as the initial bromide concentration was increased from 0.25 to 1.0 mg/L, the concentration of bromate ion increased as well, indicating that as more bromide ion was available to react with molecular ozone and/or hydroxyl radicals, more bromate was produced. This finding is consistent with the results reported by Moslemi et al., 2011 who studied the effect of the initial bromide concentration on bromate formation in the absence of NOM. As shown in Figure 6, the concentration of TTHMs formed was increased. As the initial bromide ion was reduced, less bromide would be available to participate in the reactions leading to THM formation. The steady state ozone concentrations in the permeate for the experiments with the initial bromide concentrations of 0.25 and 1.0 mg/L were equal to 0.81 and 0.72 mg/L, respectively.

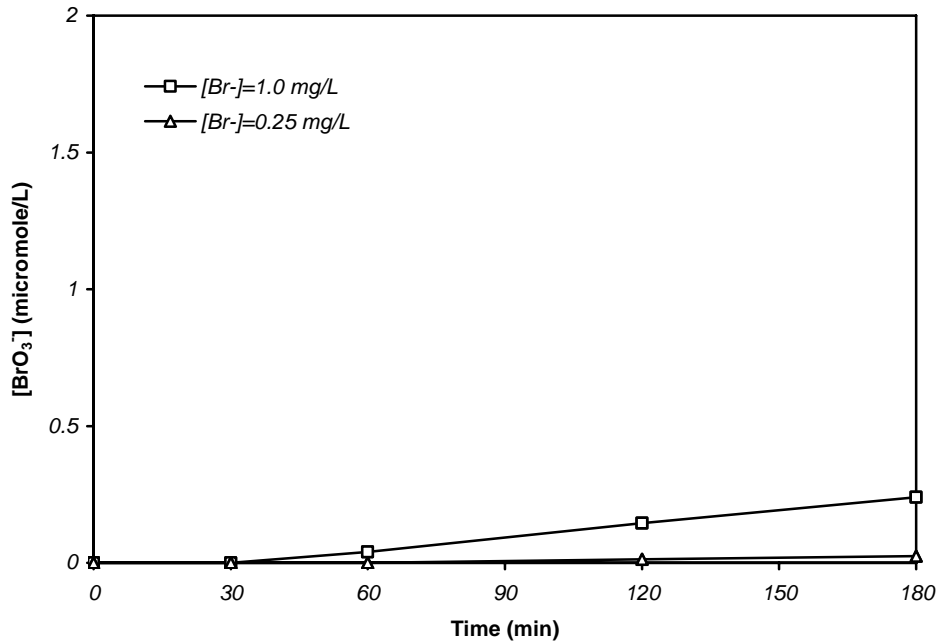


Fig. 5- Bromate concentration in the permeate vs. time at various initial bromide concentrations. Membrane: 7 channel – 5 kD, inlet O<sub>3</sub> mass injection rate: 0.5 mg/min, [NOM]<sub>0</sub>: 10 mg C/L, [CaCl<sub>2</sub>]<sub>0</sub>: 1 mM, [t-BuOH]<sub>0</sub>: 0 mM, pH: 6.0.

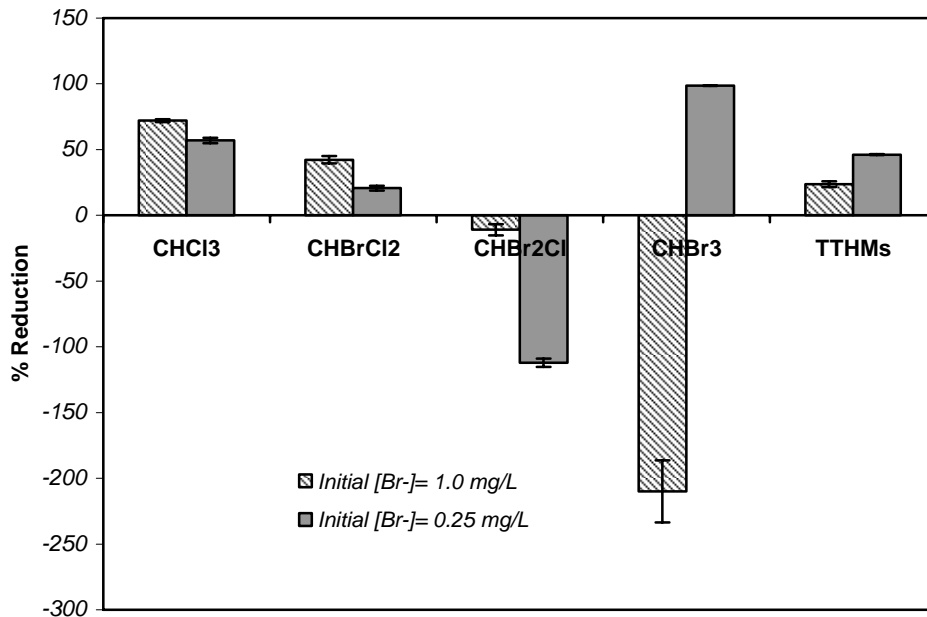


Fig. 6- Percent reduction in DBPs concentration at various initial bromide concentrations. Membrane: 7 channel – 5 kD, inlet O<sub>3</sub> mass injection rate: 0.5 mg/min, [NOM]<sub>0</sub>: 10 mg C/L, [CaCl<sub>2</sub>]<sub>0</sub>: 1 mM, [t-BuOH]<sub>0</sub>: 0 mM, pH: 6.0.

### 5.4.3. Effect of NOM Concentration

The effect of NOM concentration (1, 5, and 10 mg C/L) on disinfection by-product formation and other water quality parameters was investigated. The reaction of ozone with NOM is faster than the reaction of ozone with bromide ion (Siddiqui et al., 1995). As mentioned earlier, as the concentration of NOM is increased fewer ozone and OH radicals are available in the solution to react with the bromide ion to form bromate. NOM also reacts with the bromide ion and thus reduces the potential for bromate formation (Westerhoff et al., 1998). Our experimental results also confirm this (see Figure 7): as the NOM concentration was increased less bromate ion was formed. Westerhoff et al., 1998 and Siddiqui et al., 1993 also reported that less bromate was formed in the presence of NOM.

As shown in Figure 8, as the NOM concentration increased from 1 to 5 mgC/L, greater reductions in  $UV_{254}$ , SUVA and color were achieved. However the extent to which turbidity was reduced did not vary with inlet ozone mass injection rate, however, at all NOM concentrations, essentially 100% of the turbidity was removed. Ozone acts as an aid to coagulation of NOM through transformation of NOM to smaller and more polar compounds (Chandrakanth et al., 1996), which is believed to explain the reduction in water turbidity achieved in the presence of ozone. Also at NOM concentration equal to 1 mgC/L, an increase in the TOC after treating water using ozone-membrane system was observed. This might be due to more complete oxidation of NOM by ozone at lower NOM concentration,

which would produce lower molecular weight organics, which would likely pass more easily through membrane pores and result in TOC increase in the permeate.

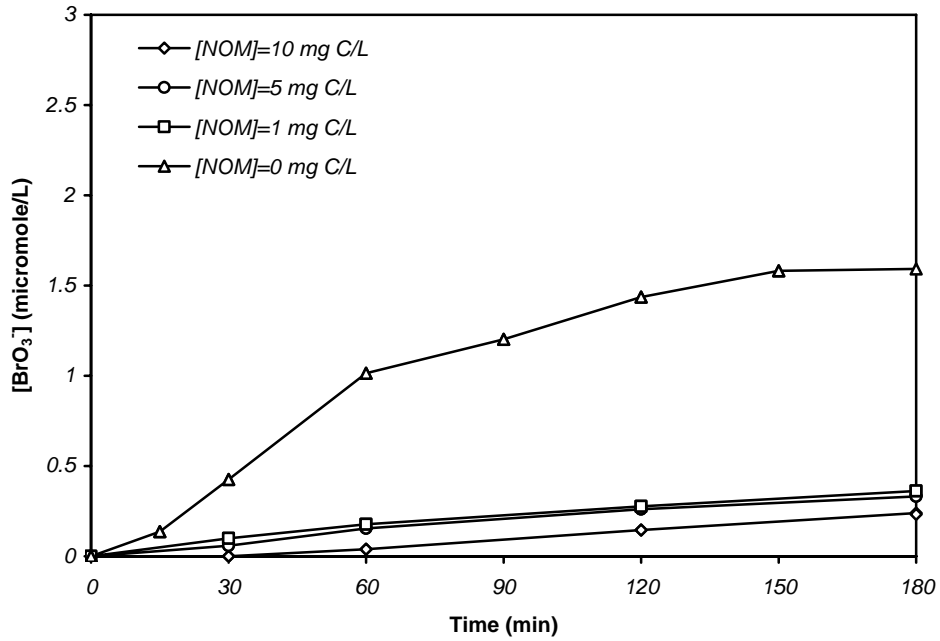


Fig. 7- Bromate concentration in the permeate vs. time at various NOM concentrations. Membrane: 7 channel – 5 kD, inlet O<sub>3</sub> mass injection rate: 0.5 mg/min, [Br<sup>-</sup>]<sub>0</sub>: 1 mg/L, [CaCl<sub>2</sub>]<sub>0</sub>: 1 mM, [t-BuOH]<sub>0</sub>: 0 mM, pH: 6.0.

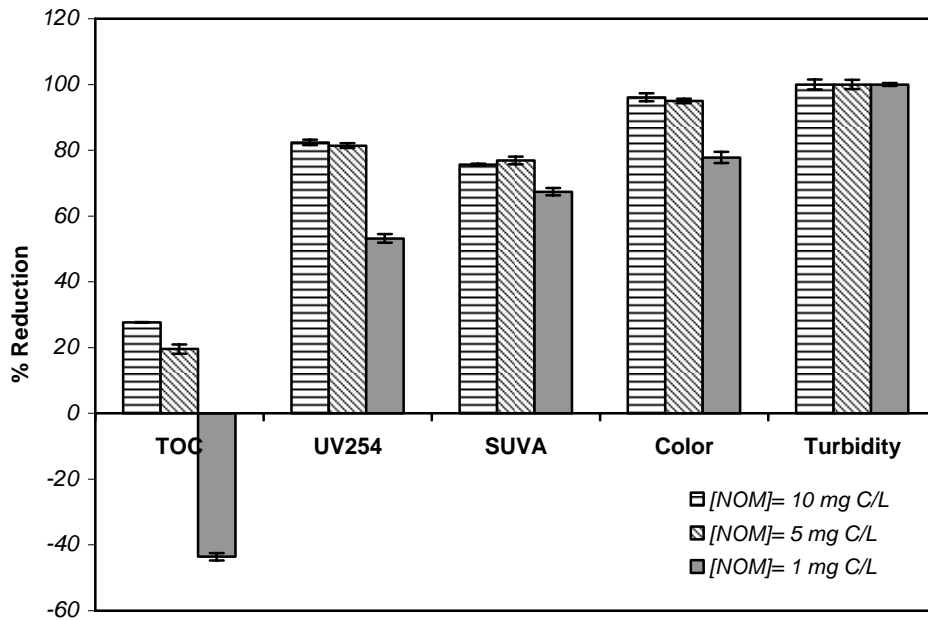


Fig. 8- Percent reduction at various NOM concentrations. Membrane: 7 channel – 5 kD, inlet O<sub>3</sub> mass injection rate: 0.5 mg/min, [Br<sup>-</sup>]<sub>0</sub>: 1 mg/L, [CaCl<sub>2</sub>]<sub>0</sub>: 1 mM, [t-BuOH]<sub>0</sub>: 0 mM, pH: 6.0.

#### 5.4.4. Effect of pH

As shown in Figure 9, in the presence of NOM and regardless of pH, a significant reduction in the concentration of bromate is observed as compared to the concentration of bromate in the absence of NOM. Moreover, the concentration of bromate at pH 6.0 is considerably less than that observed at pH 8.0. At lower pH, ozone is more stable and the concentration of hydroxyl radicals in the reactor would be expected to be less than that found at higher pH (Pinkernell and von Gunten, 2001; von Gunten, 2003). Moreover, as an intermediate step in the bromate formation mechanism, hypobromite ( $\text{OBr}^-$ ) reacts with ozone molecule.  $\text{OBr}^-$  is at equilibrium with hypobromous acid ( $\text{HOBr} \leftrightarrow \text{OBr}^- + \text{H}^+$ ). As pH decreases the equilibrium shifts towards the left and the concentration of HOBr increases. HOBr is much less reactive with ozone than is  $\text{OBr}^-$  (Mizuno et al., 2004). Hence, at low pH the rate of formation of bromate is slower and less bromate is observed.

Figure 10 represents the percent reduction in the DBP concentrations as a function of pH. Reduction in pH, reduced the formation of some of the trihalomethanes while it increased the concentration of some others and the concentration of TTHMs more or less remained the same. Hence, no specific trend for the effect of pH on the formation of trihalomethanes was observed. The influence of pH on the water quality parameters is shown in Figure 11. Again, no substantial variation in these parameters as a result of pH depression was observed.

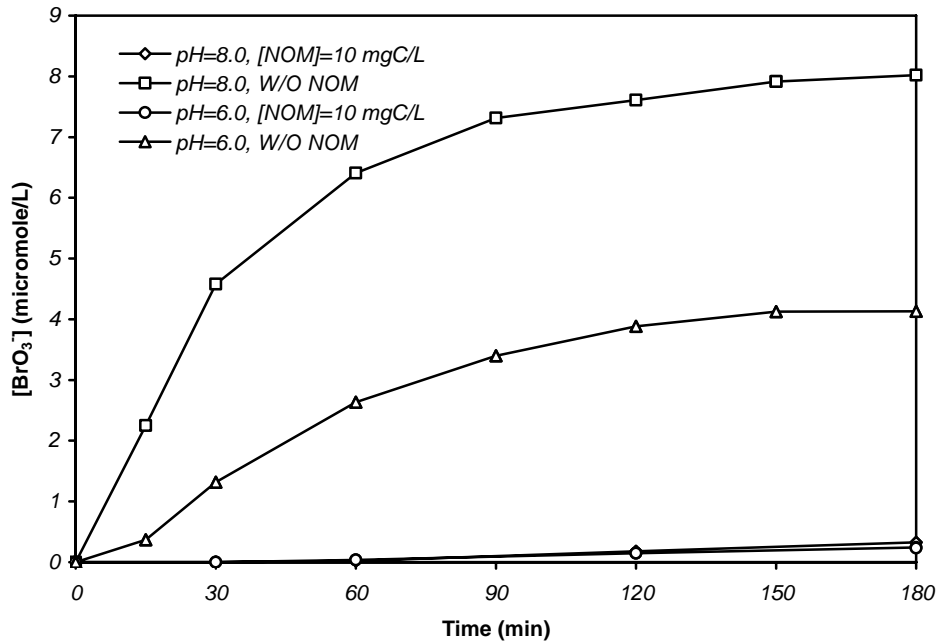


Fig. 9- Bromate concentration in the permeate vs. time at various pHs. Membrane: 7 channel – 5 kD, inlet  $O_3$  mass injection rate: 0.5 mg/min,  $[Br^-]_0$ : 1 mg/L,  $[CaCl_2]_0$ : 1 mM,  $[t-BuOH]_0$ : 0 mM.

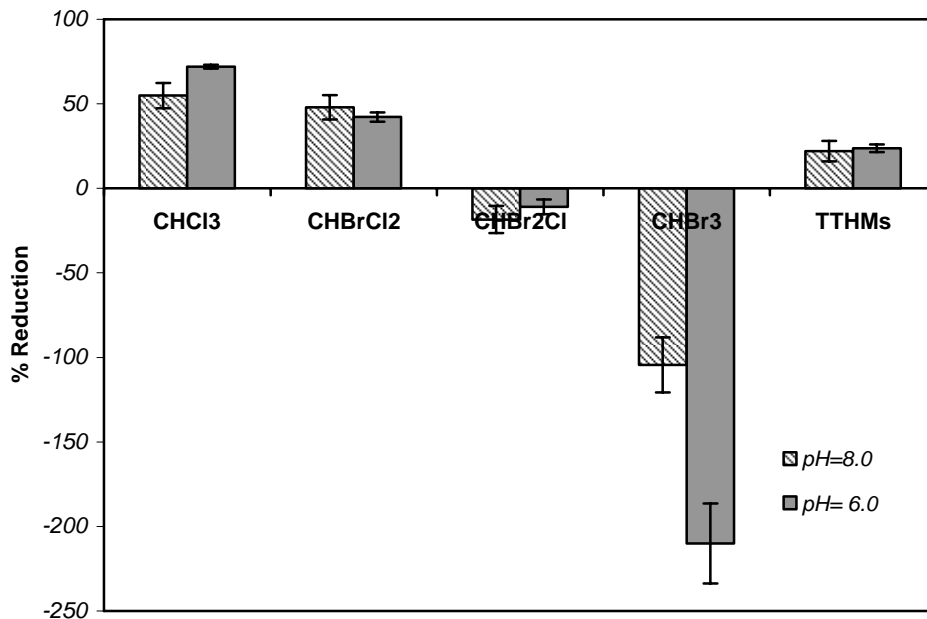


Fig. 10- Percent reduction in DBPs concentration at various pHs. Membrane: 7 channel – 5 kD, inlet  $O_3$  mass injection rate: 0.5 mg/min,  $[Br^-]_0$ : 1 mg/L,  $[NOM]_0$ : 10 mg C/L,  $[CaCl_2]_0$ : 1 mM,  $[t-BuOH]_0$ : 0 mM.

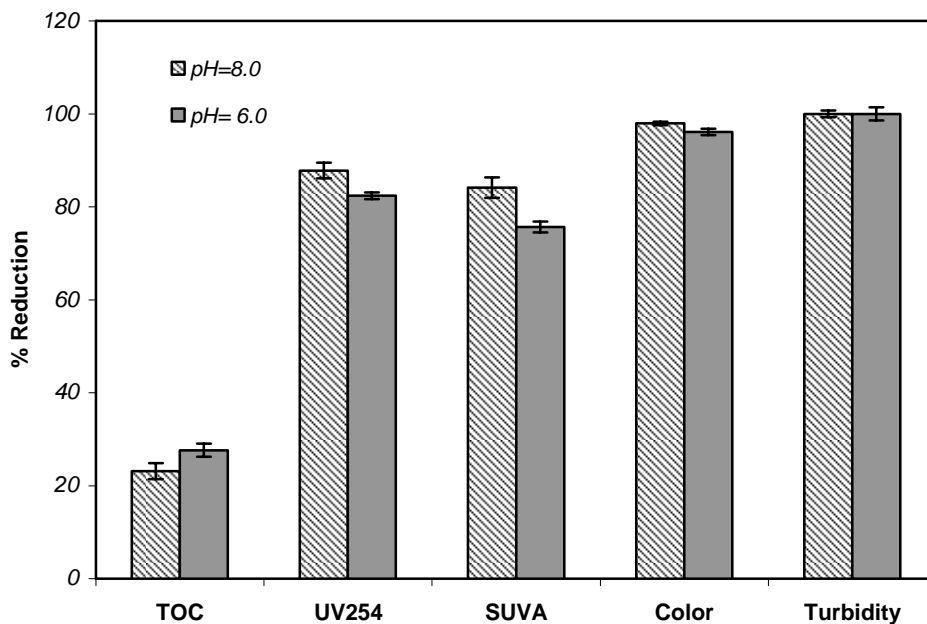


Fig. 11- Percent reduction at various NOM concentrations. Membrane: 7 channel – 5 kD, inlet  $O_3$  mass injection rate: 0.5 mg/min,  $[Br^-]_0$ : 1 mg/L,  $[NOM]_0$ : 10 mg C/L,  $[CaCl_2]_0$ : 1 mM,  $[t-BuOH]_0$ : 0 mM, pH: 6.0.

#### 5.4.5. Effect of OH Radical Scavengers

Experiments were carried out in the presence of a hydroxyl radical scavenger (t-BuOH) to study the contribution of hydroxyl radicals to DBP formation. t-BuOH is highly reactive towards hydroxyl radicals, but is essentially unreactive with molecular ozone and exerts no ozone demand. t-BuOH consumes OH radicals available in the system and hence suppresses the intermediate steps of the bromate formation mechanism which involves the OH radical and thus it should suppress bromate formation.

As shown in Figure 12, regardless of the inlet ozone mass injection rate, the addition of t-BuOH reduced bromate concentration to very low levels. This suggests that the OH radical pathway plays a significant role in bromate formation

in the hybrid ozonation membrane system. In the absence of NOM, in the presence of t-BuOH, the concentration of bromate was significantly reduced (see Chapter 4). It is noteworthy that experiments were also repeated in the presence of bicarbonate (70 mM), which is a hydroxyl radical scavenger as well. Bicarbonate also resulted in bromate suppression; however we were unable to quantify bromate concentrations in the presence of bicarbonate because of co-elution of peaks. Siddiqui et al., 1995 achieved up to 93% reduction in bromate formation using OH radical scavengers.

As shown in Figure 13, the addition of OH radical scavengers reduced TTHMs concentration. However, less reduction was observed in TOC in the presence of the scavenger (see Figure 14). An explanation for this is reduced ozone decomposition and OH radical formation in the presence of scavengers. OH is a much stronger NOM oxidized and suppression of the formation of OH radicals results in reduced TOC removal.

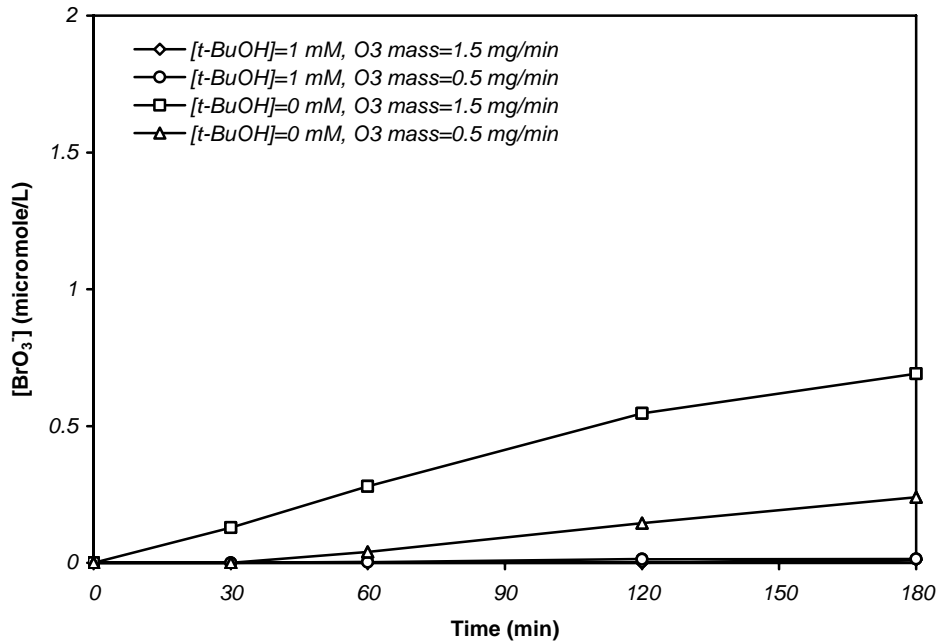


Fig. 12- Bromate concentration in the permeate vs. time in the presence of scavenger. Membrane: 7 channel – 5 kD,  $[Br^-]_0$ : 1 mg/L,  $[NOM]_0$ : 10 mg C/L,  $[CaCl_2]_0$ : 1 mM, pH: 6.0.

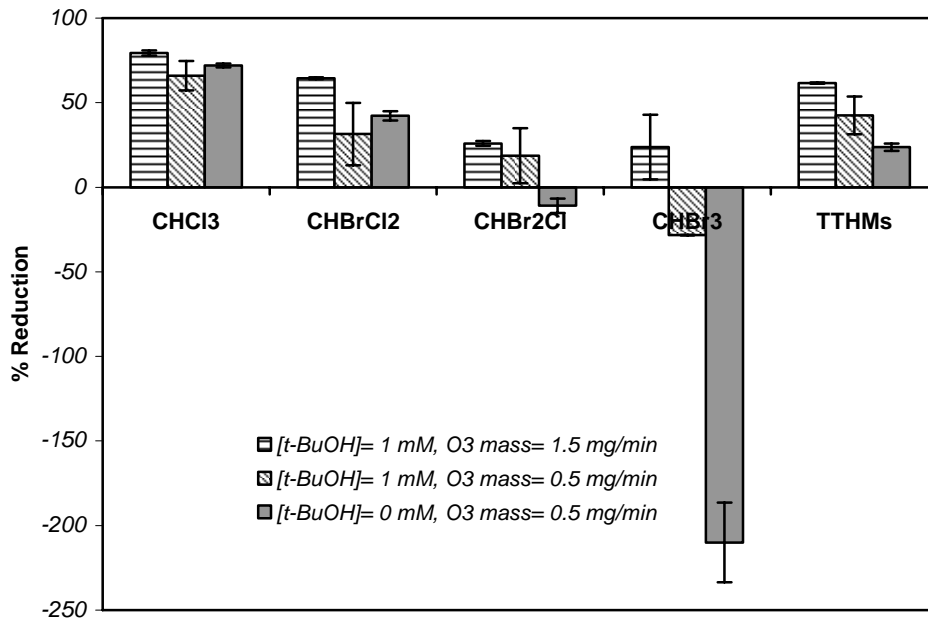


Fig. 13- Percent reduction in DBP concentrations in the presence of scavenger. Membrane: 7 channel – 5 kD,  $[Br^-]_0$ : 1 mg/L,  $[NOM]_0$ : 10 mg C/L,  $[CaCl_2]_0$ : 1 mM, pH: 6.0.

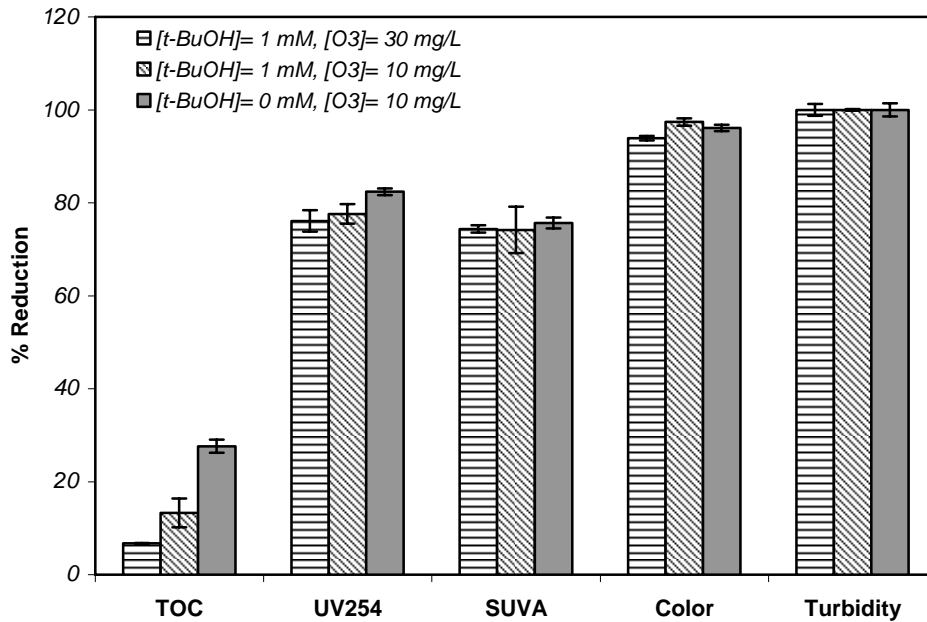


Fig. 14- Percent reduction in the presence of scavenger. Membrane: 7 channel – 5 kD, inlet  $O_3$  mass injection rate: 0.5 mg/min,  $[Br^-]_0$ : 1 mg/L,  $[NOM]_0$ : 10 mg C/L,  $[CaCl_2]_0$ : 1 mM, pH: 6.0.

#### 5.4.6. Effect of Membrane Coating

To study the effect of the manganese oxide coating on bromate formation, the performance of a 5 kD ceramic membrane, Inside Ceram (TAMI North America, Saint-Laurent, Quebec), coated with 30 layers of manganese oxide was compared with that of an uncoated membrane (see Corneal et al. (35) for the membrane preparation method). Manganese oxide is shown to be a more powerful catalyst of ozone decomposition than is titanium oxide (which is used in the fabrication of the Inside Ceram membranes) and the manganese oxide coated membrane is more effective at controlling fouling of the membrane in a hybrid ozonation-membrane system than is the uncoated membrane (36). As can be seen in Figure 15, the

bromate concentration that was observed using the coated membrane is less than that observed with the uncoated membrane. Camel et al. (6) also showed that ozonation in the presence of heterogeneous catalysts reduced bromate formation. As shown in our earlier work (see Chapter 4) the coated membrane enhanced ozone decomposition, and resulted in lower concentrations of dissolved ozone. Hence, the lower concentration of bromate ion formed when the coated membrane was used in the hybrid ozonation-membrane system may be due to the lower ozone concentration available in the system.

The coated membrane also shows promising results in terms of controlling the formation of other disinfection by-products. As it can be seen in Figure 16, the coated membrane resulted in greater reductions in the DBPs, including  $\text{CHCl}_3$ ,  $\text{CHBr}_3$ ,  $\text{CHBrCl}_2$ ,  $\text{CHBr}_2\text{Cl}$  and TTHMs. In both cases, the steady state concentrations of these DBPs in system are greater than the regulatory limits proposed by drinking water guidelines. The TTHMs concentration in the permeate using uncoated and coated membranes were 251 and 211  $\mu\text{g/L}$ , whereas as mentioned above, the MCLs proposed by USEPA, the Ontario Ministry of the Environment, and the European Union are 80, 100, and 100  $\mu\text{g/L}$ , respectively. However, the NOM concentration and also the bromide concentration that are observed in the natural waters in many cases are expected to be lower than the values used in the current study and the concentration of the DBPs resulting from the ozonation of natural waters might be within the regulatory limits.

As shown in Figure 17 a greater TOC removal was achieved using the uncoated membrane. An explanation for this results, is the more effective decomposition of NOM in the presence of the catalyst which breaks down NOM to lower molecular weight species which would pass through the membrane pores and result in an increase in the TOC in the permeate line. Gracia et al., 1996 also showed that in the presence of metal ions, the oxidation of organic compounds was promoted and the TOC removal obtained as a result of ozonation in the presence of a metal oxide was significantly greater than with ozone alone.

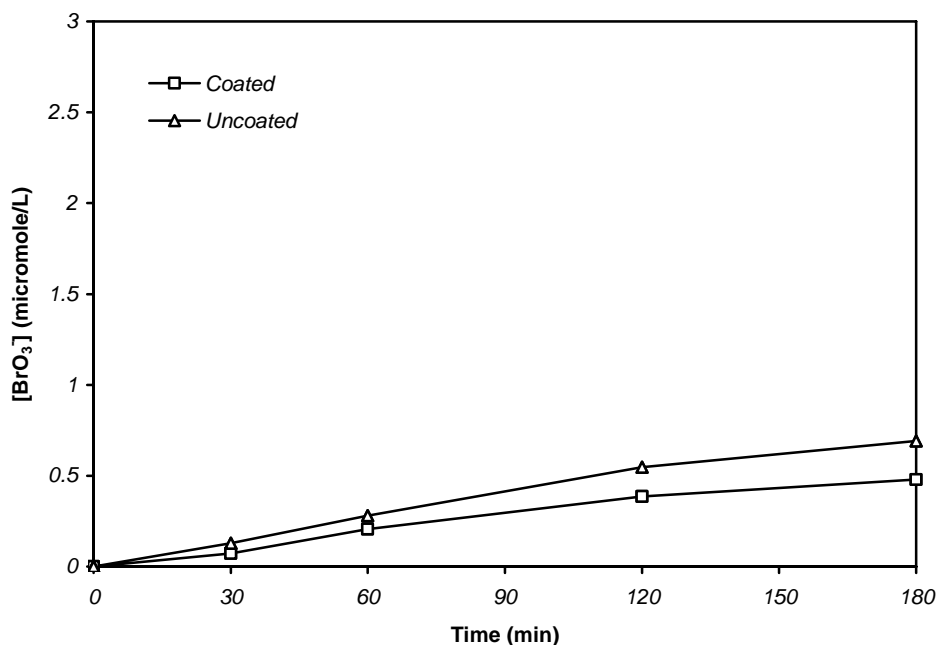


Fig. 15- Bromate concentration in the permeate vs. time. The effect of membrane coating. Membrane: 7 channel – 5 kD, inlet O<sub>3</sub> mass injection rate: 0.5 mg/min, [Br<sup>-</sup>]<sub>0</sub>: 1 mg/L, [NOM]<sub>0</sub>: 10 mg C/L, [CaCl<sub>2</sub>]<sub>0</sub>: 1 mM, [t-BuOH]<sub>0</sub>: 0 mM, pH: 6.0.

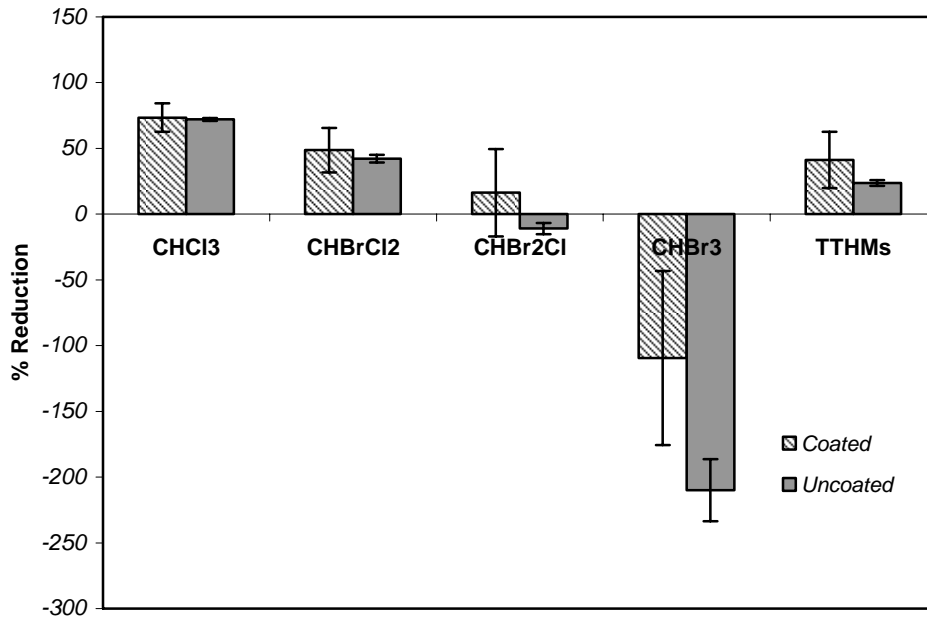


Fig. 16- Percent reduction in DBPs concentration. The effect of membrane coating. Membrane: 7 channel – 5 kD, inlet O<sub>3</sub> mass injection rate: 0.5 mg/min, [Br<sup>-</sup>]<sub>0</sub>: 1 mg/L, [NOM]<sub>0</sub>: 10 mg C/L, [CaCl<sub>2</sub>]<sub>0</sub>: 1 mM, [t-BuOH]<sub>0</sub>: 0 mM, pH: 6.0.

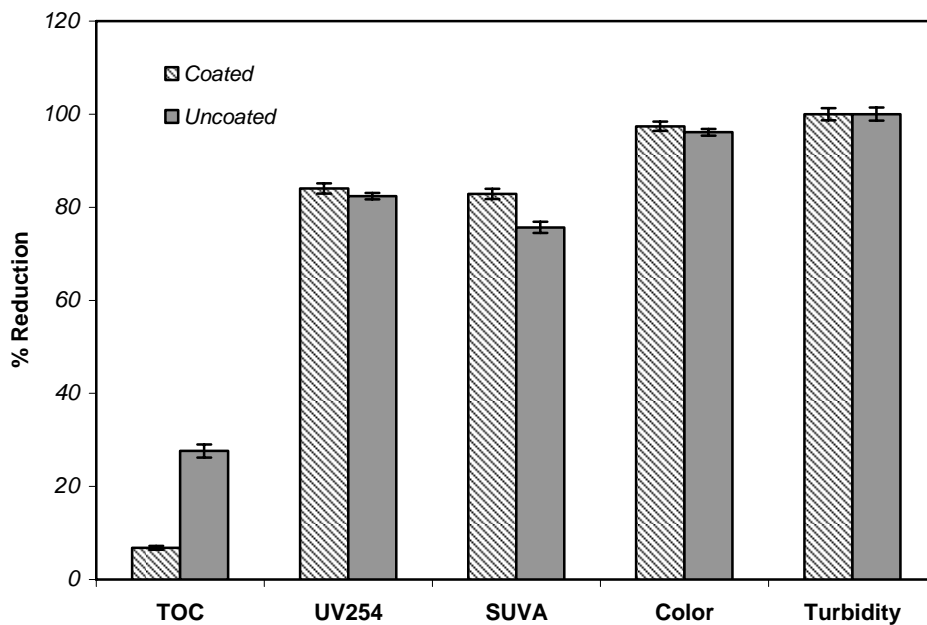


Fig. 17- Percent reduction. The effect of membrane coating. Membrane: 7 channel – 5 kD, inlet O<sub>3</sub> mass injection rate: 0.5 mg/min, [Br<sup>-</sup>]<sub>0</sub>: 1 mg/L, [NOM]<sub>0</sub>: 10 mg C/L, [CaCl<sub>2</sub>]<sub>0</sub>: 1 mM, [t-BuOH]<sub>0</sub>: 0 mM, pH: 6.0.

#### 5.4.7. Effect of MWCO

As presented in Figure 18, lower bromate concentrations were observed using membranes with greater MWCOs. The permeability of the membranes increases with MWCO, so at a constant operating pressure, as the MWCO of the membrane increases, the permeate flux also increases, and subsequently the contact time in the reactor decreases. The retention times in the system for the membranes with MWCOs of 5, 8, and 15 kD were equal to 126, 99, and 89 minutes, respectively. As a result, for membranes with higher MWCOs, the ozone exposure is reduced and less bromate is formed. Our earlier work (Moslemi et al., 2011) also indicated that, in the absence of NOM, increasing the MWCO of the membrane reduced bromate formation in the hybrid system.

Figure 19 shows percent reduction in DBPs concentrations at various MWCOs. As shown in Figure 20, a greater reduction in TOC,  $UV_{254}$ , and SUVA with membranes having lower MWCOs is achieved. This is due to the fact that finer membranes are more effective in filtering and removing NOM from water. Also as mentioned above, greater ozone exposure with membranes having lower MWCOs allows for more complete oxidation of NOM which subsequently results in greater reduction in the parameters studied. As indicated in Figures 21 to 23, membrane filtration-ozonation system is able to reduce the color, turbidity and  $UV_{254}$  of the raw water tested. After 30 min a significant reduction in these parameters was obtained. It is also evident from these figures that ozonation was

more effective in the removal of color, turbidity and  $UV_{254}$  as compared to the experiments carried out without ozonation.

MWCO of the membrane should be chosen in a way that membrane can effectively filter NOM out of the water and at the same time the retention time in the reactor is short enough that the amount of DBPs formed does not exceed corresponding the MCLs set by the drinking water regulations.

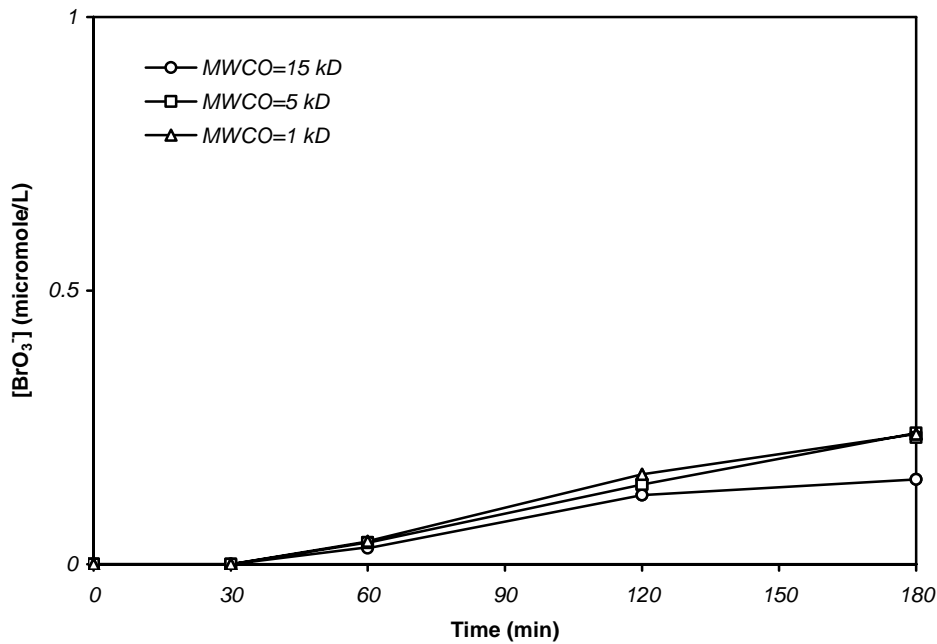


Fig. 18- Bromate concentration in the permeate vs. time using various MWCOs. Membrane: 7 channel, inlet  $O_3$  mass injection rate: 0.5 mg/min,  $[Br^-]_0$ : 1 mg/L,  $[NOM]_0$ : 10 mg C/L,  $[CaCl_2]_0$ : 1 mM,  $[t-BuOH]_0$ : 0 mM, pH: 6.0.

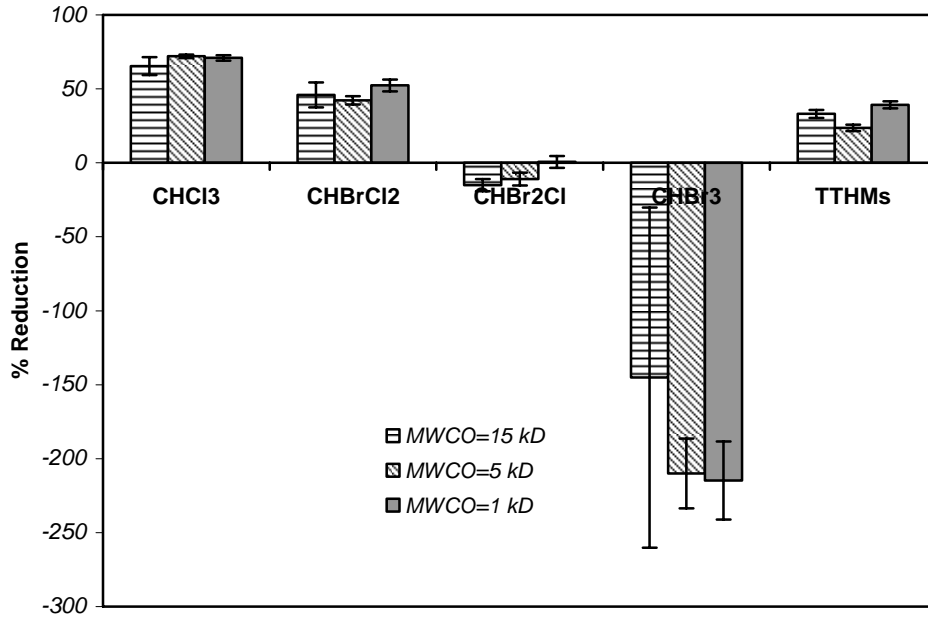


Fig. 19- Percent reduction in DBPs concentration using various MWCOs. Membrane: 7 channel, inlet O<sub>3</sub> mass injection rate: 0.5 mg/min, [Br<sup>-</sup>]<sub>0</sub>: 1 mg/L, [NOM]<sub>0</sub>: 10 mg C/L, [CaCl<sub>2</sub>]<sub>0</sub>: 1 mM, [t-BuOH]<sub>0</sub>: 0 mM, pH: 6.0.

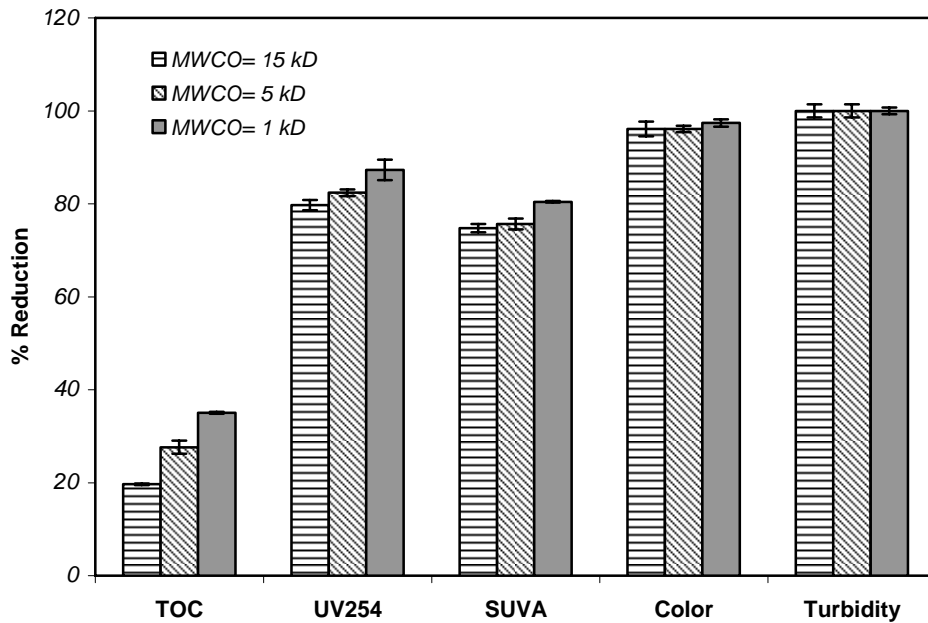


Fig. 20- Percent reduction using various MWCOs. Membrane: 7 channel, inlet O<sub>3</sub> mass injection rate: 0.5 mg/min, [Br<sup>-</sup>]<sub>0</sub>: 1 mg/L, [NOM]<sub>0</sub>: 10 mg C/L, [CaCl<sub>2</sub>]<sub>0</sub>: 1 mM, [t-BuOH]<sub>0</sub>: 0 mM, pH: 6.0.

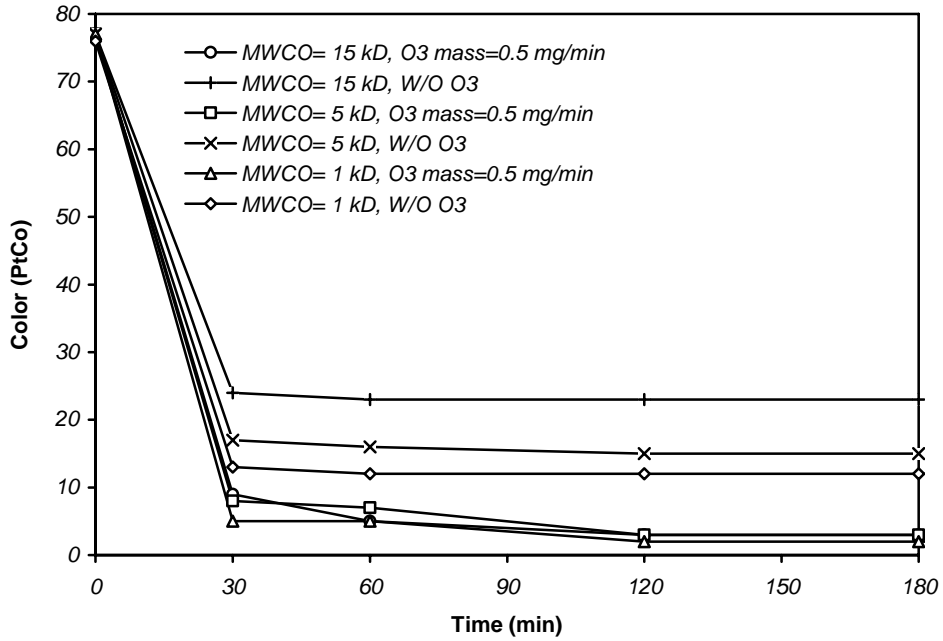


Fig. 21- Percent reduction in color using various MWCOs. Membrane: 7 channel,  $[Br^-]_0$ : 1 mg/L,  $[NOM]_0$ : 10 mg C/L,  $[CaCl_2]_0$ : 1 mM,  $[t-BuOH]_0$ : 0 mM, pH: 6.0.

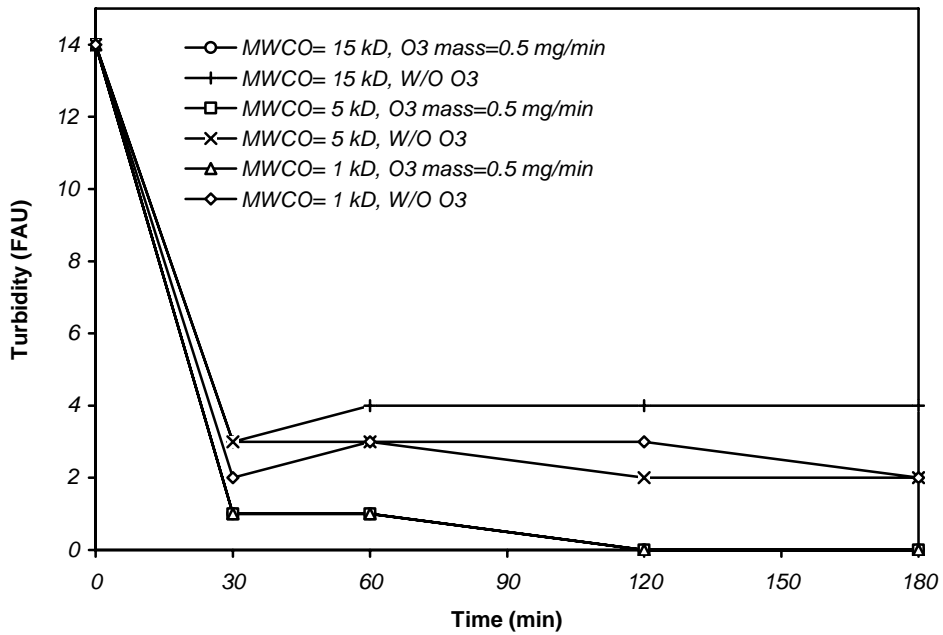


Fig. 22- Percent reduction in turbidity using various MWCOs. Membrane: 7 channel,  $[Br^-]_0$ : 1 mg/L,  $[NOM]_0$ : 10 mg C/L,  $[CaCl_2]_0$ : 1 mM,  $[t-BuOH]_0$ : 0 mM, pH: 6.0.

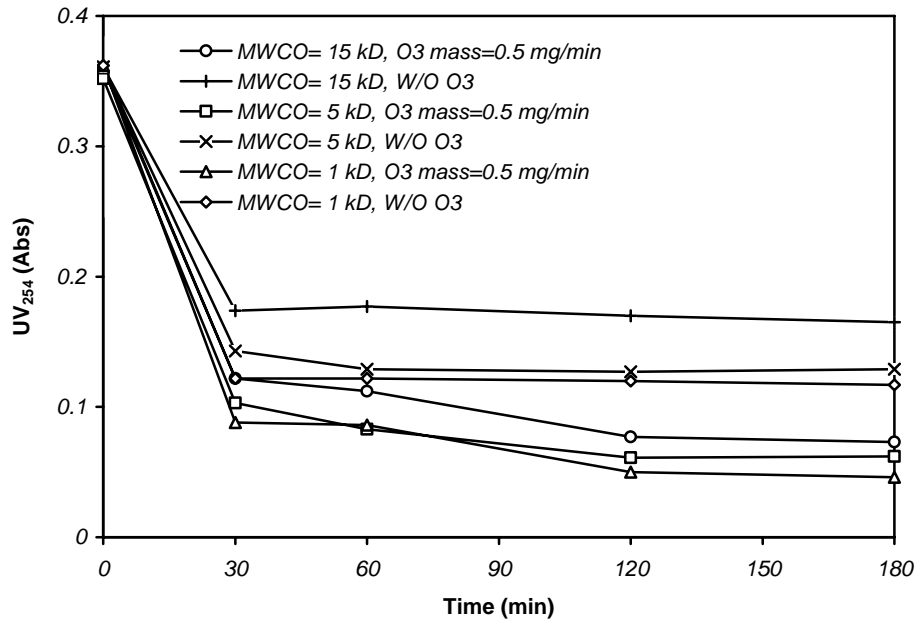


Fig. 23- Percent reduction in UV<sub>254</sub> using various MWCOs. Membrane: 7 channel, [Br<sup>-</sup>]<sub>0</sub>: 1 mg/L, [NOM]<sub>0</sub>: 10 mg C/L, [CaCl<sub>2</sub>]<sub>0</sub>: 1 mM, [t-BuOH]<sub>0</sub>: 0 mM, pH: 6.0.

#### 5.4.8. Fouling

A series of experiments was conducted to study fouling of the ceramic membrane by NOM present in the water and to investigate the influence of ozonation on membrane fouling. Table 2, lists the steady state permeate flux and residual ozone observed for the experiments with varying MWCOs and NOM concentrations. As shown in Figure 24, in the experiment with pure oxygen, permeate flux quickly dropped and after 180 min it reduced to about 50% of the initial permeate flux.

Our earlier work (Moslemi et al., 2011, Moslemi et al., 2010) indicated that in the hybrid ozonation-membrane system, dissolved ozone concentration was linearly proportional to the ozone mass injection rate. Based on the experimental

data obtained in this work, in the experiments with inlet ozone mass injection rates of 0.25 and 0.50 mg/min, the system can be operated at a constant permeate flux of about 75% and 85% of the initial flux, respectively. However, not much improvement in the permeate flux was obtained when the inlet ozone mass injection rate was increased beyond 0.50 mg/min. This is consistent with the findings of Kim et al., 2009, You et al., 2007, and Karnik et al., 2005 who showed that maintaining a minimum dissolved ozone concentration in the system allows for continuous operation of the hybrid membrane-ozone system at a constant permeate flux. Given the fact that oxygen injection did not prevent the reduction in the permeate flux, it can be inferred that fouling removal is due to ozonation, and not a scouring effect.

Table 2- Effects of MWCO, [NOM] and O<sub>3</sub> dosage on permeate flux.

MWCO (kD)	[NOM] (mg C/L)	Inlet O <sub>3</sub> mass injection rate (mg/min)	Steady state permeate flux (mL/min)	Steady state residual [O <sub>3</sub> ] (mg/L)
1	10	0.5	4.2	0.96
5	10	0.5	5.4	0.72
15	10	0.5	10.1	0.54
5	1	0.5	6.6	2.47
5	5	0.5	6.3	1.78
5	10	0.25	4.8	0.00
5	10	1.0	5.4	3.79
5	10	1.5	5.6	6.16

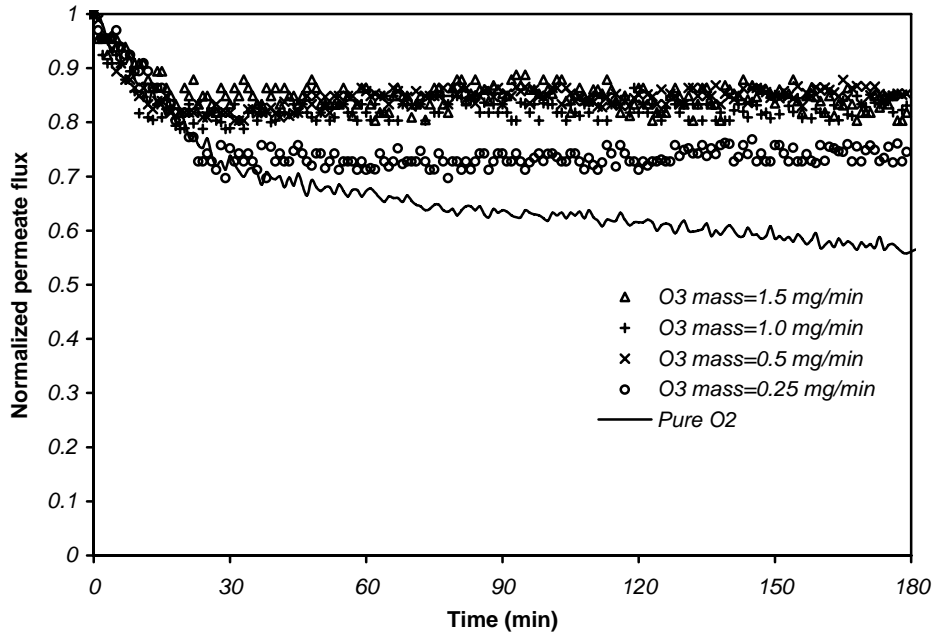


Fig. 24- Effect of ozone dosage on permeate flux. Membrane: 7 channel – 5 kD,  $[\text{Br}^-]_0$ : 1 mg/L,  $[\text{NOM}]_0$ : 10 mg C/L, inlet gas flow rate: 50 mL/min,  $[\text{CaCl}_2]_0$ : 1 mM,  $[\text{t-BuOH}]_0$ : 0 mM, pH: 6.0.

## 5.5. Empirical Bromate Model

A power function with the following general form was used for modeling.

$$[\text{BrO}_3^-] = 10^{b_0} [\text{Br}^-]^{b_1} [\text{DOC}]^{b_2} (\text{O}_3 \text{ mass rate})^{b_3} (\text{pH})^{b_4} (t)^{b_5} \quad (1)$$

where,

$[\text{BrO}_3^-]$  = bromate concentration in the permeate at time  $t$ ,  $\mu\text{g/L}$

$[\text{Br}^-]$  = bromide concentration in the feed water,  $250 \leq [\text{Br}^-] \leq 1000 \mu\text{g/L}$

$[\text{DOC}]$  = dissolved organic carbon concentration in the feed water,  $1 \leq [\text{DOC}] \leq 10 \text{ mgC/L}$

$\text{O}_3 \text{ mass rate}$  = inlet ozone mass injection rate,  $0.25 \leq \text{O}_3 \text{ mass rate} \leq 1.50 \text{ mg/min}$

pH = aqueous pH,  $6.0 \leq \text{pH} \leq 8.0$

t = reaction time,  $0 \leq t \leq 180$  min

$b_i$  = regression coefficients

After logarithmic transformation, equation 1 can be written as:

$$\log[\text{BrO}_3^-] = b_0 + b_1 \log[\text{Br}^-] + b_2 \log[\text{DOC}] + b_3 \log(\text{O}_3 \text{ mass rate}) + b_4 \log(\text{pH}) + b_5 \log(t) \quad (2)$$

Linear regression method was employed to estimate the regression coefficients. Experimental data reported in this study including eighty nine (89) data points was used to perform the regression. After calculation and substitution an empirical bromate model with the following equation was obtained:

$$[\text{BrO}_3^-] = 1.63 \times 10^{-8} [\text{Br}^-]^{1.716} [\text{DOC}]^{-0.554} (\text{O}_3 \text{ mass rate})^{1.521} (\text{pH})^{2.254} (t)^{1.497} \quad (3)$$

A negative coefficient indicates that the corresponding variable has a reverse effect on bromate formation. Hence, increase in DOC concentration reduces bromate formation. On the other hand, increase in bromide concentration, inlet ozone injection rate, pH, and residence time in the reactor favour bromate formation. The model results are consistent with the experimental findings presented earlier in this paper. Similar trend for the effect of these variables on bromate formation in the absence of NOM in the hybrid system (see Chapter 4). Unlike bromate models presented in the literature for conventional ozonation processes (Jarvis et al., 2007, Song et al., 1996), the model developed in this paper demonstrates that the initial bromide concentration plays a more important role in bromate formation than does the ozone dose. This finding is

consistent with the empirical model proposed for bromate formation in the hybrid system in the absence of NOM (see Chapter 4).

In order to validate the ability of the above model in simulating bromate formation, the predicted bromate concentrations were plotted against observed values in Figure 25. Model was able to satisfactorily predict bromate concentration in the system ( $R^2=0.815$ ). The slope of the regression line (0.916) is close to 1 meaning that the model and experimental results are very close but since it is smaller than 1 the model tends to slightly under-predict the bromate concentration.

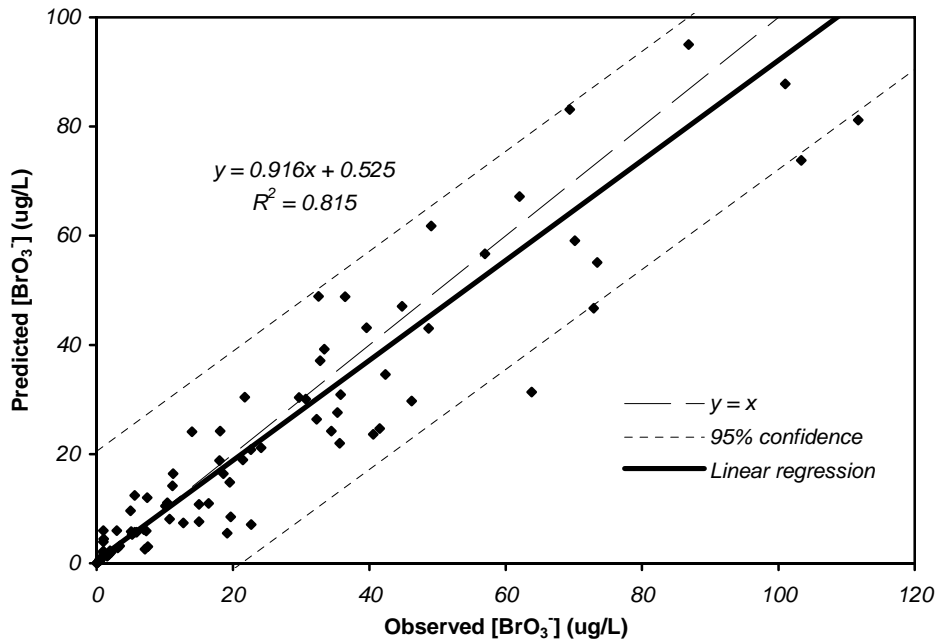


Fig. 25- Predicted bromate concentration vs. observed values.

## 5.6. References

- APHA (2005) Standard methods for the examination of water and wastewater. 21<sup>st</sup> ed.
- Byun, S., Davies, S.H., Alpatova, A.L., Corneal, L.M., Baumann, M.J., Tarabara, V.V., Masten, S.J. (2011) Mn oxide coated catalytic membranes for a hybrid ozonation-membrane filtration: Comparison of Ti, Fe and Mn oxide coated membranes for water quality. *Wat. Res.* 45, 163-170.
- Camel, V., Bermond, A. (1998) The use of ozone and associated oxidation processes in drinking water treatment. *Water Res.* 32, 3208-3222.
- Chandrakanth, M.S.; Honeyman, B.D.; Amy, G.L. (1996) Modeling the interactions between ozone, natural organic matter, and particles in water treatment. *Colloids Surf. A: Physiochem. Eng. Aspects* 107, 321-342.
- Corneal, L.M., Masten, S.J., Davies, S.H.R., Tarabara, V.V., Byun, S., Baumann, M.J. (2010) AFM, SEM and EDS characterization of manganese oxide coated ceramic water filtration membranes. *J. Mem. Sci.* 360, 292-302.
- European Union (1998) Official Journal of the European Communities, L 330, Council Directive 98/83/EC.
- Evans F.L. (1972) Ozone in water and wastewater treatment. Ann Arbor Science Publishers, Michigan.
- Gottschalk, C., Libra, J.A., Saupe, A. (2000) Ozonation of water and waste water: A practical guide to understanding ozone and its application. Wiley-VCH: New York.
- Gracia, R., Aragues, J.L., Ovelleiro, J.L. (1996) Study of the catalytic ozonation of humic substances in water and their ozonation byproducts. *Ozone Sci. Eng.* 18, 195-208.

- Jarvis, P., Parsons, S.A., Smith, R. (2007) Modeling bromate formation during ozonation. *Ozone Sci. Eng.* 29, 429-442.
- Karnik, B.S., Davies, S.H.R., Chen, K.C., Jaglowski, D.R., Baumann, M.J., Masten, S.J. (2005) Effects of ozonation on the permeate flux of nanocrystalline ceramic membranes. *Water Res.* 39, 728-734.
- Kim, J., Shan, W., Daview, S.R., Baumann, M.J., Masten, S.J., Tarabara, V. (2009) Interactions of aqueous NOM with nanoscale TiO<sub>2</sub>: Implications for ceramic membrane filtration-ozonation hybrid process. *Environ. Sci. Technol.* 43, 5488-5494.
- Kim, J., Van der Bruggen, B. (2010) The use of nanoparticles in polymeric and ceramic membrane structures: Review of manufacturing procedures and performance improvement for water treatment. *Environmental Pollution* 158, 2335-2349.
- Legube, B., Parinet, B., Gelinet, K., Berne, F., Croue, J.P. (2004) Modeling of bromate formation by ozonation of surface waters in drinking water treatment. *Water Res.* 38, 2185-2195.
- Mizuno, T., Yamada, H., Tsuno, H. (2004) Formation of bromate ion through a radical pathway in a continuous flow reactor. *Ozone Sci. Eng.* 26, 573-584.
- Mizuno, T., Tsuno, H., Yamada, H. (2007) A simple model to predict formation of bromate ion and hypobromous acid/hypobromite ion through hydroxyl radical pathway during ozonation. *Ozone Sci. Eng.* 29, 3-11.

- Morris, R.D., Audet, A.M., Angelillo, I.F., Chalmers, T.C., Mosteller, F. (1992) Chlorination, chlorination by-products, and cancer: A metaanalysis, *Am. J. Public. Health* 82, 955-963.
- Moslemi, M., Davies, S.H., Masten, S.J. (2010). Ozone mass transfer in a recirculating loop semibatch reactor operated at high pressure. *Adv. Oxidation Technol.* 13, 79-88
- Moslemi, M., Davies, S.H., Masten, S.J. (2011) Bromate formation in a hybrid ozonation-ceramic membrane filtration system, *Water Res.* 45, 5529-5534.
- Moza, S., Tomaszewska, M., Morawski, A.W. (2006) Application of an ozonation-adsorption-ultrafiltration system for surface water treatment. *Desalination* 190, 308-314.
- Ontario drinking-water quality standards (2002) Safe Drinking Water Act, Ontario regulation 169/03.
- Pinkernell, U., von Gunten, U. (2001) Bromate minimization during ozonation: Mechanistic considerations. *Environ. Sci. Technol.* 35, 2525-2531.
- Schlichter, B., Mavrov, V., Chmiel, H. (2003) Study of a hybrid process combining ozonation and membrane filtration - filtration of model solutions. *Desalination* 156, 257-265.
- Siddiqui, M.S., Amy, G.L. (1993) Factors affecting DBP formation during ozone-bromide reactions. *J. AWWA* 85, 63-72.
- Siddiqui, M.S., Amy, G.L., Rice, R.G. (1995) Bromate ion formation: A critical review, *J. AWWA* 87, 58-70.

- Sohn, J., Amy, G., Cho, J., Lee, Y., Yoon, Y. (2004) Disinfectant decay and disinfection by-products formation model development: chlorination and ozonation by-products. *Wat. Res.* 38, 2461–2478.
- Song, R., Donohoe, C., Minear, R., Westerhoff, P., Ozekin, K., Amy, G. (1996) Empirical modeling of bromate formation during ozonation of bromide-containing water. *Wat. Res.* 30, 1161-1168.
- USEPA (1998) National primary drinking water regulations: Disinfection and disinfection byproducts. *Federal Register* 63, 69390-69476.
- USEPA (2003) Determination of haloacetic acids and dalapon in drinking water by liquide-liquid microextraction, derivatization, and gas chromatography with electron capture detection, 815-B-03-002.
- Van Geluwe, S., Braeken, L., Van der Bruggen, B. (2011) Ozone oxidation for the alleviation of membrane fouling by natural organic matter: A review. *Water Res.* 45, 3551-3570.
- von Gunten, U., Oliveras, Y. (1998) Advanced oxidation of bromide-containing waters: Bromate formation mechanisms. *Environ. Sci. Technol.* 32, 63-70.
- Westerhoff, P., Song, R., Amy, G., Minear, R. (1998) NOM's role in bromine and bromate formation during ozonation. *AWWA* 89, 82-94.
- You, S.H., Tseng, D.H., Hsu, W.C. (2007) Effect and mechanism of ultrafiltration membrane fouling removal by ozonation. *Desalination* 202, 224-230.

## **Chapter 6: Conclusions and Recommendations**

### **6.1. Conclusions**

The mass transfer of ozone gas to water plays a pivotal role in the performance and efficacy of ozonation systems. As a preliminary step, the effects of water flow rate, mixing, gaseous ozone concentration, inlet gas flow rate, temperature, and pH on ozone hydrodynamics in a recirculating loop semibatch reactor operated at high pressure were studied. Variations in the water cross flow rate only slightly affected the ozone mass transfer rates, suggesting that sufficient mixing in the reactor was achieved at the low flow rates used. The addition of an inline static mixer had a negligible effect on aqueous ozone concentrations in the reactor, indicating that mixing was sufficient without the mixer and adequate mass transfer can be achieved using a simple tee to inject the ozone gas into the pressurized water stream. The dissolved ozone concentration increased with increasing gaseous ozone concentration and with the inlet gas flow rate. The final dissolved ozone concentration was found to be proportional to the inlet ozone concentration. The dissolved ozone concentration decreased with increasing pH due to the greater rate of ozone decomposition at higher pH. The mass transfer of ozone increased slightly with temperature, however, due to the lower solubility of ozone at higher temperature, the final ozone concentration achieved decreased with increasing temperature. A model to describe the ozone mass transfer was

developed. Good agreement between the model predictions and the experimental data was achieved.

The aim of the second phase of the experiments was to study the formation of bromate in the hybrid ozonation-membrane filtration system in the absence of natural organic matter (NOM). To achieve this goal the effects of important variables including pH, inlet ozone mass injection rate, initial bromide concentration, membrane molecular weight cut off (MWCO), the nature of the membrane surface (coating), hydroxyl radical scavengers, and temperature on bromate formation in a hybrid membrane filtration–ozonation reactor was studied. According to our experimental findings, decreasing the pH, significantly reduced bromate formation. Bromate formation increased with increasing inlet gaseous ozone mass injection rate, due to increase in dissolved ozone concentrations. Greater initial bromide concentrations resulted in higher bromate concentrations. An increase in the bromate concentration was observed by reducing MWCO, which resulted in a concomitant increase in the retention time in the system.

Presence of hydroxyl radical scavengers (tertiary butyl alcohol) suppressed the indirect bromate formation pathway and less bromate was formed, suggesting that, the hydroxyl radical pathway plays a significant role in bromate formation. The Mn oxide coated membrane enhanced ozone decomposition, which resulted in lower concentrations of dissolved ozone. The bromate concentration that resulted with the coated membrane was less than that formed with the uncoated

TiO<sub>2</sub> membrane. As the temperature was increased, bromate formation was enhanced, which was attributed to greater reaction rates.

In order to simulate bromate formation in the hybrid system, a kinetic-based model was developed. Good correlation between the model simulation and the experimental data was achieved. An empirical model was also developed to predict bromate formation in the hybrid system. The model was generated using multiple linear regression method with logarithmic transformations and takes into account the effects of important experimental variables including initial bromide concentration, inlet ozone mass injection rate, pH, temperature, and reaction time. Good correlation was achieved between the model predictions and the experimental data ( $R^2=0.903$ ). Modeling results indicated that bromate formation was favoured at high bromide concentration, ozone dose, pH, and temperature.

In the final phase of research, formation of bromate and organic disinfection by-products in the presence of NOM was investigated. To this end, the effect of pH, inlet ozone mass injection rate, NOM concentration, initial bromide concentration, membrane coating, hydroxyl radical scavenger, and membrane MWCO on the formation of disinfection by-products including bromate, total trihalomethanes (TTHMs), and halo-acetic acids (HAAs) in the hybrid system was studied. Furthermore, variations in the TOC, UV<sub>254</sub>, SUVA, color and turbidity of water as function of these parameters were investigated. Bromate and TTHMs formation increased with increasing inlet gaseous ozone mass injection rate, and initial bromide concentration. In the presence of NOM less bromate was

formed. The extent of bromate formation decreased with decreasing pH. The presence of tertiary butyl alcohol significantly reduced bromate and TTHM formation. The bromate and TTHM concentrations that were observed with the Mn oxide coated membrane were less than that formed with the uncoated TiO<sub>2</sub> membrane. An increase in the bromate concentration was observed with decreasing MWCO of the filtration membrane.

An empirical model using multiple linear regression method was developed to predict bromate formation in the presence of NOM. The variables included in the model consist of bromide concentration, dissolved organic carbon concentration, ozone mass injection rate, pH, and reaction time. Good correlation was achieved between the model predictions and the experimental data ( $R^2=0.815$ ). According to this model, bromate formation was favoured at high bromide concentration, ozone mass injection rate, and pH. However, bromate formation reduced as dissolved carbon concentration was increased.

Experimental results also indicated that ozonation can be used to overcome membrane fouling problem by maintaining a minimum dissolved ozone concentration in the system. This allows for continuous operation of the hybrid ozonation-membrane filtration system at a relatively high permeate flux as compared to the original permeate flux obtained with pure water.

## 6.2. Recommendations for Future Research

In order to enhance the understanding of disinfection by-product formation in the hybrid ozonation–membrane system, the following are suggested for future research:

1. Optimization of the hybrid ozonation-membrane filtration system. Experimental results indicated that for a gaseous ozone concentration of 10.0 mg/L, the total ozone losses from the system at gas flow rates of 25, 50, 75 and 100 mL/min were 83.5, 87.5, 90.0 and 91.0 %, respectively. Given the high ozone loss from the experimental setup, efforts should be made to optimize the ozone hydrodynamics in the hybrid system in order to make the most of the ozone mass delivered to the system.
2. Duplication of the experiments using natural water source. Model water made with Suwannee River NOM was used in the existing research. Given the fact that
3. type and nature of NOM can play role in DBP formation, it is recommended that complementary experiments to be conducted using natural waters containing various concentrations and types of organic materials.
4. Expanding the theoretical and empirical bromate formation models developed in this research to account for a wider range of independent variables.

5. Modeling trihalomethane and halo-acetic acids formation in the hybrid ozonation-ceramic filtration system treating bromide containing waters.
6. Studying the effect of ammonia on DBP formation in the hybrid ozonation-membrane reactor. Ammonia has been reported to reduce bromate formation in conventional ozonation systems [70,73,75].
7. Investigation of the effect of Mn oxides particles on DBP formation in the hybrid system and compare the results with the results obtained in this research using the Mn oxide coated membrane.

### **6.3. Implications of Research for Full-scale Operation**

Ceramic membranes owing to their catalytic nature have shown very promising results in terms of oxidation and removal of organic foulants from the membrane surface. Ceramic membranes are made of a combination of metal oxides such as titanium dioxide, iron oxide, aluminum oxide and zirconium dioxide and, hence, they are catalytic in nature. Experimental results also indicated that in the presence of metal oxides less bromate and TTHM was formed. Therefore, ceramic membranes can be used to reduce disinfection by-products formation in the treatment of bromide containing waters using ozonation processes.

Since ceramic membranes are not commercially available right now, their major drawback is the high initial cost associated with the purchase of the membranes. However, ceramic membranes are physically more durable and long lasting as compared to polymeric membranes and in the long run the use of ceramic

membranes could be more economical than the use of polymeric membranes. Moreover, using ceramic membranes, the inlet ozone dosage can be lowered. Ceramic membranes are believed to promote ozone decomposition and thereby enhance the formation of hydroxyl radicals. Hydroxyl radicals are much stronger oxidants than ozone and can more effectively oxidize and remove foulants. Therefore, it is expected that in the presence of ceramic membrane less ozone dosage is required to overcome membrane fouling and hence the ozone dose can be reduced. Lowering the ozone dosage reduces the cost of the treatment process. Therefore, it is believed that advantages offered by ceramic membranes justify the high initial cost associated with their installation.

## References

- [1] M. L. Davis, S. J. Masten, Principles of environmental engineering and science, (2004) McGraw-Hill, New York.
- [2] P. Hillis, Membrane technology in water and wastewater treatment, (2000) Royal Society of Chemistry, Cambridge.
- [3] T. Chaiket, P. C. Singer, A. Miles, M. Moran, C. Pallotta, Effectiveness of coagulation, ozonation, and biofiltration in controlling DBPs, J. AWWA 94 (2002) 12: 81-95.
- [4] G. F. Craun, S. A. Hubbs, F. Frost, R. L. Calderon, S. H. Via, Waterborne outbreaks of cryptosporidiosis, J. AWWA 90 (1998) 9: 81-91.
- [5] USEPA, National primary drinking water regulations: Interim enhanced surface water treatment, Federal Register 63 (1998) 241: 69478-69521.
- [6] J. Crittenden, M. W. Harza (firm), Water treatment: Principles and design, 2nd ed. (2005) MWH, John Wiley, New Jersey.
- [7] G. Belfort, R. H. Davis, A. L. Zydney, Behavior of suspensions and macromolecular solutions in crossflow microfiltration, J. Membr. Sci. 96 (1994) 1-58.
- [8] AWWA membrane technology research committee, Membrane processes in potable water treatment, J. AWWA 84 (1992) 1: 59-67.
- [9] AWWA membrane technology research committee, Membrane processes, J. AWWA 90 (1998) 6: 91-105.

- [10] B. S. Karnik, S.H. Davies, M.J. Baumann, S.J. Masten, The effect of combined ozonation and filtration on disinfection by-product formation, *Wat. Res.* 39 (2005) 2839-2850.
- [11] C. T. Cleveland, Big advantages in membrane filtration, *J. AWWA* 91 (1999) 6: 10.
- [12] S. Nakatsuka, I. Nakate, T. Miyano, Drinking water treatment by using ultrafiltration hollow fiber membranes, *Desalination* 106 (1996) 1-3: 55-61.
- [13] B. S. Karnik, S. H. R. Davies, K. C. Chen, D. R. Jaglowski, M. J. Baumann, S. J. Masten, Effects of ozonation on the permeate flux of nanocrystalline ceramic membranes, *Wat. Res.* 39 (2005) 728-734.
- [14] R. Ghosh, Protein bioseparation using ultrafiltration, (2003) Imperial College Press, London.
- [15] C. Jucker, M. M. Clark, Adsorption of aquatic humic substances on hydrophobic ultrafiltration membranes, *J. Membr. Sci.* 97 (1994) 37-52.
- [16] C. Combe, E. Molis, P. Lucas, R. Riley, M. M. Clark, The effect of CA membrane properties on adsorptive fouling by humic acid, *J. Membr. Sci.* 154 (1999) 73-87.
- [17] W. Yuan, A. L. Zydney, Humic acid fouling during ultrafiltration, *Environ. Sci. Technol.* 34 (2000) 5043-5050.
- [18] B. Schlichter, V. Mavrov, H. Chmiel, Study of a hybrid process combining ozonation and membrane filtration - filtration of model solutions, *Desalination* 156 (2003) 257-265.

- [19] S. H. You, D. H. Tseng, W. C. Hsu, Effect and mechanism of ultrafiltration membrane fouling removal by ozonation, *Desalination*, 202 (2007) 224-230.
- [20] Y. G. Park, Effect of ozonation for reducing membrane-fouling in the UF membrane, *Desalination* 147 (2002) 43-48.
- [21] S. Mozia, M. Tomaszewska, A. W. Morawski, Application of an ozonation-adsorption-ultrafiltration system for surface water treatment, *Desalination* 190 (2006) 308-314.
- [22] B. Schlichter, V. Mavrov, H. Chmiel, Study of a hybrid process combining ozonation and microfiltration/ultrafiltration for drinking water production from surface water, *Desalination* 168 (2004) 307-317.
- [23] R. G. Rice, C. M. Robson, G. W. Miller, A. G. Hill, Use of ozone in drinking water treatment, *J. AWWA* 73 (1981) 1: 44-57.
- [24] B. Legube, N. K. V. Leitner, Catalytic ozonation: a promising advanced ozidation technology for water treatment, *Catal. Today* 53 (1999) 61-72.
- [25] C. Gottschalk, J. A. Libra, A. Saupe, Ozonation of water and waste water: A practical guide to understanding ozone and its application, (2000) Wiley-VCH, New York.
- [26] B. Langlais, D. A. Reckhow, D. R. Brink, Ozone in water treatment: Application and engineering: Cooperative research report, (1991) AWWA Research Foundation, Lewis Publishers, Michigan.
- [27] W. J. Masschelein, Ozonization manual for water and wastewater treatment, (1982) Wiley, New York.

- [28] C. Gomella, Ozone practice in France, *J. AWWA* 64 (1972) 1:39-46.
- [29] M. S. Chandrakanth, B. D. Honeyman, G. L. Amy, Modeling the interactions between ozone, natural organic matter, and particles in water treatment, *Colloids Surf. A: Physiochem. Eng. Aspects* 107 (1996) 321-342.
- [30] A. Peter, U. von Gunten, Oxidation kinetics of selected taste and odor compounds during ozonation of drinking water, *Environ. Sci. Technol.* 41 (2007) 626-631.
- [31] V. Camel, A. Bermond, The use of ozone and associated oxidation processes in drinking water treatment, *Wat. Res.* 32 (1998) 11: 3208-3222.
- [32] W. H. Glaze, Drinking water treatment with ozone, *Environ. Sci. Technol.* 21 (1987) 3: 224-230.
- [33] U. von Gunten, Ozonation of drinking water: Part II. Disinfection and by-product formation in presence of bromide, iodide or chlorine, *Wat. Res.* 37 (2003) 1469-1487.
- [34] F. L. Evans III, Ozone in water and wastewater treatment, (1972) Ann Arbor Science Publishers, Michigan.
- [35] R. D. Morris, A. M. Audet, I. F. Angelillo, T. C. Chalmers, F. Mosteller, Chlorination, chlorination by-products, and cancer: A metaanalysis, *Am. J. Public Health* 82 (1992) 7: 955-963.
- [36] EU, Official journal of European Communities, L 330 (1998) Council Directive 98/83/EC.

- [37] WHO, Guidelines for drinking-water quality, Vol. 1, Recommendations, 3rd ed. (2006) World Health Organization (Electronic version).
- [38] Ontario drinking-water quality standards, Safe drinking water act, (2002) Ontario regulation 169/03 (Electronic version).
- [39] USEPA, National primary drinking water regulations: Disinfection and disinfection byproducts, Federal Register 63 (1998) 241: 69390-69476.
- [40] USEPA, Stage 2 microbial and disinfection byproducts federal advisory committee agreement in principle, Federal Register 65 (2000) 251: 83015-83024.
- [41] Canada. Environmental Health Directorate, A one-year survey of halogenated disinfection by-products in the distribution system of treatment plants, (1996) Environmental Health Directorate, Health Protection Branch, Ottawa.
- [42] G. L. Amy, R. Bull, G. F. Craun, G. Craun, Disinfection and disinfectant by-products, (2000) WHO, Geneva.
- [43] P. H. S. Kim, J. M. Symons, Using anion exchange resins to remove THM precursors, J. AWWA 83 (1991) 12: 61-68.
- [44] J. C. Crittenden, D. W. Hand, H. Arora, B. W. Lykins, Design consideration for GAC treatment of organic chemicals, J. AWWA 79 (1987) 1: 74-82.
- [45] T. H. Boyer, P. C. Singer, Bench-scale testing of a magnetic ion exchange resin for removal of disinfection by-product precursors, Wat. Res. 39 (2005) 1265-1276.

- [46] M. Fielding, M. Farrimond, Disinfection by-products in drinking water: current issues, (1999) Royal Society of Chemistry, Cambridge.
- [47] S. D. Faust, O. M. Aly, Chemistry of water treatment, (1983) Butterworths, Boston.
- [48] J. Hoigne, H. Bader, Rate constants of reactions of ozone with organic and inorganic compounds in water-I : Non-dissociating organic compounds, *Wat. Res.* 17 (1983) 173-183.
- [49] J. Hoigne, H. Bader, Rate constants of reactions of ozone with organic and inorganic compounds in water-II : Dissociating organic compounds, *J. AWWA* 17 (1983) 185-194.
- [50] J. Hoigne, H. Bader, W. R. Haag, J. Staehelin, Rate constants of reactions of ozone with organic and inorganic compounds in water-III. Inorganic compounds and radicals, *Wat. Res.* 19 (1985) 8: 993-1004.
- [51] U. von Gunten, Ozonation of drinking water: Part I. Oxidation kinetics and product formation, *Wat. Res.* 37 (2003) 1443-1467.
- [52] D. A. Reckhow, B. Legube, P. C. Singer, The ozonation of organic halide precursors: effect of bicarbonate, *Wat. Res.* 20 (1986) 8: 987-998.
- [53] J. Hoigne, H. Bader, Ozonation of water: Role of hydroxyl radicals as oxidizing intermediate, *Sci.* 190 (1975) 4216: 782-784.
- [54] G. V. Buxton, C. L. Greenstock, W. P. Helman, A. B. Ross, Critical review of rate constants for reactions of hydrated electrons, hydrogen atoms and

- hydroxyl radicals ( $\cdot\text{OH}/\cdot\text{O}$ ) in aqueous solution, *J. Phys. Chem. Ref. Data* 17 (1988) 2: 513-886.
- [55] J. Hoigne, H. Bader, The role of hydroxyl radical reactions in ozonation processes in aqueous solutions, *Wat. Res.* 10 (1976) 377-386.
- [56] J. J. McCarthy, C. H. Smith, A review of ozone and its application to domestic wastewater treatment, *J. AWWA* 66 (1974) 12: 718-725.
- [57] J. Staehelin, J. Hoigne, Decomposition of ozone in water: Rate of initiation by hydroxide ions and hydrogen peroxide, *Environ. Sci. Technol.* 16 (1982) 16: 676-681.
- [58] R. E. Buhler, J. Staehelin, J. Hoigne, Ozone decomposition in water studied by pulse radiolysis. 1.  $\text{HO}_2/\text{O}_2^-$  and  $\text{HO}_3/\text{O}_3^-$  as intermediates, *J. Phys. Chem.* 88 (1984) 2560-2564.
- [59] P. Westerhoff, R. Song, G. Amy, R. Minear, Numerical kinetic models for bromide oxidation to bromine and bromate, *Wat. Res.*, 32 (1998) 5: 1687-1699.
- [60] H. Tomiyasu, H. Fukutomi, G. Gordon, Kinetics and mechanism of ozone decomposition in basic aqueous solution, *Inorg. Chem.* 24 (1985) 19: 2962-2966.
- [61] J. Staehelin, R. E. Buler, J. Hoigne, Ozone decomposition in water studied by pulse radiolysis. 2.  $\text{OH}$  and  $\text{HO}_4$  as chain intermediates, *J. Phys. Chem.* 88 (1984) 5999-6004.
- [62] U. von Gunten, J. Hoigne, Bromate formation during ozonation of bromide containing waters: interaction of ozone and hydroxyl radical reactions, *Environ. Sci. Technol.* 28 (1994) 1234-1242.

- [63] J. Staehelin, J. Hoigne, Decomposition of ozone in water in the presence of organic solutes acting as promoters and inhibitors of radical chain reactions, *Environ. Sci. Technol.* 19 (1985) 12: 1206-1213.
- [64] T. Mizuno, H. Tsuno, H. Yamada, Effect of inorganic carbon on ozone self-decomposition, *Ozone Sci. Eng.* 29 (2007) 31-40.
- [65] M. S. Siddiqui, G. L. Amy, R. G. Rice, Bromate ion formation: A critical review, *J. AWWA* 87 (1995) 10: 58-70.
- [66] U. von Gunten, U. Pinkernell, Ozonation of bromide-containing drinking waters: a delicate balance between disinfection and bromate formation, *Wat. Sci. Technol.* 41 (2000) 7: 53-59.
- [67] S. W. Krasner, W. H. Glaze, H. S. Weinberg, P. A. Daniel, I. N. Najm, Formation and control of bromate during ozonation of waters containing bromide, *J. AWWA* 85 (1993) 1: 73-81.
- [68] W. R. Haag, J. Hoigne, Ozonation of bromide-containing waters: Kinetics of formation of hypobromous acid and bromate, *Environ. Sci. Technol.* 17 (1983) 17: 261-267.
- [69] J. Tanaka, M. Matsumura, Kinetic studies of removal of ammonia from seawater by ozonation, *J. Chem. Technol. Biotechnol.* 77 (2002) 649-656.
- [70] R. Song, P. Westerhoff, R. Minear, G. Amy, Bromate minimization during ozonation, *J. AWWA* 89 (1997) 6: 69-78.

- [71] T. Mizuno, H. Yamada, H. Tsuno, Formation of bromate ion through a radical pathway in a continuous flow reactor, *Ozone Sci. Eng.* 26 (2004) 573-584.
- [72] B. Legube, B. Parinet, K. Gelinet, F. Berne, J. P. Croue, Modeling of bromate formation by ozonation of surface waters in drinking water treatment, *Wat. Res.* 38 (2004) 2185-2195.
- [73] F. Berne, G. Chasson, B. Legube, Effect of addition of ammonia on the bromate formation during ozonation, *Ozone Sci. Eng.* 26 (2004) 267-276.
- [74] U. von Gunten, Y. Oliveras, Advanced oxidation of bromide-containing waters: Bromate formation mechanisms, *Environ. Sci. Technol.* 32 (1998) 63-70.
- [75] U. Pinkernell, U. von Gunten, Bromate minimization during ozonation: Mechanistic considerations, *Environ. Sci. Technol.* 35 (2001) 2525-2531.
- [76] P. Westerhoff, R. Song, G. Amy, R. Minear, NOM's role in bromine and bromate formation during ozonation, *J. AWWA* 89 (1998) 11: 82-94.
- [77] S. W. Krasner, M. J. Scilimenti, E. G. Means, Quality degradation: Implications for DBP formation, *J. AWWA* 86 (1994) 6: 34-47.
- [78] B. S. Karnik, M. J. Baumann, S. J. Masten, S. H. Davies, AFM and SEM characterization of iron oxide coated ceramic membranes, *J. Mater. Sci.* 41 (2006) 6861-6870.
- [79] B. S. Karnik, S. H. Davies, M. J. Baumann, S. J. Masten, Fabrication of catalytic membranes for the treatment of drinking water using combined ozonation and ultrafiltration, *Environ. Sci. Technol.* 39 (2005) 7656-7661.

- [80] K. Kusakabe, S. Aso, J. I. Hayashi, K. Isomura, S. Morooka, Decomposition of humic acid and reduction of trihalomethane formation potential in water by ozone with u.v. irradiation, *Wat. Res.* 24 (1990) 6: 781-785.
- [81] H. Arai, M. Arai, A. Sakumoto, Exhaustive degradation of humic acid in water by simultaneous application of radiation and ozone, 20 (1986) 7: 885-891.
- [82] A. Chin, P. R. Berube, Removal of disinfection by-product precursors with ozone-UV advanced oxidation process, *Wat. Res.* 39 (2005) 2136-2144.
- [83] M. S. Siddiqui, G. L. Amy, Factors affecting DBP formation during ozone-bromide reactions, *J. AWWA* 85 (1993) 1: 63-72.
- [84] R. Hofmann, R. C. Andrews, Ammoniacal bromamines: a review of their influence on bromate formation during ozonation, *Wat. Res.* 35 (2001) 3: 599-604.
- [85] M. L. Bao, O. Griffini, D. Santianni, K. Barbieri, D. Burrini, F. Pantani, Removal of bromate ion from water using granular activated carbon, *Wat. Res.* 33 (1999) 2959-2970.
- [86] R. D. Letterman, *Water quality and treatment: A handbook of community water supplies*, 5th ed. (1999) AWWA, McGraw-Hill, New York.
- [87] M. Siqueiri, G. Amy, K. Ozekin, W. Zhai, P. Westerhoff, Alternative strategies for removing bromate, *J. AWWA* 86 (1994) 10: 81-96.
- [88] I. Ilisz, A. Bokros, A. Dombi, TiO<sub>2</sub>-based heterogeneous photocatalytic water Treatment combined with ozonation, *Ozone Sci. Eng.* 26 (2004) 585-594.

- [89] E. M. Aieta, K. M. Reagan, J. S. Lang, L. McReynolds, J. W. Kang, W. H. Glaze, Advanced oxidation process for treating groundwater contaminated with TCE and PCE: Laboratory studies, *J. AWWA* 81 (1988) 5: 64-72.
- [90] P. L. Clech, E. K. Lee, V. Chen, Hybrid photocatalysis/membrane treatment for surface waters containing low concentrations of natural organic matters, *Wat. Res.* 40 (2006) 323-330.
- [91] A. Mills, S. K. Lee, A web-based overview of semiconductor photochemistry-current commercial applications, *J. Photochem. Photobiol. A: Chem.* 152 (2002) 233-247.
- [92] D. Robert, S. Malato, Solar photocatalysis: a clean process for water detoxification, *Sci. Total Environ.* 291 (2002) 85-97.
- [93] R. P. Schwarzenbach, P. M. Gschwend, D. M. Imboden, *Environmental organic chemistry*, 2nd ed. (2003) Wiley, New Jersey.
- [94] G. Wittmann, I. Horvath, A. Dombi, UV-induced decomposition of ozone and hydrogen peroxide in the aqueous phase at pH 2-7, *Ozone Sci. Eng.* 24 (2002) 281-291.
- [95] Y. Zhang, J. C. Crittenden, D. W. Hand, D. L. Perram, Fixed-bed photocatalysis for solar decontamination of water, *Environ. Sci. Technol.* 28 (1994) 435-442.
- [96] Z. Bukhari, F. Abrams, M. LeChevallier, Using ultraviolet light for disinfection of finished water, *Wat. Sci. Technol.* 50 (2004) 1: 173-178.

- [97] D. E. Huffman, A. Gennaccaro, J. B. Rose, B. W. Dussert, Low- and medium-pressure UV inactivation of microsporidia *Encephalitozoon intestinalis*, *Wat. Res.* 26 (2002) 3161-3164.
- [98] N. H. Phillip, E. Gurten, V. Diyamandoglu, Transformation of bromine species during decomposition of bromate under UV light from low pressure mercury vapor lamps, *Ozone Sci. Eng.* 28 (2006) 217-228.
- [99] A. Mills, A. Gelghazi, D. Rodman, Bromate removal from drinking water by semiconductor photocatalysis, *Wat. Res.* 30 (1996) 9: 1973-1978.
- [100] A. Mills, G. Meadows, Heterogeneous redox catalysis: A novel route for removing bromate ions from water, *Wat. Res.* 29 (1995) 9: 2181-2185.
- [101] J. J. Wu, S. J. Masten, Mass transfer of ozone in semibatch stirred reactor, *J. Environ. Eng.* 127 (2001) 12: 1089-1099.
- [102] M. R. Wiesner, S. Chellam, Mass transport consideration for pressure driven membrane processes, *J. AWWA* 84 (1992) 1: 88-95.
- [103] J. L. Sotelo, F. J. Beltran, F. J. Benitez, J. B. Heredia, Henry's law constant for the ozone-water system, *Wat. Res.* 23 (1989) 10: 1239-1246.
- [104] F. J. Rivas, F. J. Beltran, M. Carbajo, O. Gimeno, Homogeneous catalyzed ozone decomposition in the presence of Co (II), *Ozone Sci. Eng.* 25 (2003) 261-271.
- [105] M. D. Gurol, P. C. Singer, Kinetics of ozone decomposition: A dynamic approach, *Environ. Sci. Technol.* 16 (1982) 7: 377-383.
- [106] D. Grasso, W. J. Weber, Mathematical interpretation of aqueous-phase ozone decomposition rates, *J. Environ. Eng.* 115 (1989) 3: 541-559.

- [107] S. W. Hermanowicz, W. D. Bellamy, L. C. Fung, Variability of ozone reaction kinetics in batch and continuous flow reactors, *Wat. Res.* 33 (1999) 9: 2130-2138.
- [108] H. Matsuda, Y. Ose, T. Sato, H. Nagase, H. Kito, K. Sumida, Mutagenicity from ozonation of humic substances, *Sci. Total Environ.* 117/118 (1992) 521-529.
- [109] H. Matsuda, T. Sato, H. Nagase, Y. Ose, H. Kito, K. Sumida, Aldehydes as mutagens formed by ozonation of humic substances, *Sci. Total Environ.* 114 (1992) 205-213.
- [110] V. Fontanier, V. Farines, J. Albet, S. Baig, J. Molinier, Oxidation of organic pollutants of water to mineralization by catalytic ozonation, *Ozone Sci. Eng.* 27 (2005) 115-128.

## Appendix



Fig. A1- Experimental apparatus: Hybrid ozonation – membrane filtration.



Fig. A2- High-pressure stainless steel tank.



Fig. A3- Water coil inside the tank.

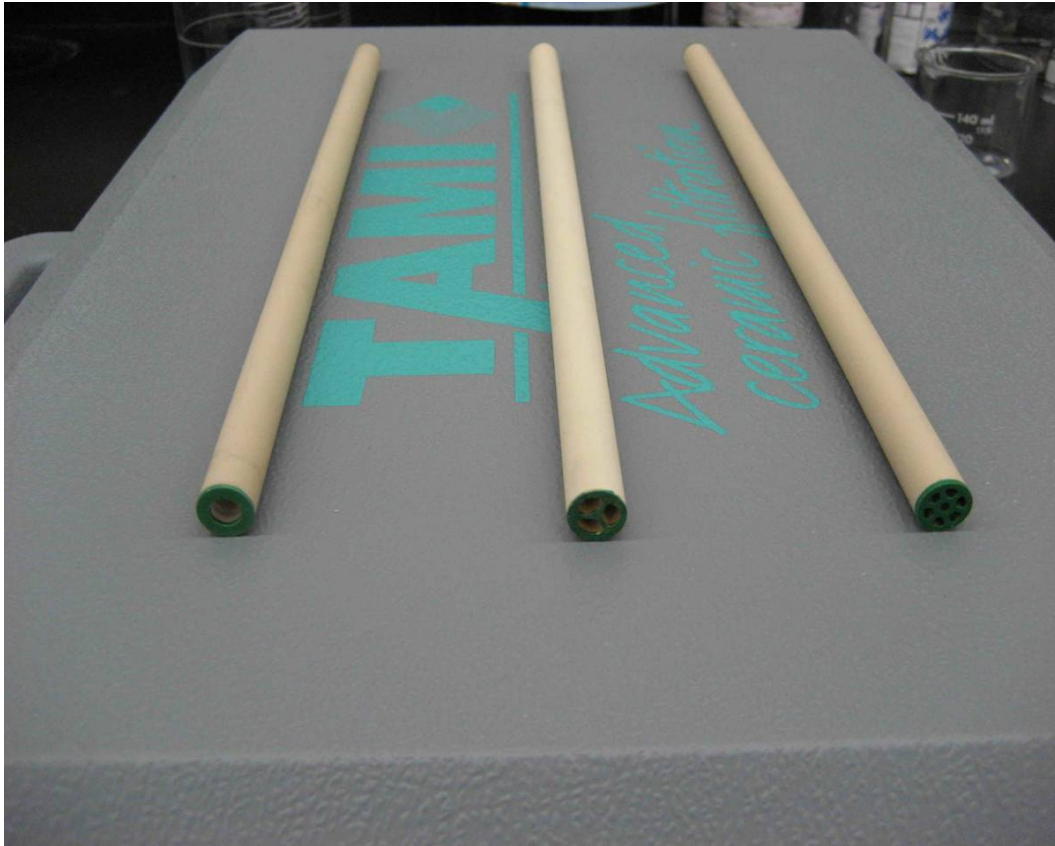


Fig. A4- Ceramic membranes (from left to right: one, three and seven channels).